SIMULATION OF ABSORPTION OF PHOTONS AT VARIOUS ANGLES AND ITS EFFECT ON IMAGING (SLANT RAY BLUR) USING GEANT–4.7.0

M.V.Amaresh Kumar

under the guidance of Dipankar Bhattacharya

Astronomy & Astrophysics Group, Raman Research Institute, Bangalore 560 080

(Sept 2005)

Abstract

This report is based on simulation of particle-matter interaction using Geant software. It is about studying the detector gas efficiency and Slant Ray Blur that arises due to photons incident on the detector at off-normal angles in the Scanning Sky Monitor (SSM).

The report discusses about efficiency of the detector gas mixture and the concept of Slant Ray Blur, considering a single cell of the detector based on the data obtained from the simulation. All the simulations are done using "GEANT 4.7" version. A brief study of statistical error present in the data and its effect are discussed, which are important in the calculation of centroid for various energies and the effect of incidence angle on the concept of Slant Ray Blur.

Contents

List of Figures

List of Tables

Chapter 1

INTRODUCTION

Report is divided into three chapters.

• Data to be obtained for the study of efficiency of the detector gas mixture and for the study of Slant Ray Blur using Geant software.

• Design of Detector Gas mixture and its effects on efficiency at various energies.

• Study of Slant Ray Blur arising due to the incident angle of X-ray photons along the anode wire and its corrections.

To begin with, we describe the detector cell on which our work will be based. The Scanning Sky Monitor is made up of three X-Ray Detecting cameras and each is made up of position sensitive multi-wire proportional counter as shown in the *figure1.1*

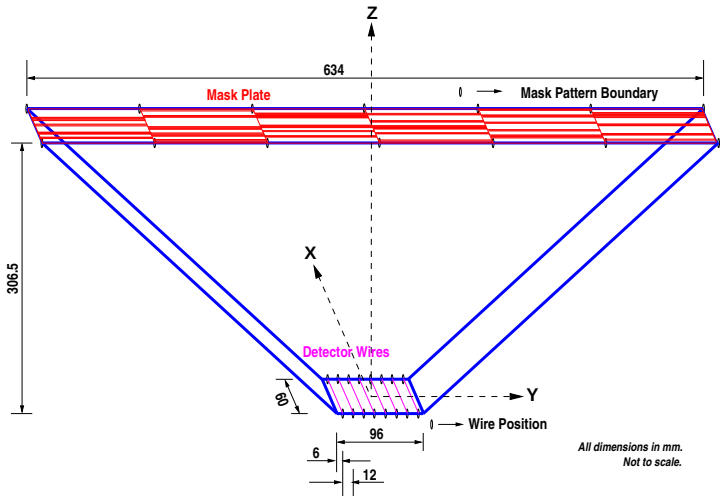

Figure 1.1: A single X-ray detecting multi-wire proportional counter with the dimensions as specified.

Here each anode/veto wire is caged by cathode wires. For the present simulation we are considering one such position sensitive anode wire caged by cathode wires as single cell is shown in the figure below, where the central dark spot is the anode wire and the circle with a dot around the dark spot are the cathode wires.

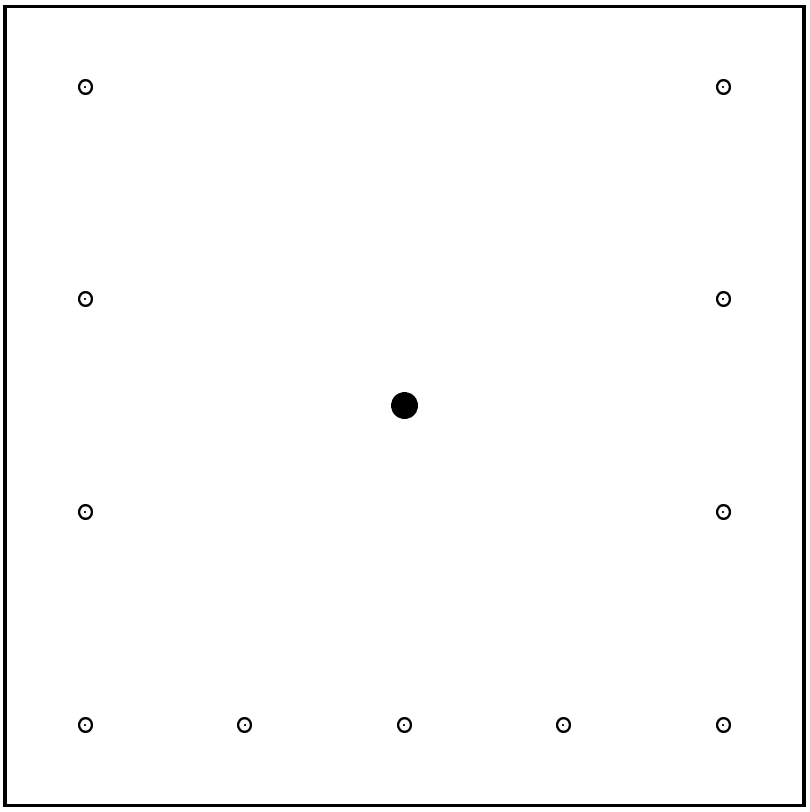

Chapter 2

GEANT 4.7

For the study of particle-matter interaction many softwares are available. According to our need and specifications we opted for Geant[1] (version 4.7) software which is a toolkit for the simulation of the passage of particles through matter. In our case it is extensively used to study the efficiency of detector gas mixture in an energy range of 2 KeV - 10 KeV and the effect of incident X-ray photon at various angles on the detector. This study analyzes slant ray blur.

While writing the code in Geant we keep in mind to divide the code in different sections to make it simple for debugging and for further enhancement and development in the code. In general each code is divided into four or five sections:

- *Detector Construction:*

  In this section detector definition and response is explained in detail. The detector definition requires the representation of its geometrical elements, their materials and their electronic properties, together with visualization attributes and user defined properties. The geometrical representation of the detector elements focuses on the solid models definition and their spatial position, as well as their logical relations.

  Geant 4.7 manages the representation of the detector element properties via the concept of Logical Volume. Geant 4.7 even manages the representation of the detector element spatial positioning and their logical relation via the concept of Physical Volume. Geant 4.7 also manages the representation of the detector element solid modeling via the concept of Solid. Much more can be learned about the geometry construction from Geant 4.7

[1] http://wwwasd.web.cern.ch/wwwasd/geant4/

Homepage[2].

In our case, we specify the dimensions of the detector, the detecting material, temperature, pressure and density in the code. Presently the detector cell that we have considered is 60*mm* in length, 12*mm* in breadth and 12*mm* in depth of the cell. The gas that is used as detecting material is a mixture of Xenon and P10 gas in proportions of 25% and 75% by volume. This part is of importance and is discussed in a separate section (*Gas Mixture and Related Calculations*).

- *Tracking and Physics:*

  All physics processes, including the transportation of particles, are treated generically. The tracking manager and stepping manager play an essential role in tracking the particle. Track information can be accessed by invoking *GET* methods provided in the *G4Track* class. For further details see the *Software Reference Manual*[3]. Step information can be retrieved by invoking various *GET* methods provided in the *G4Step* class. Again, for further details see the *Software Reference Manual*.

Physics processes describe how particles interact with a material. Seven major categories of processes are provided by Geant 4.7:

- Electromagnetic.
- Hadronic.
- Decay.
- PhotoLepton Hadron.
- Optical.
- Parametrization.
- Transportation.

[2]http://wwwasd.web.cern.ch/wwwasd/geant4/G4UsersDocuments/UsersGuides/ForApplicationDeveloper/html/Detector/index.html

[3]http://wwwasd.web.cern.ch/wwwasd/geant4/G4UsersDocuments/Overview/html/

Each of these headings is further subdivided, for example the category **Electromagnetic Interaction** which summarizes the electromagnetic processes. The following is a summary of the Low Energy Electromagnetic processes available in Geant4.7.

- **Photon Processes**

  Compton Scattering.

  Polarized Compton Scattering.

  Rayleigh Scattering.

  Gamma Conversion.

  Photoelectric effect.

- **Electron Processes**

  Bremsstrahlung.

  Ionization.

- **Hadron and Ion Processes**

  Ionization.

Among the above processes Photoelectric effect is of prime importance for the present simulation which should be used in the physics processes.

- Event Generator:

  The G4PrimaryParticle class represents a primary particle with which Geant 4.7 starts simulating an event. This class object has information on the particle type and its three momenta. The positional and time information of primary particle is stored in the G4PrimaryVertex class object and, thus this class object can have one or more G4PrimaryParticle class objects which share the same vertex. Further details are available in Software Reference Manual.

  In this section X-ray photons of the range of 2 KeV to 10 KeV are generated for our simulation.

- Event Action:

  In this section Geant detects the photon matter interaction (photoelectric effect) and writes the values of the energy and the interaction depth of the cell in a file. The file in which this data is written is named as **raw.dat**. Further calculations and refinement of this data are done using a **C** code named **util.c** and the different output files are named as follows:

  ThetaX*(0-11)*_Energy*(2-10)*.dat which is a replica of **raw.dat**.

  ThetaX*(0-11)*_Energy*2-10*_col.dat which consists of three columns: sub-cell number, the number of photons deposited and the interaction-depth in mm. At the end, the values of the number of photons detected in the full cell, the centroid of the detector and the standard deviation are also written as comment-lines.

  ThetaX*(0-11)*_Energy*(2-10)*_logmat.dat is a matrix of 80×100 in the log scale where 80 rows represent the number of sub-cells and 100 columns represent energy-bins in the range 0.1-10 KeV. The elements of the matrix represent the number of photons detected. This data is required to produce the 3-D graph of number of photons as a function of the energy deposited and the sub-cell at which the interaction took place.

  ThetaX*(0-11)*_Energy*(2-10)*_mat.dat is similar to the previous one but it is without log scale.

Chapter 3

DETECTOR GAS

A multi-wire Proportional counter is a type of gas-filled detector which is always operated in pulse mode and rely on the phenomenon of *gas multiplication* to amplify the charge represented by the original ion-pairs created within the gas. Pulses are therefore considerably larger than those from ion chambers used under the same conditions, and proportional counters can be applied to situations in which the number of ion pairs generated by the radiation is too small to permit satisfactory operation in pulse type ion chambers. One important application of proportional counters has therefore been in the detection, spectroscopy and imaging of low energy X-ray photon sources.

3.1 Design of Detector Gas Mixture

While designing the Detector Gas Mixture for multi-wire proportional counters, the high efficiency of the detector should be of higher priority. Mostly a mono-atomic gas operated at high values satisfy this condition. But in such cases spurious pulses and photon induced effects arise which increases the possible dead time and spoil the position resolution in multi-wire proportional counters. To overcome this hurdle a fraction of polyatomic stabilizing additive is mixed with detector gas which is known as quench gas. In our case we use a mixture of xenon and P10 gas (P10 is a mixture of Argon and methane in 90% and 10% ratio by volume). The pressure at which the detector was proposed to operate is 800 torr and the density of the gas mixture which is calculated to be 2.574075 mg/cc (calculations are present in the coming section) and the temperature at which the detector will operate is around the standard temperature. The ef-

ficiency curve for normal incidence and normal incidence - each incident angle are as shown in the figures 3.1 and 3.2. There was hardly any change in efficiency that was found due to various incident angles. In the figure 3.2 the different lines represents the ratio between normal incidence and the angles at which the photons are incident on the detector.

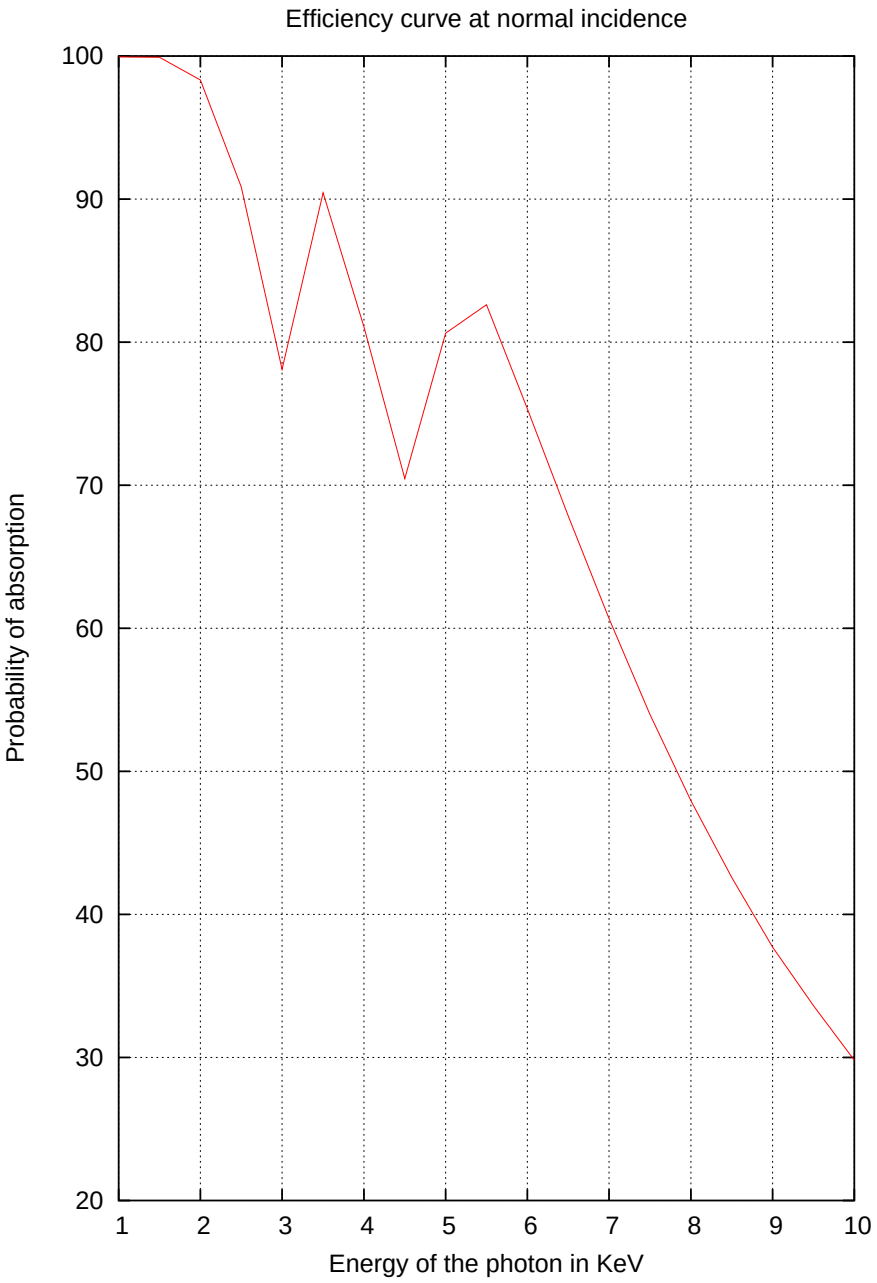

Figure 3.1: Efficiency curve of Detector Gas mixture at normal incidence.

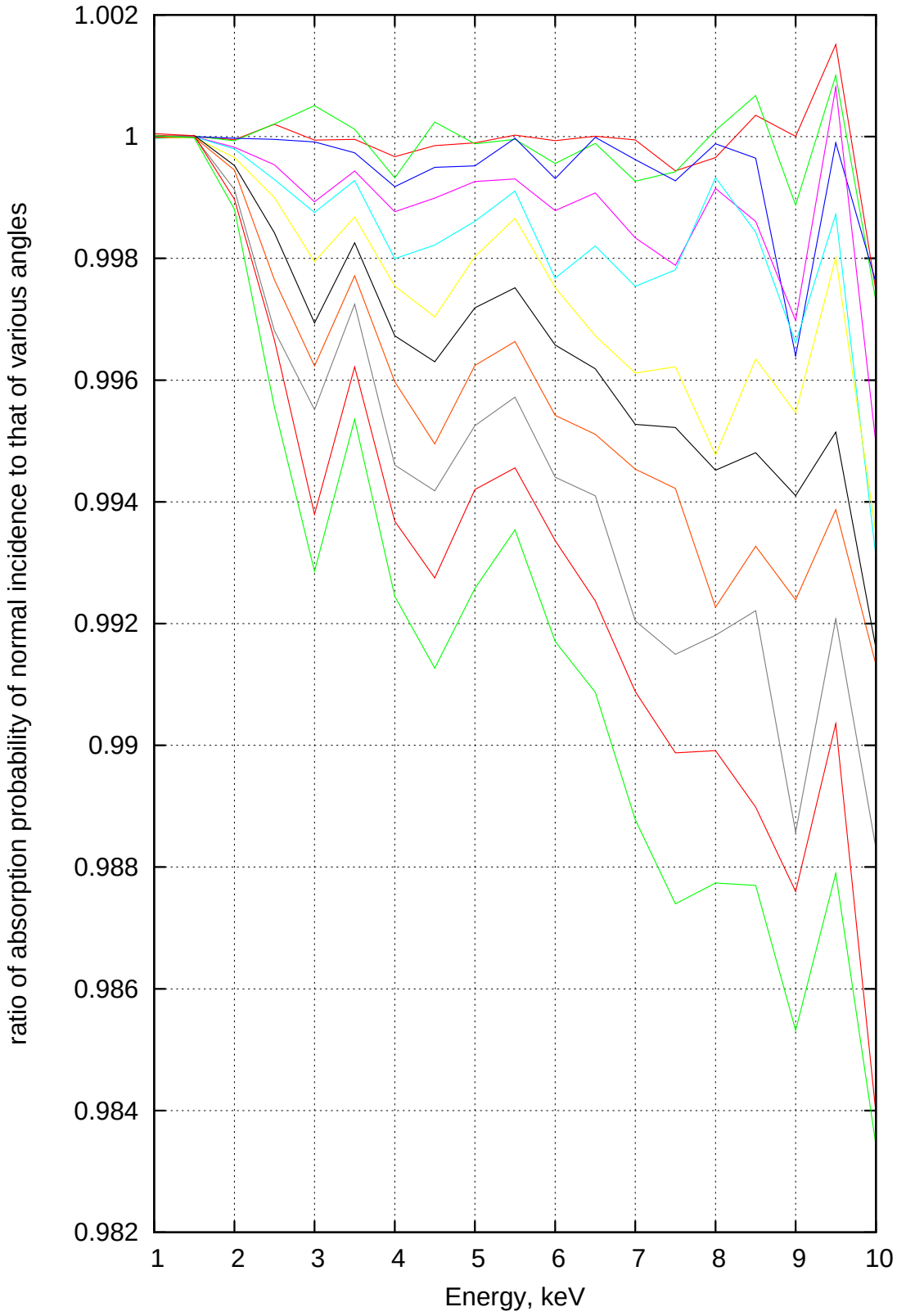

Figure 3.2: Ratio of Efficiency curves for X-ray photons at normal incidence to that of incident angles from 1° to 11°. The first curve belongs to 1° and it continues downward till 11°.

3.2 Gas Mixture and Related Calculations:

The gas mixture that was proposed for Scanning Sky Monitor (SSM) was 25%Xe and 75%P10 gas which has to modelled in Geant code where each element has to be defined with its atomic number, temperature and pressure at which it is operating and density of the element.

As we know P10 gas which is a mixture of 90%Ar and 10%CH_4. Therefore, the detector gas mixture that is proposed has

25%Xe + 67.5%Ar + 7.5%CH_4

This ratio is by volume and Geant code takes the mass fraction not volume fraction as such, so the following calculation were put to use for achieving the mass fraction of each element in the given composition. The calculations are in the following way.

Density of Xe at STP $\longrightarrow$ 5.541mg/cm^3

Density of Ar at STP $\longrightarrow$ 1.686mg/cm^3

Density of CH_4 at STP $\longrightarrow$ 0.677mg/cm^3

Molecular weight of Xe $\longrightarrow$ 131.3gm/mole

Molecular weight of Ar $\longrightarrow$ 39.948gm/mole

Molecular weight of CH_4 $\longrightarrow$ 0.667gm/mole

The volume of the cell is 8.64*ml* and the volume occupied by Xe, Ar and CH_4 are

V_{Xe} = 25%ofXe $\longrightarrow$ 2.16ml

$V_{Ar} = 67.5\% of Ar \longrightarrow 5.832\text{ml}$

$V_{CH_4} = 7.5\% of CH_4 \longrightarrow 0.648\text{ml}$

at pressure of 1.0526 atm (800 torr).

Ideal Gas Formula.

$\text{PV} = \text{nRT} \Longrightarrow \text{n} = \frac{\text{PV}}{\text{RT}}$

Notation Used

fractional $\text{n} = \text{n}_{\text{xxx}}$ for a given volume.

$\text{n}_{\text{Xe}} = \frac{\text{PV}_{\text{Xe}}}{\text{RT}} = \frac{1.05236\text{atm} \times 2.16\text{ml}}{\text{R} \times 300\text{Kelvin}}$

$\text{n}_{\text{Xe}} = \frac{\text{PV}_{\text{Ar}}}{\text{RT}} = \frac{1.05236\text{atm} \times 5.832\text{ml}}{\text{R} \times 300\text{Kelvin}}$

$\text{n}_{\text{Xe}} = \frac{\text{PV}_{\text{CH}_4}}{\text{RT}} = \frac{1.05236\text{atm} \times 0.648\text{ml}}{\text{R} \times 300\text{Kelvin}}$

3.2.1 Density of the gas mixture

The density of the gas mixture is given by the following formula:

$\text{Density} = \rho = \frac{\text{m}}{\text{V}} = \frac{\text{Mass}}{\text{Volume}} = \frac{\text{molarmass} \times \text{no.ofatoms/Na}}{\text{Volume}}$

where the total density of a gas mixture is given by

$\rho_{\text{Total}} = \frac{(\rho_1 \text{V}_1 + \rho_2 \text{V}_2 + ...)}{\text{V}_1 + \text{V}_2 + ...}$

And the total density of the gas mixture in the detector is given by

$$\rho_{\text{Detector}} = \frac{\rho_{Xe}V_{Xe}+\rho_{Ar}V_{Ar}+\rho_{CH_4}V_{CH_4}}{V_{Ar}+V_{Xe}+V_{CH_4}}$$

3.2.2 Partial Densities

The partial densities of each of the element present in the mixture of gas are given as follows:

$$\rho_{Xe} = \frac{\text{molarmass}\times\text{no.ofatoms/Na}}{\text{Volume}} = 1.38523\text{mg/cc}$$

where $n_{Xe} = \text{numberofatoms/Na}$

Similarly

$$\rho_{Ar} = 0.480265241\text{mg/cc}$$

And

$$\rho_{CH_4} = 0.02142741325\text{mg/cc}$$

$$\text{mass} = \text{molarmass} \times (\text{No.ofatoms/Na})$$

$$m_{total} = m_{Xe} + m_{Ar} + m_{CH_4}$$

$$m_{Xe}\% = 53.81544827\%$$

$$m_{Ar}\% = 44.2199848\%$$

$$m_{CH_4}\% = 1.972553247\%$$

and $m_C\% = 1.479191493\%$

$m_H\% = 0.495627762\%$

So, the mass fraction of each element in the detector gas mixture is

Mass fraction of Xenon gas is 53.81544827%

Mass fraction of Argon gas is 44.2199848%

Mass fraction of Methane gas is 1.972553247%

These three mass fractions have to be given as input to Geant code in the Detector Construction section.

Chapter 4

STUDY OF SLANT RAY BLUR

Slant ray blur is a problem related to the position sensing of the absorbed X-ray photon when it is incident at an angle on the multi-wire proportional counter. Since the detector is collimated as shown in the figure 1.1, so the incident angle along the x-axis which results in blurring the image is reduced to $\pm 11.3099^{o}$. If the incident ray is normal to the detector then there is no blur as the possibility of the photon getting absorbed at any depth is not going to matter at what position of the wire the electrons are going to be absorbed. The position sensitiveness of the wire is 1mm and at any angle between the $\pm 11.3099^{o}$ the possibility of the photon getting absorbed in the cell results in finding its position more than 1mm on the position sensitive wire results blurring of the image. For visualization we can refer the figure below. In the below figure the up and down arrows show the range in which the probability of finding the photon on the position sensitive wire.

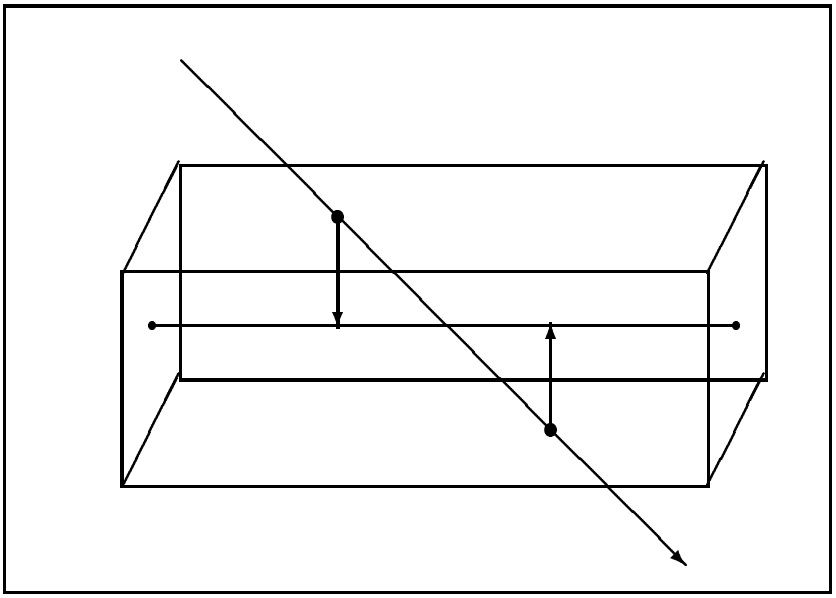

Now, finding the maximum probability at which the incident photon of a specific energy and angle can get absorbed is by calculating the Centroid of the curve. The equation for finding the centroid of the curve is

$$\text{Centroid} = \frac{\sum_{i=1}^{80} n_i x_i}{\sum_{i=1}^{80} x_i} \tag{4.1}$$

And the Standard Deviation of the curve is given as

$$\text{StandardDeviation(SD)} = \frac{\sum_{i=1}^{80} n_i (x_i - \overline{x})^2}{\sum_{i=1}^{80} n_i} \tag{4.2}$$

The *tables no.4.1 to no.4.20* and *figures 4.1(a,b,c,d) to 4.62(a)* give the information of centroid, standard deviation and the efficiency of absorption of photons for various incident angles at certain energies.

E (KeV)	*θ (deg)*	*CENTROID (mm)*	*σ (mm)*	*η (%)*
1	0	0	0	99.9322
1	1	0.0087	0.01001	99.9307
1	2	0.0175	0.02003	99.9324
1	3	0.0263	0.03004	99.9314
1	4	0.0351	0.04014	99.9342
1	5	0.0439	0.05011	99.9356
1	6	0.0526	0.06016	99.9344
1	7	0.0614	0.07010	99.9323
1	8	0.0701	0.08011	99.9340
1	9	0.0789	0.09015	99.9313
1	10	0.0875	0.10000	99.9274
1	11	0.0961	0.10987	99.9305
1	11.3099	0.0988	0.11290	99.9279

Table 4.1: 1 KeV source incident at various angles.

E (KeV)	*θ (deg)*	*CENTROID (mm)*	*σ (mm)*	*η (%)*
1.5	0	0	0	99.9134
1.5	1	0.0243	0.02544	99.9134
1.5	2	0.0508	0.0486	99.9123
1.5	3	0.0730	0.07639	99.9132
1.5	4	0.0974	0.10182	99.9134
1.5	5	0.1217	0.12734	99.9137
1.5	6	0.1458	0.15262	99.9152
1.5	7	0.1703	0.17817	99.9114
1.5	8	0.1945	0.20350	99.9142
1.5	9	0.2185	0.22856	99.9134
1.5	10	0.2428	0.25431	99.9118
1.5	11	0.2667	0.27953	99.9156
1.5	11.3099	0.2738	0328689	99.9159

Table 4.2: 1.5 KeV source incident at various angles.

E (KeV)	*θ (deg)*	*CENTROID (mm)*	*σ (mm)*	*η (%)*
2	0	0	0	98.3267
2	1	0.0458	0.0427	98.3316
2	2	0.0917	0.0856	98.3336
2	3	0.1374	0.1282	98.3292
2	4	0.1834	0.1713	98.3438
2	5	0.2293	0.2143	98.3467
2	6	0.2756	0.2577	98.3604
2	7	0.3210	0.3003	98.3734
2	8	0.3668	0.3434	98.380
2	9	0.3866	0.3866	98.4123
2	10	0.4588	0.4300	98.4280
2	11	0.5039	0.4728	98.4439
2	11.3099	0.5182	0.4858	98.4510

Table 4.3: 2 KeV source incident at various angles.

E (KeV)	*θ (deg)*	*CENTROID (mm)*	*σ (mm)*	*η (%)*
2.5	0	0	0	90.8605
2.5	1	0.0648	0.0527	90.8419
2.5	2	0.1295	0.1054	90.8414
2.5	3	0.1943	0.1582	90.8646
2.5	4	0.2597	0.2114	90.9025
2.5	5	0.3245	0.2643	90.9245
2.5	6	0.3903	0.3178	90.9515
2.5	7	0.4552	0.3709	90.0042
2.5	8	0.5204	0.4244	91.0746
2.5	9	0.5862	0.4787	91.1511
2.5	10	0.6518	0.5323	91.1648
2.5	11	0.7176	0.5860	91.2661
2.5	11.3099	0.7377	0.6027	91.2834

Table 4.4: 2.5 KeV source incident at various angles.

E (KeV)	*θ (deg)*	*CENTROID (mm)*	*σ (mm)*	*η (%)*
3	0	0	0	78.0976
3	1	0.0774	0.0569	78.1020
3	2	0.1550	0.1138	78.0578
3	3	0.2326	0.1708	78.1044
3	4	0.3109	0.2283	78.1812
3	5	0.3884	0.2855	78.1951
3	6	0.4673	0.3434	78.2584
3	7	0.5457	0.4010	78.3373
3	8	0.6242	0.4589	78.3929
3	9	0.7026	0.5171	78.4494
3	10	0.7820	0.5758	78.5852
3	11	0.8606	0.6344	78.6594
3	11.3099	0.8857	0.6527	78.6999

Table 4.5: 3 KeV source incident at various angles.

E (KeV)	*θ (deg)*	*CENTROID (mm)*	*σ (mm)*	*η (%)*
3.5	0	0	0	90.4398
3.5	1	0.0656	0.0530	90.4439
3.5	2	0.1309	0.1059	90.4287
3.5	3	0.1961	0.1588	90.4639
3.5	4	0.2623	0.2124	90.4908
3.5	5	0.3281	0.2658	90.5051
3.5	6	0.3940	0.3194	90.5594
3.5	7	0.4598	0.3728	90.5979
3.5	8	0.5258	0.4267	90.6471
3.5	9	0.5914	0.4802	90.6894
3.5	10	0.6580	0.5347	90.7832
3.5	11	0.7238	0.5889	90.8618
3.5	11.3099	0.7446	0.6055	90.8596

Table 4.6: 3.5 KeV source incident at various angles.

E (KeV)	*θ (deg)*	*CENTROID (mm)*	*σ (mm)*	*η (%)*
4	0	0	0	81.0685
4	1	0.0753	0.0563	81.0952
4	2	0.1507	0.1126	81.1234
4	3	0.2260	0.1691	81.1352
4	4	0.3019	0.2258	81.1686
4	5	0.3776	0.2825	81.2313
4	6	0.4536	0.3396	81.2680
4	7	0.5297	0.3966	81.3346
4	8	0.6056	0.4539	81.3963
4	9	0.6813	0.5115	81.5083
4	10	0.7584	0.5695	81.5840
4	11	0.8362	0.6278	81.6854
4	11.3099	0.8591	0.6456	81.6926

Table 4.7: 4 KeV source incident at various angles.

E (KeV)	*θ (deg)*	*CENTROID (mm)*	*σ (mm)*	*η (%)*
4.5	0	0	0	70.4628
4.5	1	0.0822	0.0580	70.4733
4.5	2	0.1647	0.1161	70.4459
4.5	3	0.2469	0.1741	70.4983
4.5	4	0.3300	0.2325	70.5340
4.5	5	0.4127	0.2910	70.5886
4.5	6	0.4959	0.3499	70.6721
4.5	7	0.5782	0.4083	70.7243
4.5	8	0.6620	0.4677	70.8203
4.5	9	0.7457	0.5268	70.8752
4.5	10	0.8300	0.5869	70.9773
4.5	11	0.9148	0.6467	71.0836
4.5	11.3099	0.9401	0.6651	71.1873

Table 4.8: 4.5 KeV source incident at various angles.

E (KeV)	*θ (deg)*	*CENTROID (mm)*	*σ (mm)*	*η (%)*
5	0	0	0	80.6273
5	1	0.0757	0.0564	80.6356
5	2	0.1514	0.1128	80.6367
5	3	0.2269	0.1693	80.6661
5	4	0.3033	0.2264	80.6868
5	5	0.3794	0.2830	80.7396
5	6	0.4562	0.3405	80.7865
5	7	0.5323	0.3974	80.8546
5	8	0.6086	0.4549	80.9316
5	9	0.6855	0.5124	80.0120
5	10	0.7626	0.5707	81.0976
5	11	0.8396	0.6285	81.2302
5	11.3099	0.8636	0.6466	81.2379

Table 4.9: 5 KeV source incident at various angles.

E (KeV)	*θ (deg)*	*CENTROID (mm)*	*σ (mm)*	*η (%)*
5.5	0	0	0	82.6224
5.5	1	0.0740	0.0559	82.6203
5.5	2	0.1481	0.1120	82.6262
5.5	3	0.2220	0.1678	82.6245
5.5	4	0.2968	0.2245	82.6798
5.5	5	0.3709	0.2807	82.6965
5.5	6	0.4461	0.3377	82.7334
5.5	7	0.5205	0.3940	82.8281
5.5	8	0.5955	0.4510	82.9015
5.5	9	0.6702	0.5081	82.9775
5.5	10	0.7460	0.5659	82.0744
5.5	11	0.8207	0.6231	83.1596
5.5	11.3099	0.8442	0.6408	83.1880

Table 4.10: 5.5 KeV source incident at various angles.

E (KeV)	*θ (deg)*	*CENTROID (mm)*	*σ (mm)*	*η (%)*
5.96	0	0	0	75.9329
5.96	1	0.0790	0.0573	75.9555
5.96	2	0.1582	0.1146	75.9626
5.96	3	0.2370	0.1720	75.9854
5.96	4	0.3169	0.2301	75.0348
5.96	5	0.3964	0.2877	76.0666
5.96	6	0.4763	0.3458	76.1235
5.96	7	0.5558	0.4035	76.2002
5.96	8	0.6363	0.4622	76.2415
5.96	9	0.7162	0.5206	76.3755
5.96	10	0.7971	0.5798	76.4705
5.96	11	0.8779	0.6388	76.5626
5.96	11.3099	0.9033	0.6573	76.6008

Table 4.11: 5.96 KeV source incident at various angles.

E (KeV)	*θ (deg)*	*CENTROID (mm)*	*σ (mm)*	*η (%)*
6	0	0	0	75.3417
6	1	0.0794	0.0574	75.3467
6	2	0.1589	0.1148	75.3749
6	3	0.2383	0.1722	75.3936
6	4	0.3185	0.2302	75.4334
6	5	0.3985	0.2881	75.5172
6	6	0.4789	0.3465	75.5289
6	7	0.5588	0.4043	75.6005
6	8	0.6392	0.4628	75.6883
6	9	0.7191	0.5215	75.7657
6	10	0.8009	0.5808	75.8449
6	11	0.8827	0.6402	75.9717
6	11.3099	0.9078	0.6587	75.9947

Table 4.12: 6 KeV source incident at various angles.

E (KeV)	*θ (deg)*	*CENTROID (mm)*	*σ (mm)*	*η (%)*
6.5	0	0	0	67.8555
6.5	1	0.0835	0.0583	67.8551
6.5	2	0.1672	0.1166	67.8630
6.5	3	0.2509	0.1750	67.8563
6.5	4	0.3355	0.2339	67.9183
6.5	5	0.4190	0.2924	67.9776
6.5	6	0.5039	0.3516	68.0782
6.5	7	0.5880	0.4107	68.1153
6.5	8	0.6728	0.4702	68.1890
6.5	9	0.7581	0.5300	68.2582
6.5	10	0.8436	0.5901	68.3771
6.5	11	0.9295	0.6503	68.4806
6.5	11.3099	0.9557	0.6690	68.5230

Table 4.13: 6.5 KeV source incident at various angles.

E (KeV)	*θ (deg)*	*CENTROID (mm)*	*σ (mm)*	*η (%)*
7	0	0	0	60.6836
7	1	0.0870	0.0589	60.6869
7	2	0.1740	0.1179	60.7280
7	3	0.2610	0.1768	60.7066
7	4	0.3490	0.2364	60.7847
7	5	0.4362	0.2959	60.8331
7	6	0.5245	0.3556	60.9202
7	7	0.6120	0.4153	60.9719
7	8	0.7005	0.4753	61.0168
7	9	0.7890	0.5357	61.1702
7	10	0.8789	0.5964	61.2419
7	11	0.9678	0.6573	61.3723
7	11.3099	0.9951	0.6763	61.4183

Table 4.14: 7 KeV source incident at various angles.

E (KeV)	*θ (deg)*	*CENTROID (mm)*	*σ (mm)*	*η (%)*
7.5	0	0	0	53.9895
7.5	1	0.0895	0.0593	54.0198
7.5	2	0.1792	0.1186	54.0207
7.5	3	0.2687	0.1779	54.0287
7.5	4	0.3590	0.2378	54.1039
7.5	5	0.4492	0.2976	54.1080
7.5	6	0.5402	0.3576	54.1944
7.5	7	0.6302	0.4180	54.2487
7.5	8	0.7220	0.4784	54.3034
7.5	9	0.8134	0.5393	54.4527
7.5	10	0.9058	0.6004	54.5416
7.5	11	0.9970	0.6613	54.6786
7.5	11.3099	1.0254	0.6805	54.6599

Table 4.15: 7.5 KeV source incident at various angles.

E (KeV)	*θ (deg)*	*CENTROID (mm)*	*σ (mm)*	*η (%)*
8	0	0	0	47.9503
8	1	0.0917	0.0595	47.9668
8	2	0.1833	0.1191	47.9453
8	3	0.2750	0.1787	47.9560
8	4	0.3679	0.2389	47.9912
8	5	0.4599	0.2988	47.9827
8	6	0.5531	0.3595	48.2023
8	7	0.6457	0.4194	48.2146
8	8	0.7384	0.4807	48.3239
8	9	0.8322	0.5417	48.3463
8	10	0.9263	0.6025	48.4389
8	11	1.0203	0.6642	48.5456
8	11.3099	1.0502	0.6837	48.6032

Table 4.16: 8 KeV source incident at various angles.

E (KeV)	*θ (deg)*	*CENTROID (mm)*	*σ (mm)*	*η (%)*
8.5	0	0	0	42.5755
8.5	1	0.0932	0.0597	42.5606
8.5	2	0.1866	0.1194	42.5468
8.5	3	0.2799	0.1791	42.5905
8.5	4	0.3743	0.2397	42.6349
8.5	5	0.4683	0.2996	42.6424
8.5	6	0.5626	0.3607	42.7316
8.5	7	0.6565	0.4205	42.7978
8.5	8	0.7519	0.4817	42.8640
8.5	9	0.8470	0.5426	42.9097
8.5	10	0.9433	0.6044	43.0497
8.5	11	1.0392	0.6663	43.1057
8.5	11.3099	1.0676	0.6852	43.1593

Table 4.17: 8.5 KeV source incident at various angles.

E (KeV)	*θ (deg)*	*CENTROID (mm)*	*σ (mm)*	*η (%)*
9	0	0	0	37.7087
9	1	0.0946	0.0598	37.7059
9	2	0.1890	0.1195	37.7511
9	3	0.2838	0.1793	37.8450
9	4	0.3789	0.2398	37.8230
9	5	0.4738	0.2997	37.8369
9	6	0.5698	0.3606	37.8806
9	7	0.6656	0.4212	37.9324
9	8	0.7620	0.4824	37.9979
9	9	0.8586	0.5435	38.1446
9	10	0.9563	0.6054	38.1822
9	11	1.0531	0.6666	38.2706
9	11.3099	1.0833	0.6865	38.3440

Table 4.18: 9 KeV source incident at various angles.

E (KeV)	*θ (deg)*	*CENTROID (mm)*	*σ (mm)*	*η (%)*
9.5	0	0	0	33.6210
9.5	1	0.0956	0.0597	33.5702
9.5	2	0.1912	0.1195	33.5873
9.5	3	0.2867	0.1795	33.6244
9.5	4	0.3831	0.2398	33.5936
9.5	5	0.4796	0.3004	33.6640
9.5	6	0.5770	0.3609	33.6879
9.5	7	0.6733	0.4215	33.7850
9.5	8	0.7707	0.4827	33.8283
9.5	9	0.8690	0.5443	33.8896
9.5	10	0.9670	0.6054	33.9484
9.5	11	1.0673	0.6675	33.0330
9.5	11.3099	1.0981	0.6869	34.1017

Table 4.19: 9.5 KeV source incident at various angles.

E (KeV)	*θ (deg)*	*CENTROID (mm)*	*σ (mm)*	*η (%)*
10	0	0	0	29.8092
10	1	0.0963	0.0598	29.8848
10	2	0.1928	0.1196	29.8900
10	3	0.2894	0.1794	29.8808
10	4	0.3866	0.2398	29.9604
10	5	0.4838	0.3001	30.0164
10	6	0.5828	0.3612	30.0051
10	7	0.6796	0.4213	30.0619
10	8	0.7781	0.4827	30.0700
10	9	0.8761	0.5433	30.1618
10	10	0.9750	0.6055	30.2951
10	11	1.0762	0.6674	30.3114
10	11.3099	1.1049	0.6869	30.3833

Table 4.20: 10 KeV source incident at various angles.

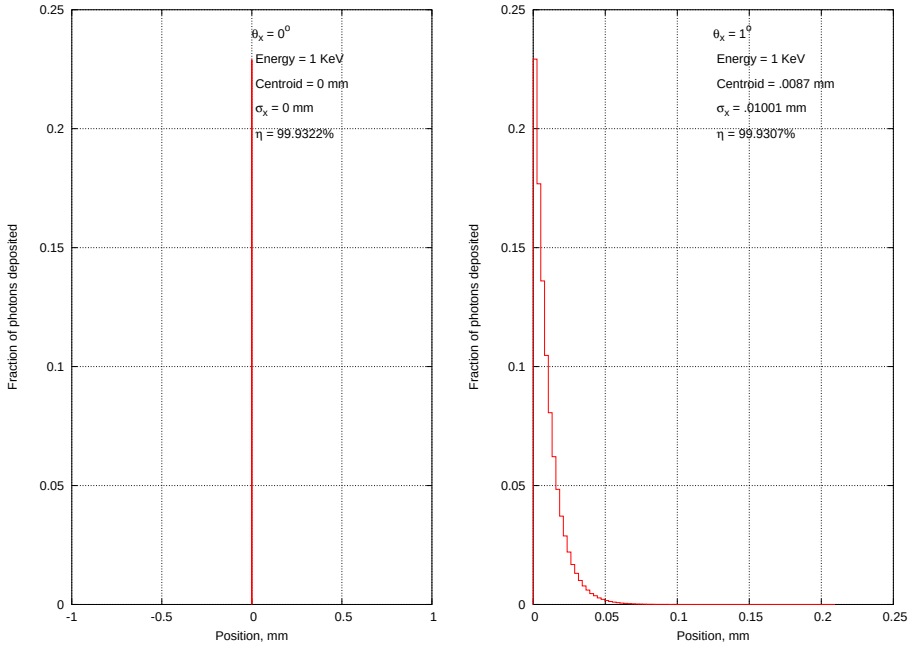

(a) 1 KeV X-ray photon incident at 0° (b) 1 KeV X-ray photon incident at 1°

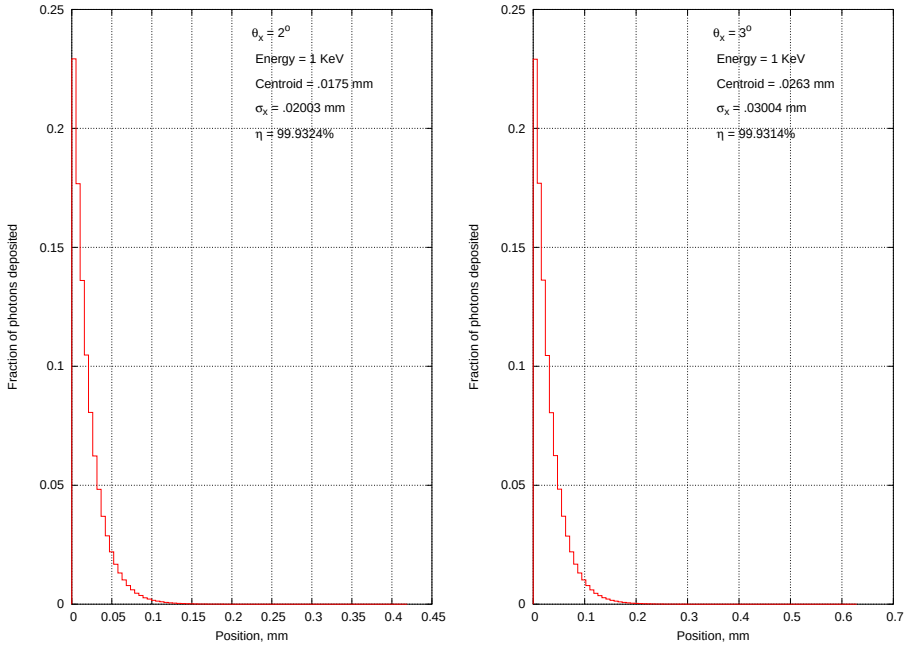

(c) 1 KeV X-ray photon incident at 2° (d) 1 KeV X-ray photon incident at 3°

Figure 4.1: Probability of absorption of 1 KeV photon when incident at 0°, 1°, 2° and 3°

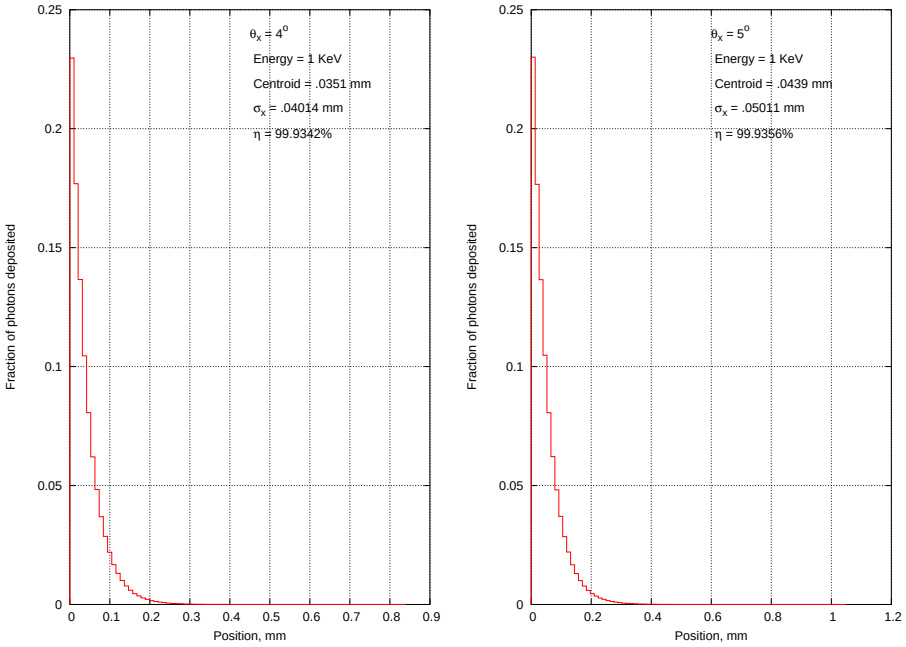

(a) 1 KeV X-ray photon incident at 4°

(b) 1 KeV X-ray photon incident at 5°

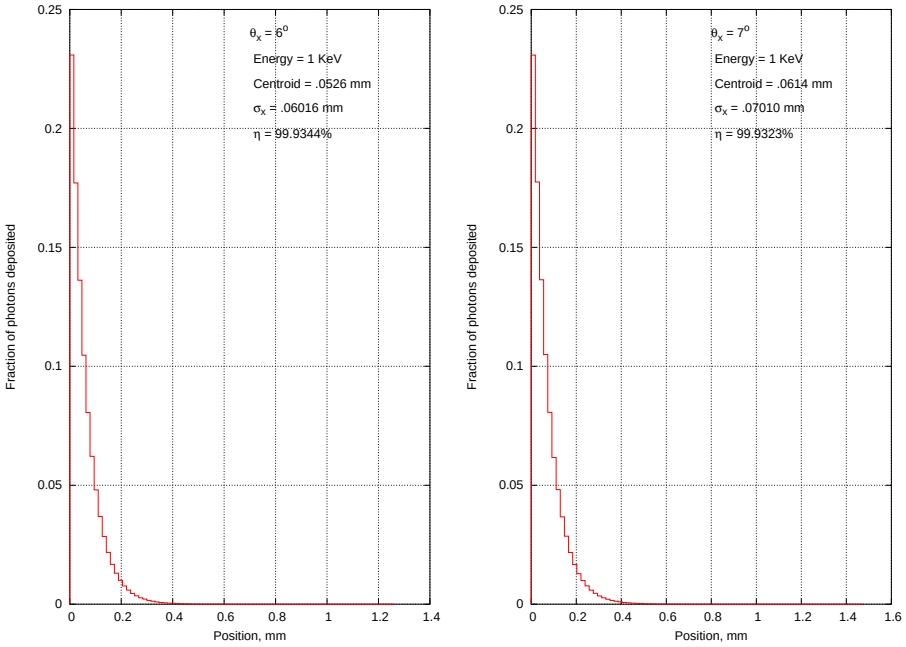

(c) 1 KeV X-ray photon incident at 6°

(d) 1 KeV X-ray photon incident at 7°

Figure 4.2: Probability of absorption of 1 KeV photon when incident at 4°, 5°, 6° and 7°

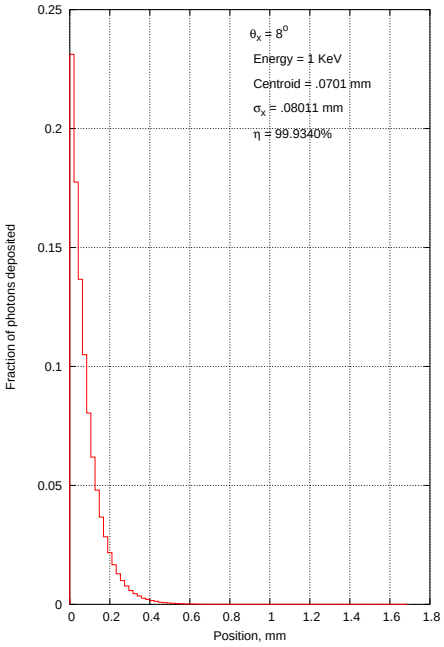

(a) 1 KeV X-ray photon incident at 8°

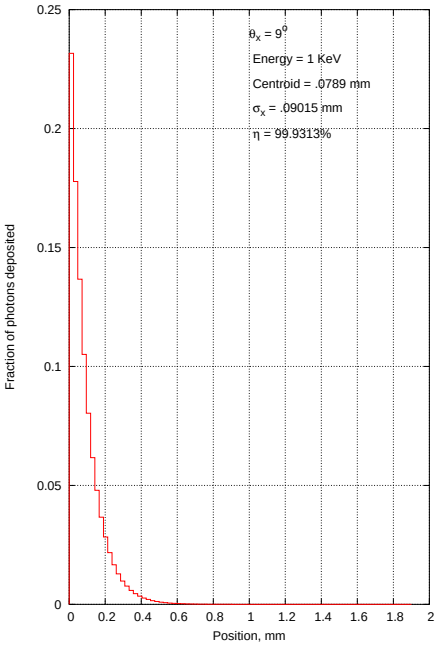

(b) 1 KeV X-ray photon incident at 9°

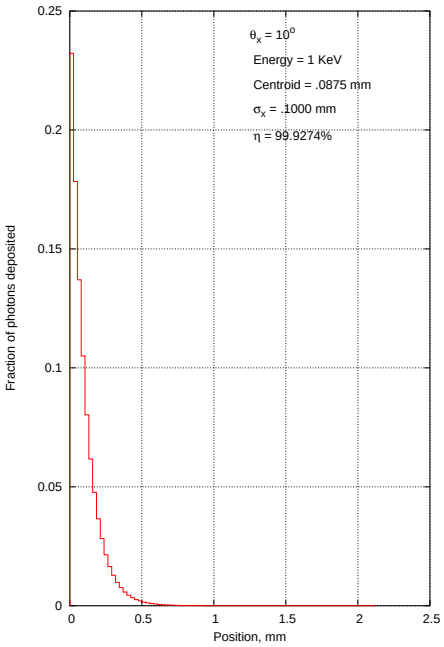

(c) 1 KeV X-ray photon incident at 10°

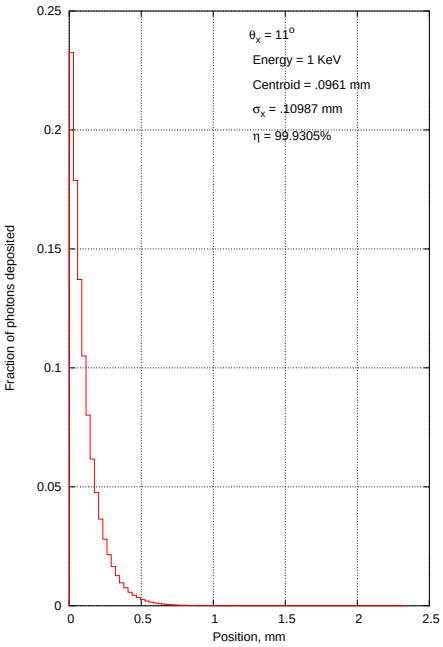

(d) 1 KeV X-ray photon incident at 11°

Figure 4.3: Probability of absorption of 1 KeV photon when incident at 8°, 9°, 10° and 11°

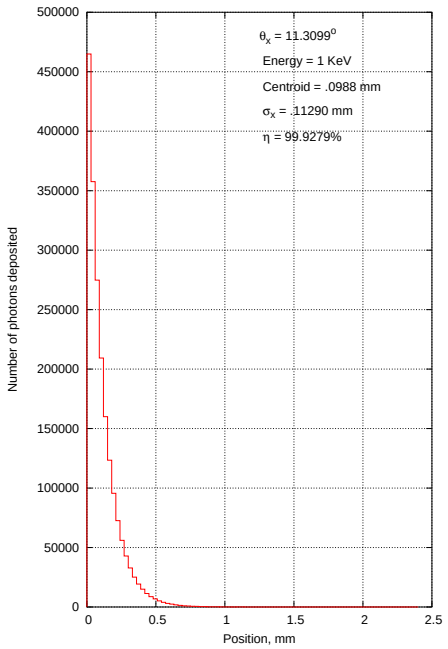

(a) 1 KeV X-ray photon incident at 11.3099°

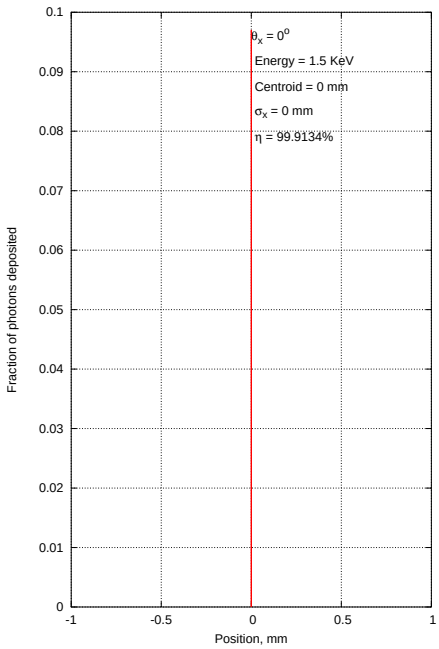

(b) 1.5 KeV X-ray photon incident at 0°

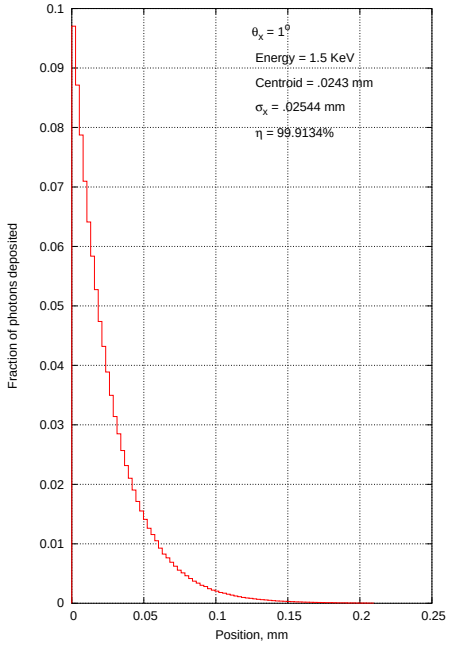

(c) 1.5 KeV X-ray photon incident at 1°

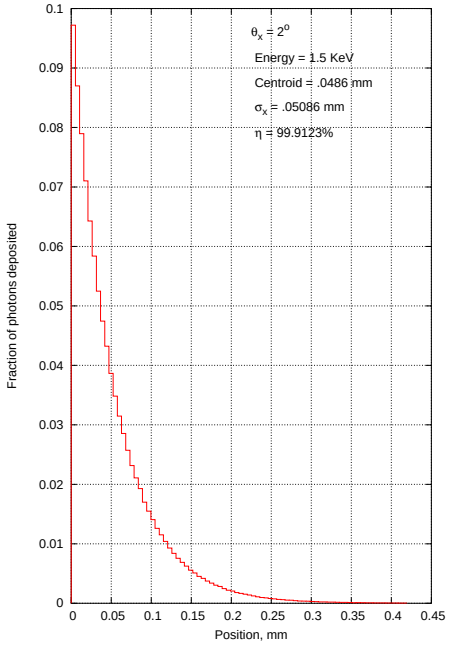

(d) 1.5 KeV X-ray photon incident at 2°

Figure 4.4: Probability of absorption of 1 KeV photon when incident at 11.3099° and 1.5 KeV at 0°, 1°, 2°

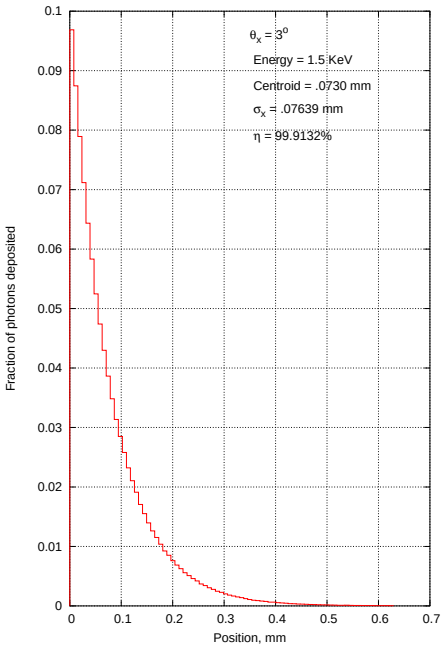

(a) 1.5 KeV X-ray photon incident at 3°

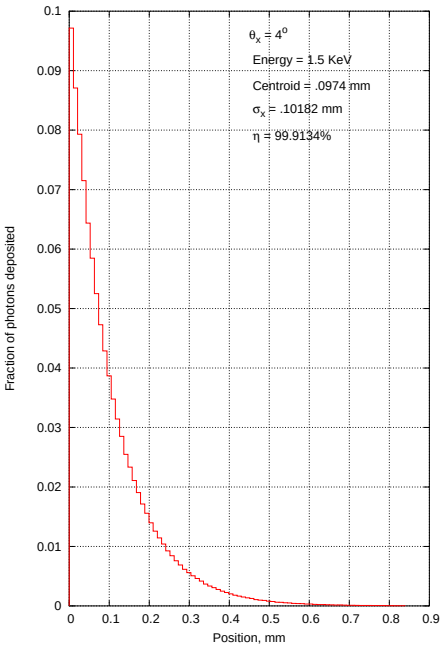

(b) 1.5 KeV X-ray photon incident at 4°

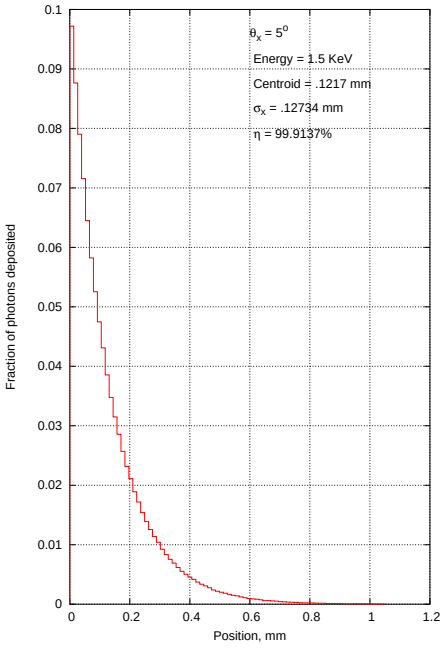

(c) 1.5 KeV X-ray photon incident at 5°

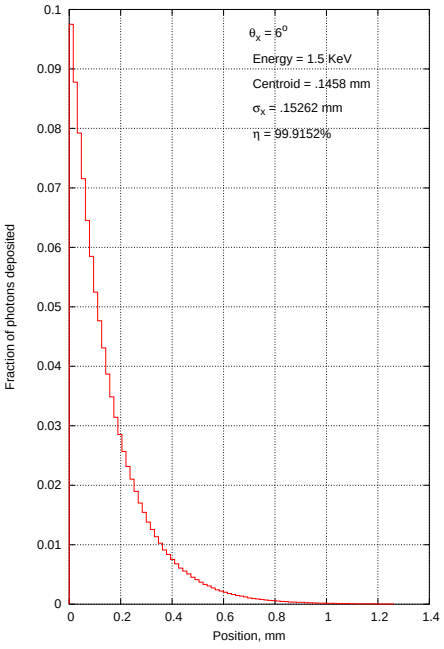

(d) 1.5 KeV X-ray photon incident at 6°

Figure 4.5: Probability of absorption of 1.5 KeV photon when incident at 3°, 4°, 5° and 6°

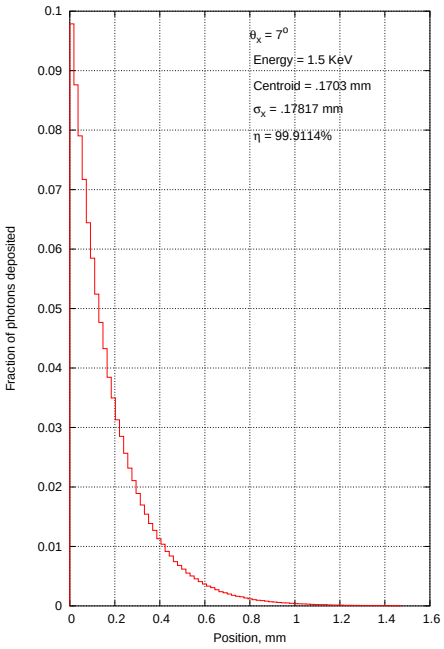

(a) 1.5 KeV X-ray photon incident at 7°

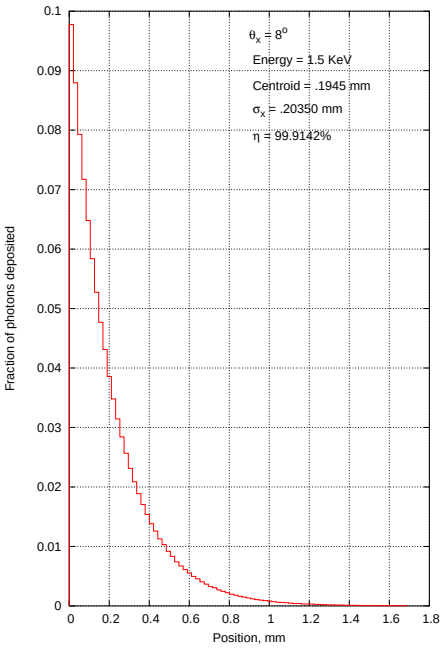

(b) 1.5 KeV X-ray photon incident at 8°

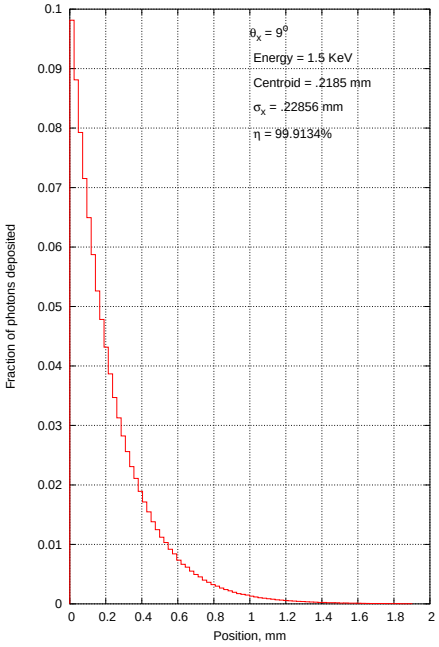

(c) 1.5 KeV X-ray photon incident at 9°

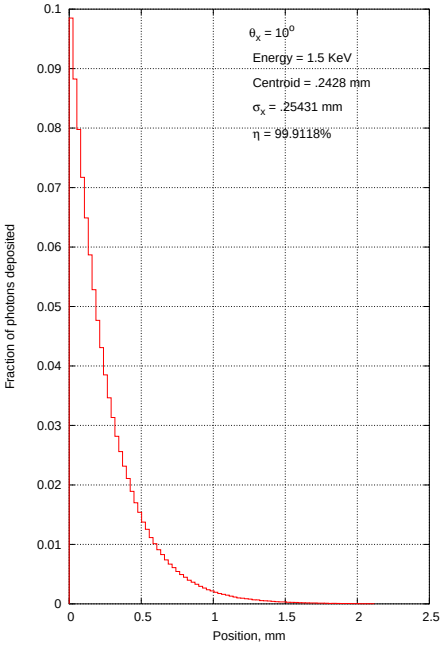

(d) 1.5 KeV X-ray photon incident at 10°

Figure 4.6: Probability of absorption of 1.5 KeV photon when incident at 7°, 8°, 9° and 10°

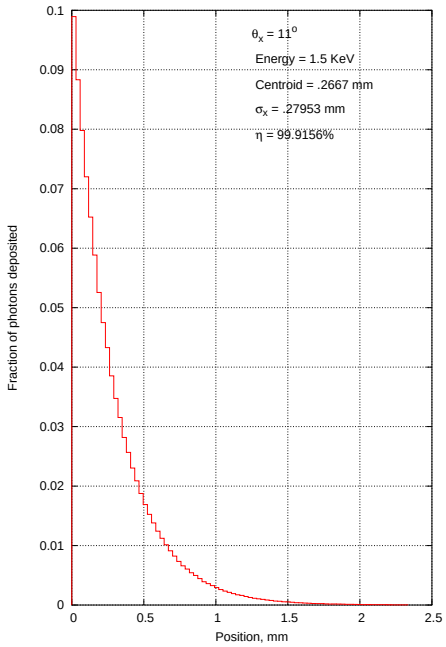

(a) 1.5 KeV X-ray photon incident at 11°

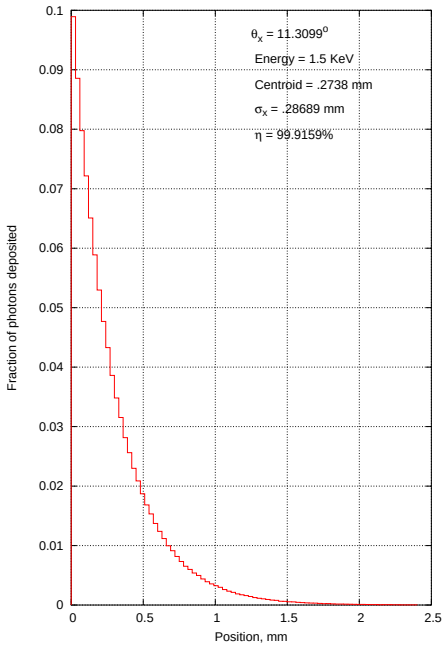

(b) 1.5 KeV X-ray photon incident at 11.3099°

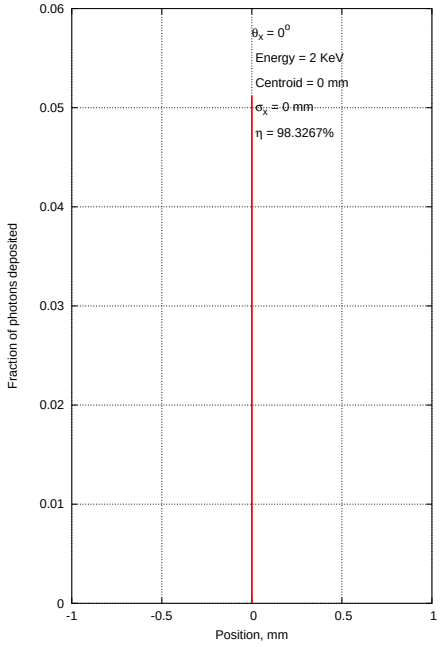

(c) 2 KeV X-ray photon incident at 0°

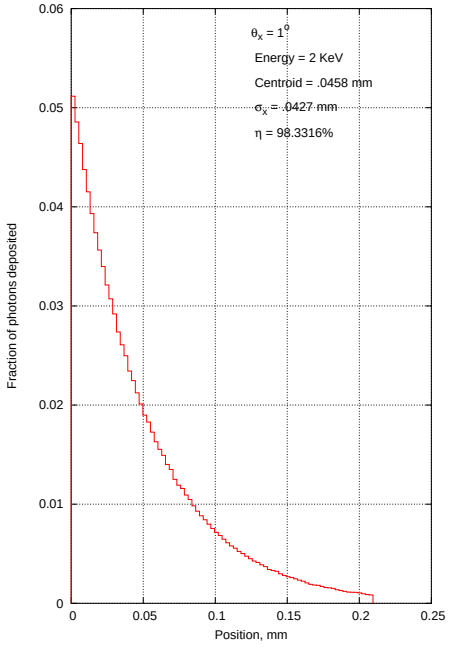

(d) 2 KeV X-ray photon incident at 1°

Figure 4.7: Probability of absorption of 1.5 KeV photon when incident at 11°, 11.3099° and 2 KeV at 0° and 1°

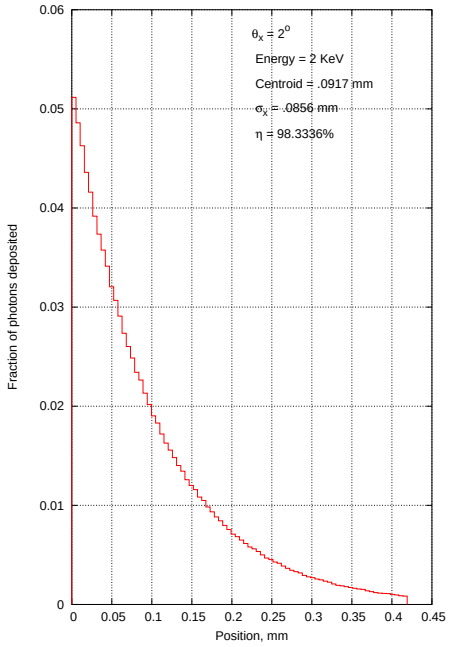

(a) 2 KeV X-ray photon incident at 2°

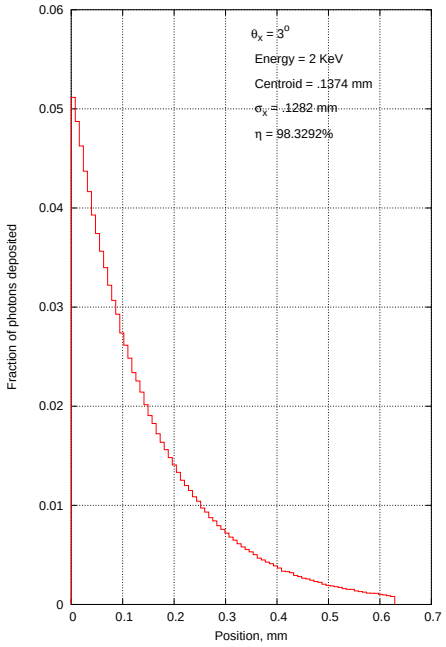

(b) 2 KeV X-ray photon incident at 3°

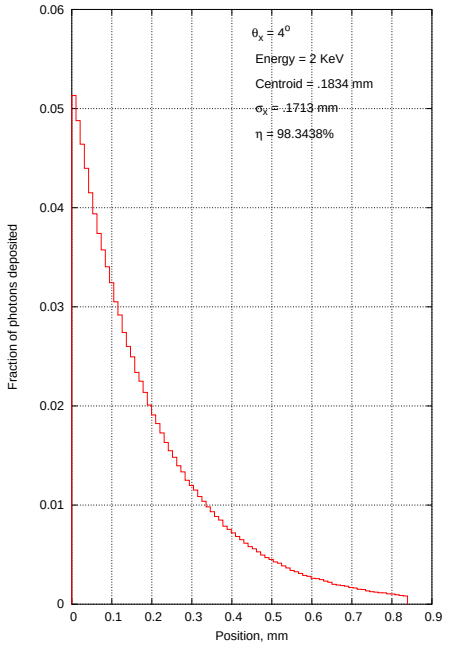

(c) 2 KeV X-ray photon incident at 4°

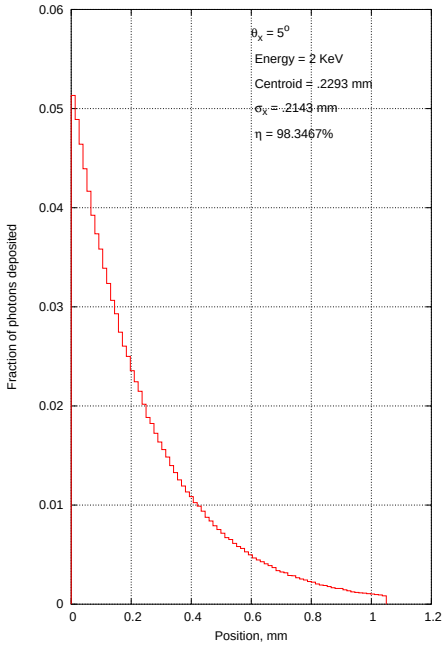

(d) 2 KeV X-ray photon incident at 5°

Figure 4.8: Probability of absorption of 2 KeV photon when incident at 2°, 3°, 4° and 5°

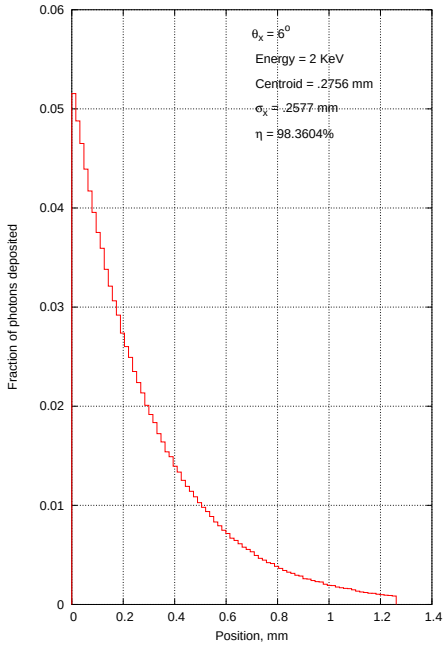

(a) 2 KeV X-ray photon incident at 6°

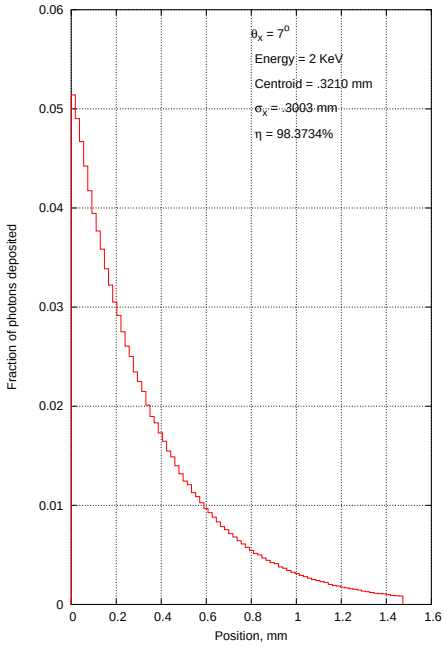

(b) 2 KeV X-ray photon incident at 7°

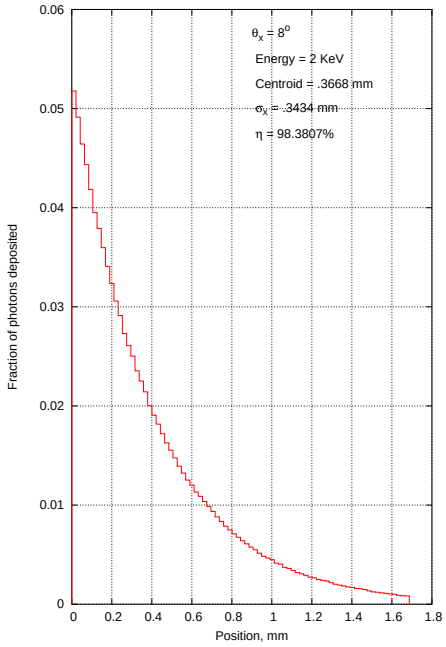

(c) 2 KeV X-ray photon incident at 8°

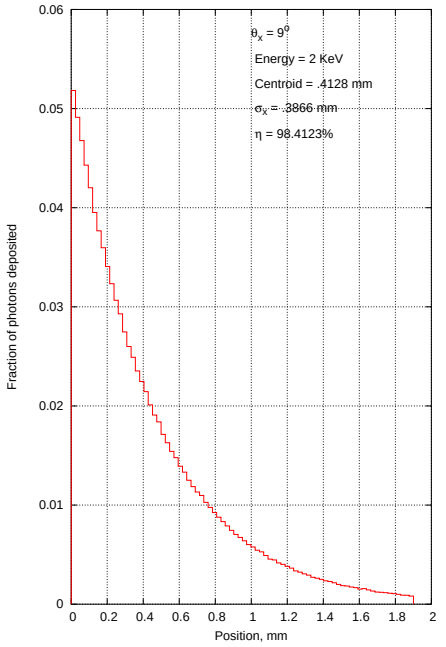

(d) 2 KeV X-ray photon incident at 9°

Figure 4.9: Probability of absorption of 2 KeV photon when incident at 6°, 7°, 8° and 9°

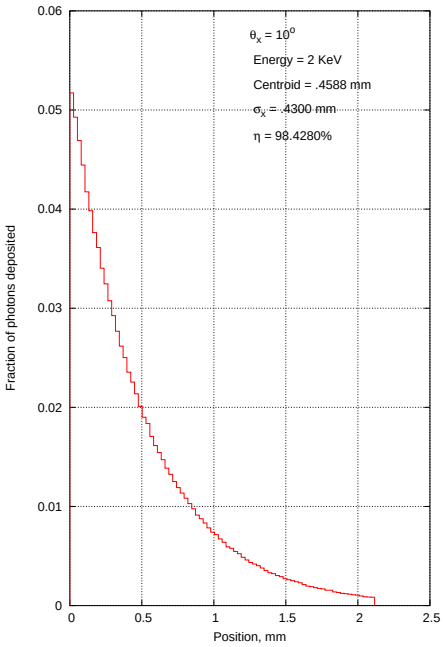

(a) 2 KeV X-ray photon incident at 10°

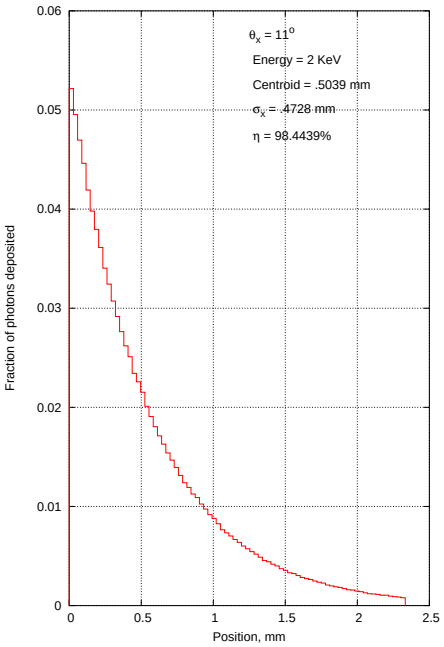

(b) 2 KeV X-ray photon incident at 11.3099°

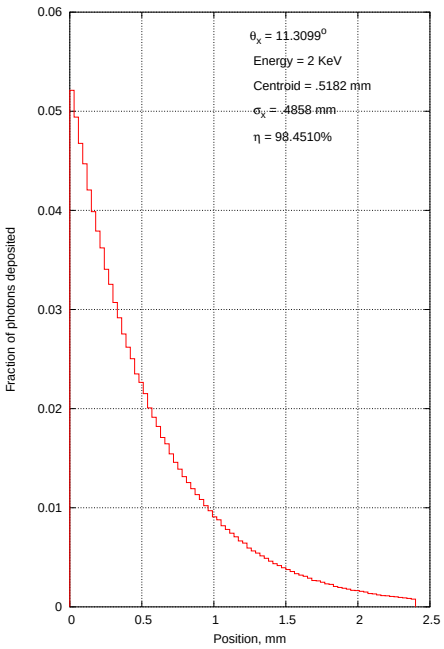

(c) 2 KeV X-ray photon incident at 11.3099°

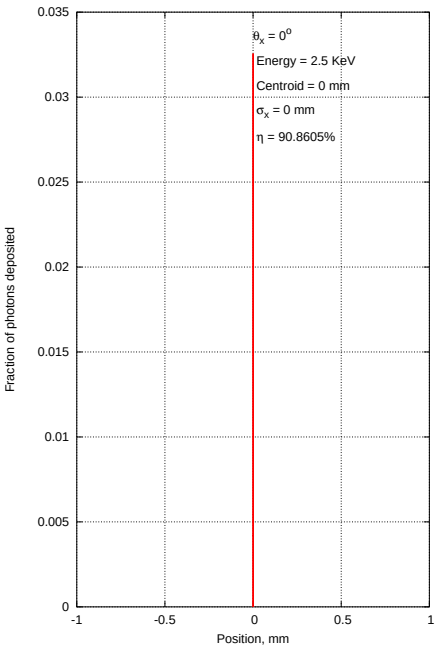

(d) 2.5 KeV X-ray photon incident at 0°

Figure 4.10: Probability of absorption of 2 KeV photon when incident at 10°, 11°, 11.3099° and 2.5 KeV at 0°

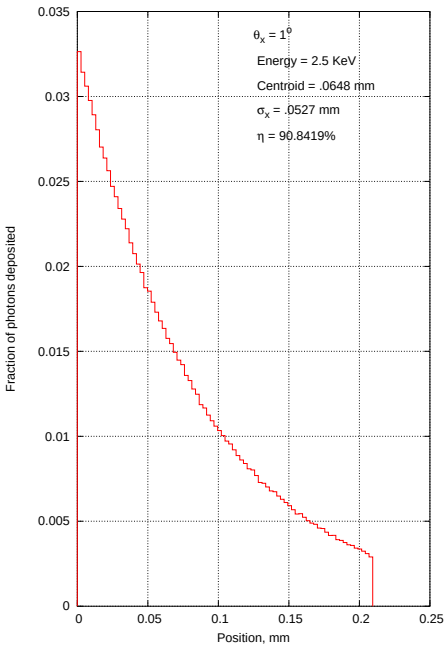

(a) 2.5 KeV X-ray photon incident at 1°

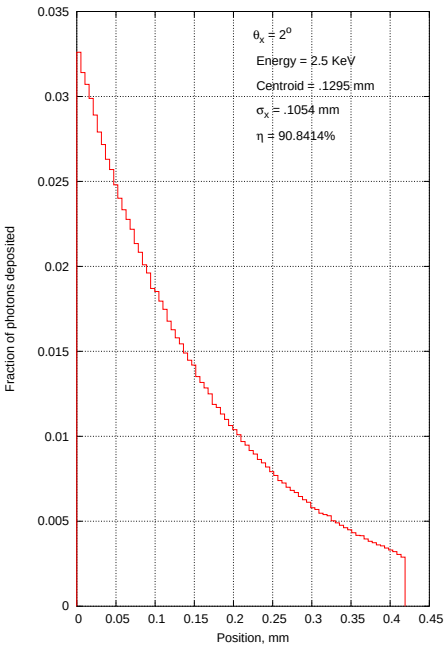

(b) 2.5 KeV X-ray photon incident at 2°

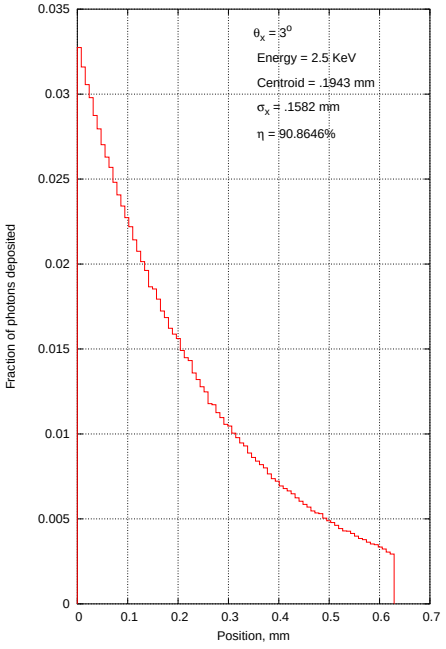

(c) 2.5 KeV X-ray photon incident at 3°

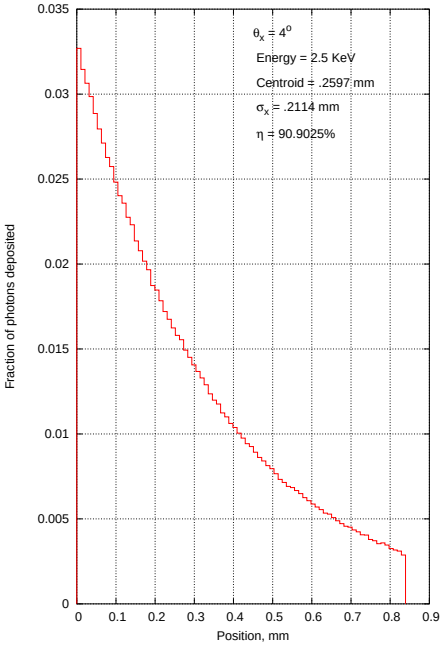

(d) 2.5 KeV X-ray photon incident at 4°

Figure 4.11: Probability of absorption of 2.5 KeV photon when incident at 1°, 2°, 3° and 4°

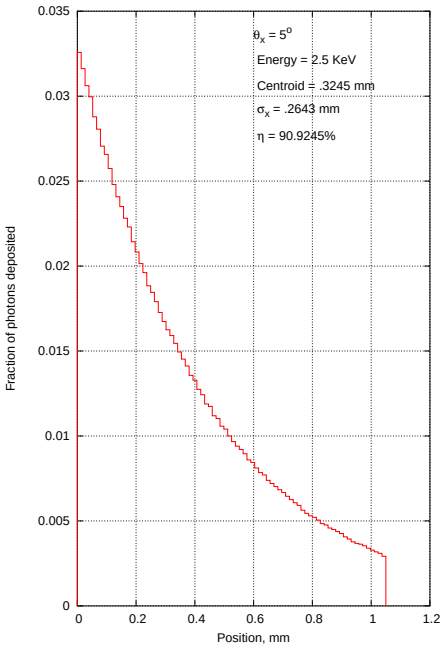

(a) 2.5 KeV X-ray photon incident at 5°

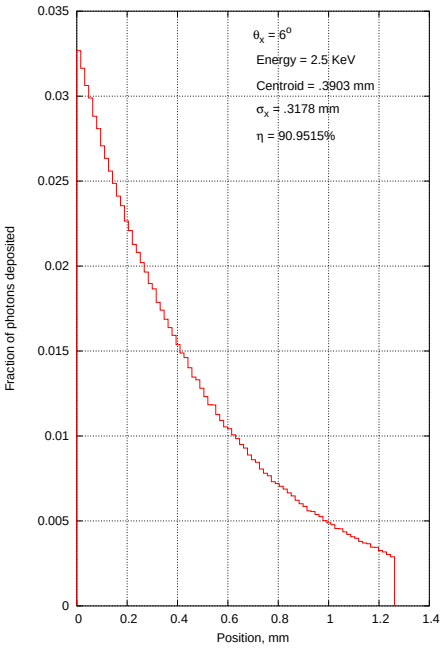

(b) 2.5 KeV X-ray photon incident at 6°

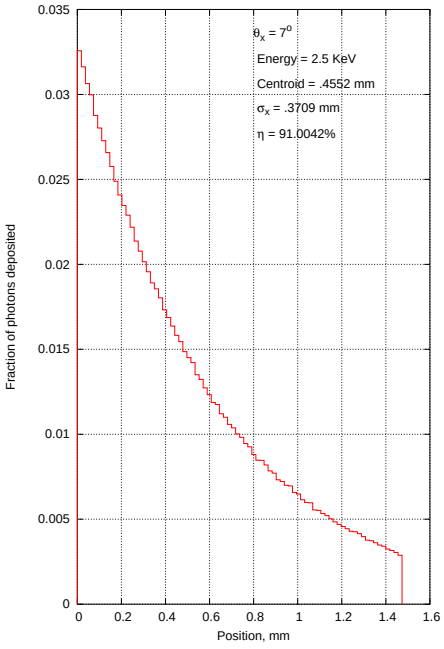

(c) 2.5 KeV X-ray photon incident at 7°

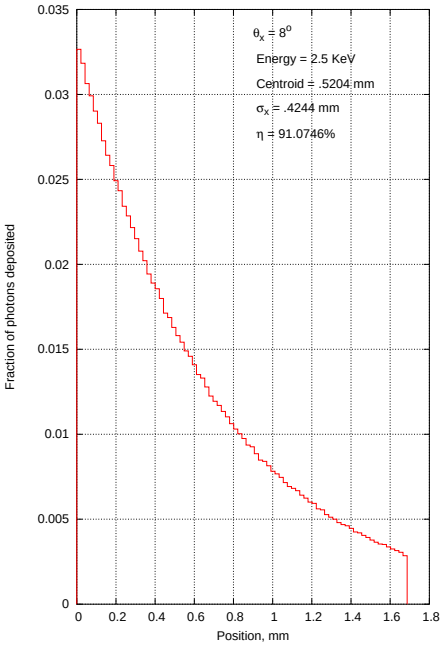

(d) 2.5 KeV X-ray photon incident at 8°

Figure 4.12: Probability of absorption of 2.5 KeV photon when incident at 5°, 6°, 7° and 8°

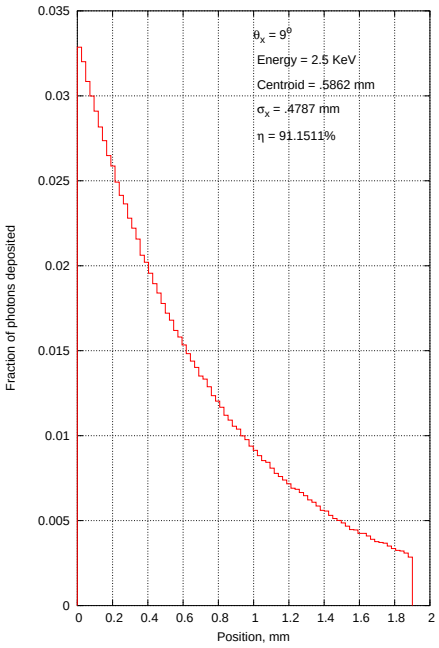

(a) 2.5 KeV X-ray photon incident at 9°

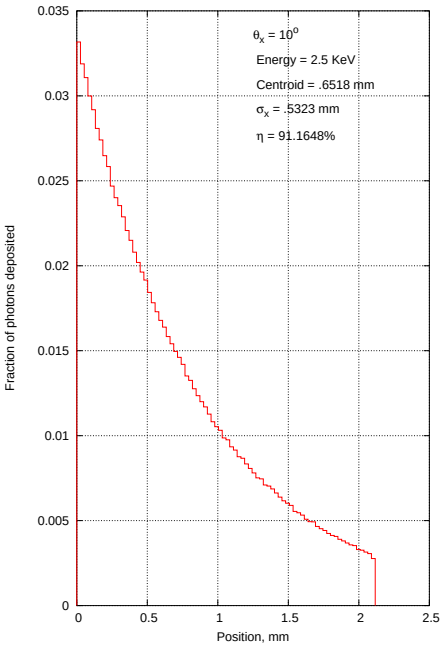

(b) 2.5 KeV X-ray photon incident at 10°

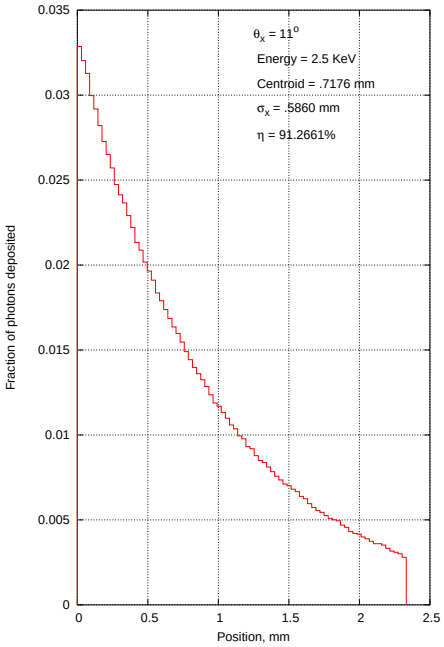

(c) 2.5 KeV X-ray photon incident at 11°

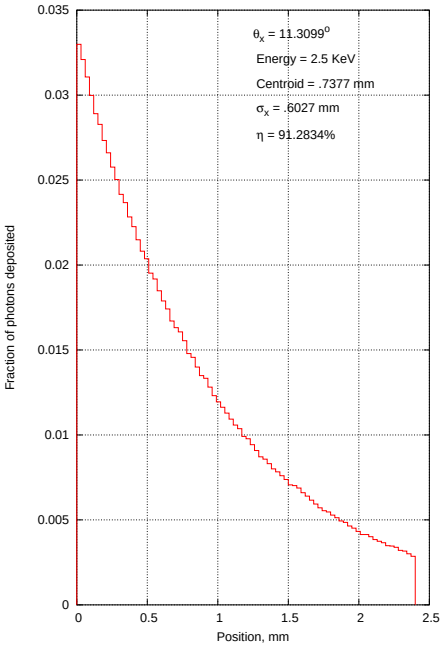

(d) 2.5 KeV X-ray photon incident at 11.3099°

Figure 4.13: Probability of absorption of 2.5 KeV photon when incident at 9°, 10°, 11° and 11.3099°

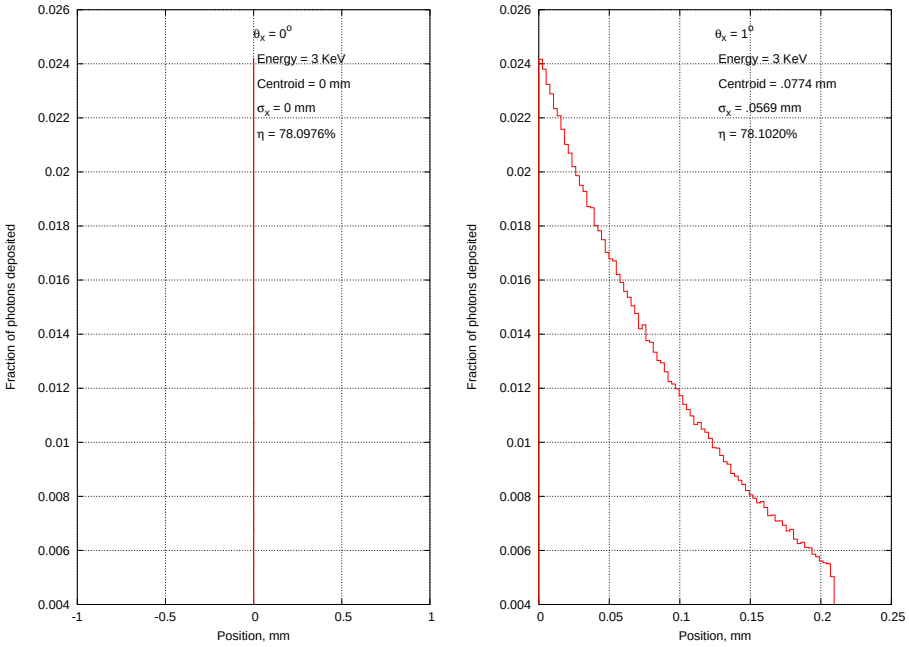

(a) 3 KeV X-ray photon incident at 0°

(b) 3 KeV X-ray photon incident at 1°

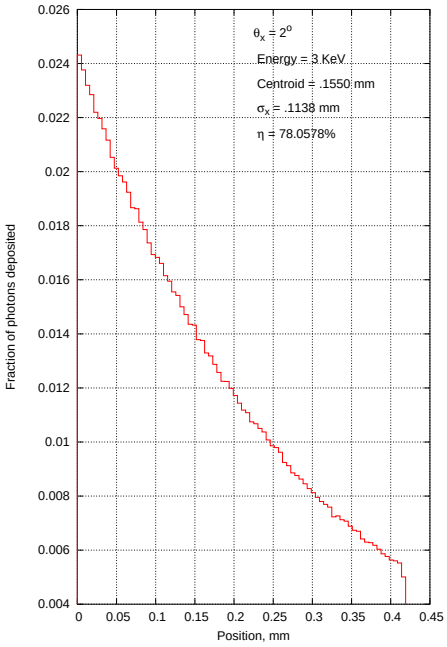

(c) 3 KeV X-ray photon incident at 2°

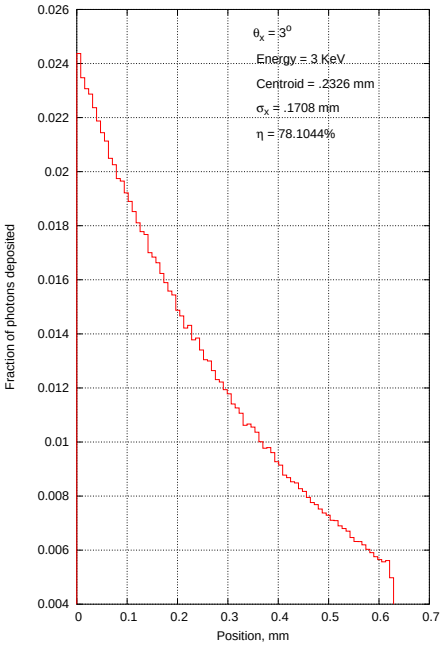

(d) 3 KeV X-ray photon incident at 3°

Figure 4.14: Probability of absorption of 3 KeV photon when incident at 0°, 1°, 2° and 3°

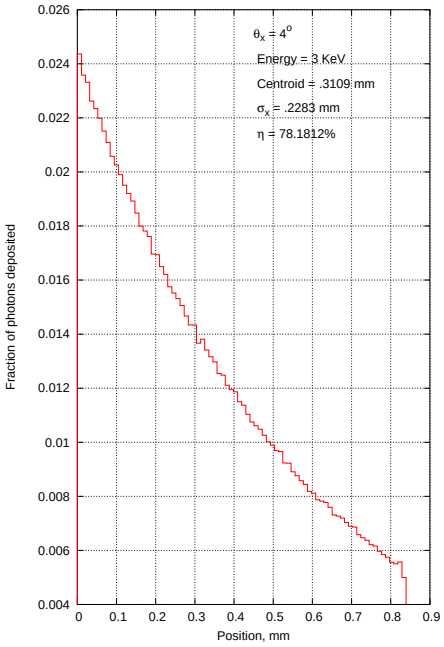

(a) 3 KeV X-ray photon incident at 4°

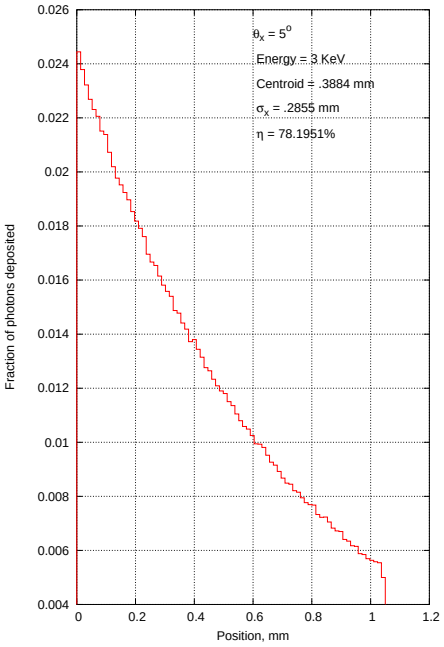

(b) 3 KeV X-ray photon incident at 5°

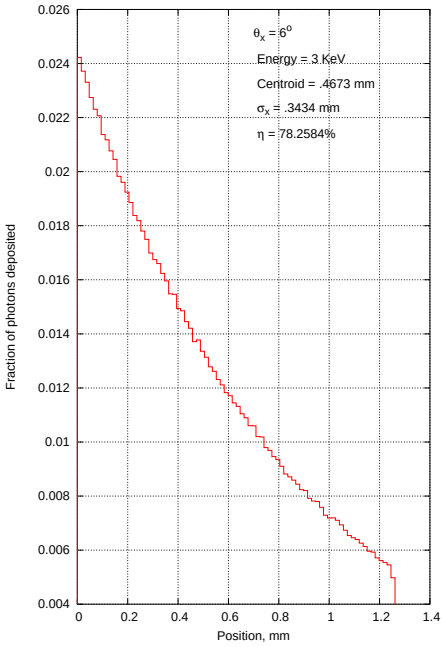

(c) 3 KeV X-ray photon incident at 6°

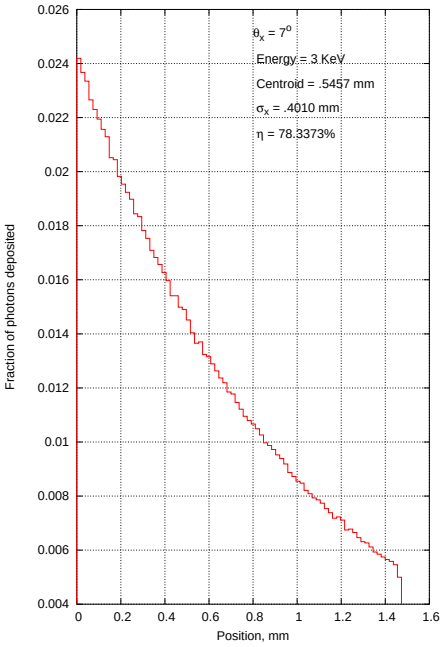

(d) 3 KeV X-ray photon incident at 7°

Figure 4.15: Probability of absorption of 3 KeV photon when incident at 4°, 5°, 6° and 7°

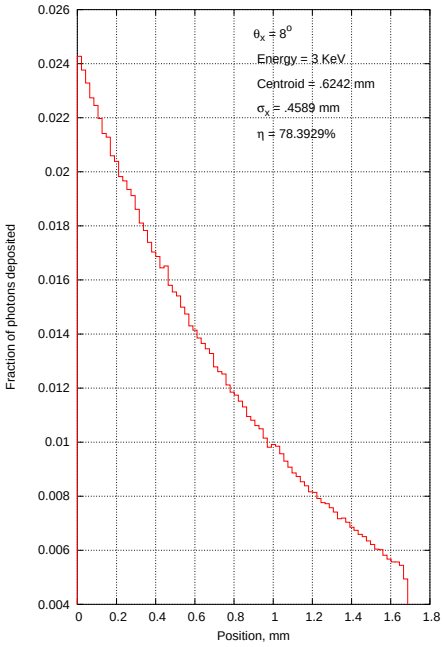

(a) 3 KeV X-ray photon incident at 8°

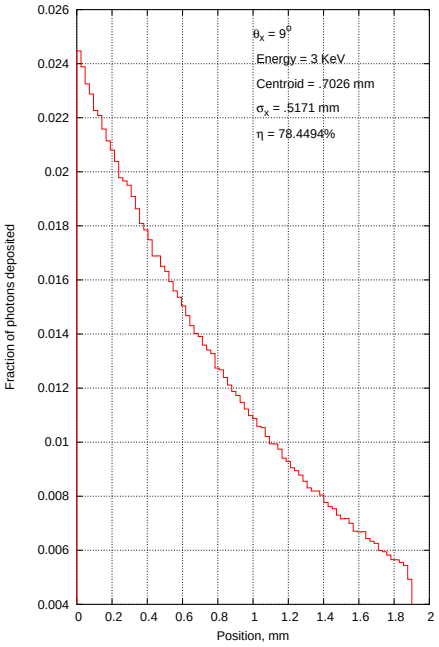

(b) 3 KeV X-ray photon incident at 9°

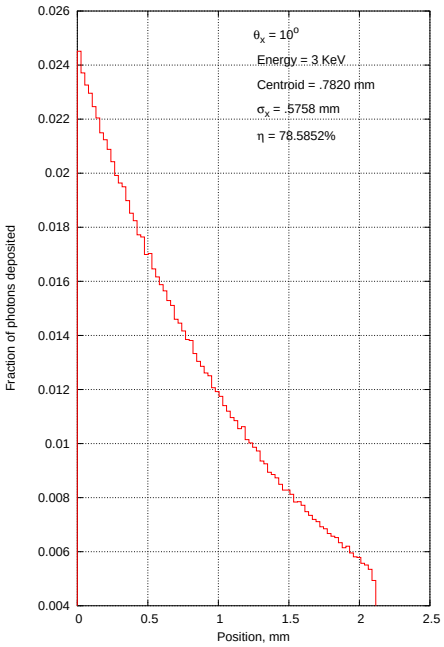

(c) 3 KeV X-ray photon incident at 10°

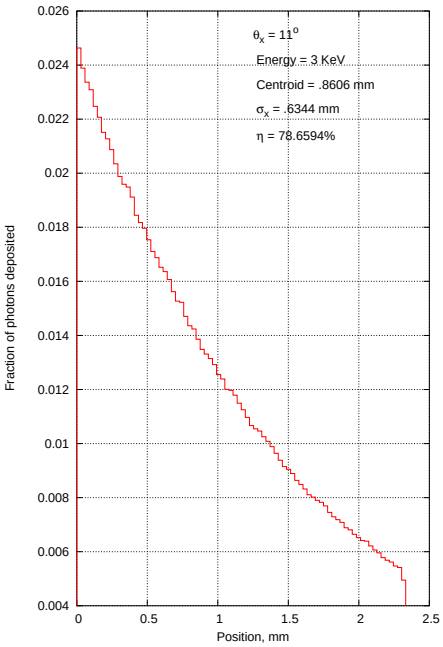

(d) 3 KeV X-ray photon incident at 11°

Figure 4.16: Probability of absorption of 3 KeV photon when incident at 8°, 9°, 10° and 11°

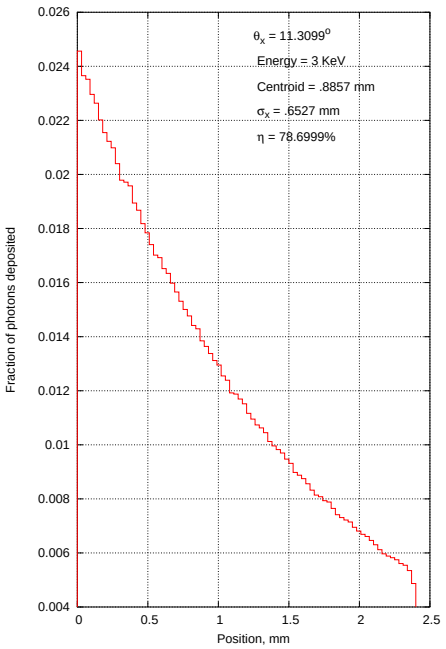

(a) 3 KeV X-ray photon incident at 11.3099°

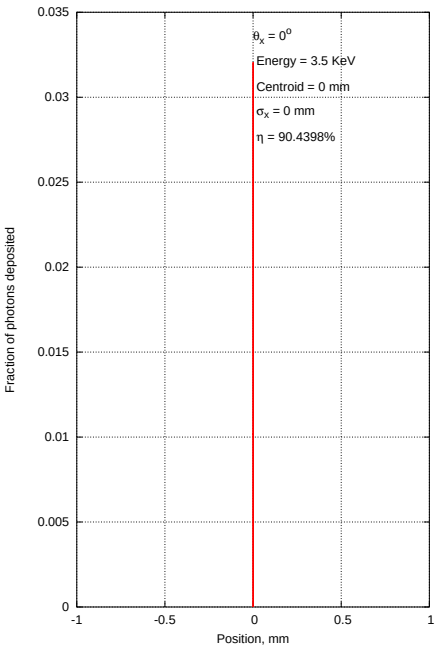

(b) 3.5 KeV X-ray photon incident at 0°

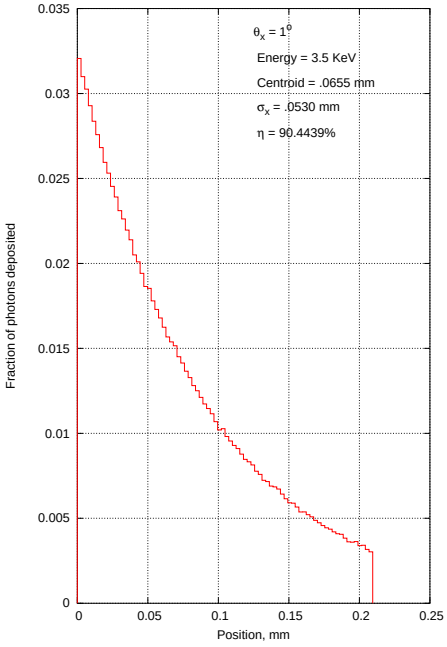

(c) 3.5 KeV X-ray photon incident at 1°

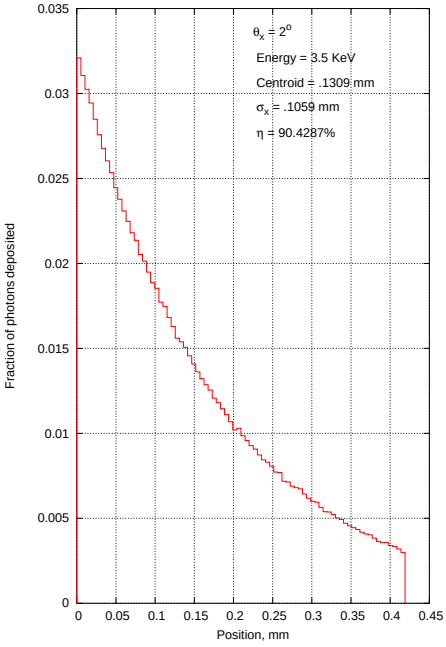

(d) 3.5 KeV X-ray photon incident at 2°

Figure 4.17: Probability of absorption of 3 KeV photon when incident at 0° and 3.5 KeV at 1°, 2°, 3°

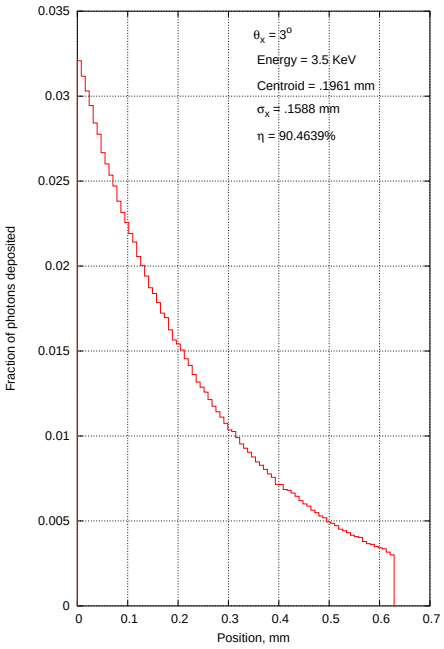

(a) 3.5 KeV X-ray photon incident at 3°

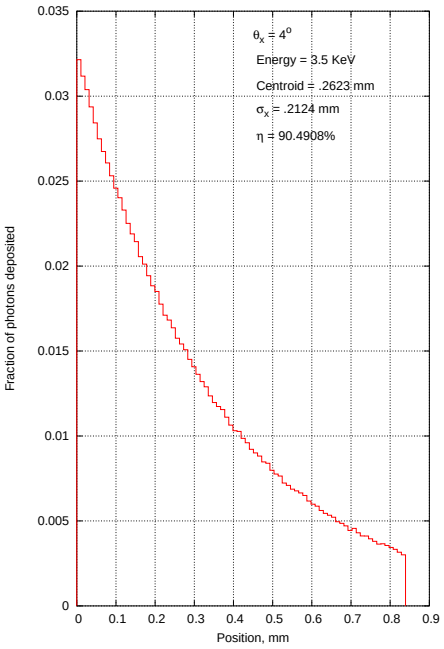

(b) 3.5 KeV X-ray photon incident at 4°

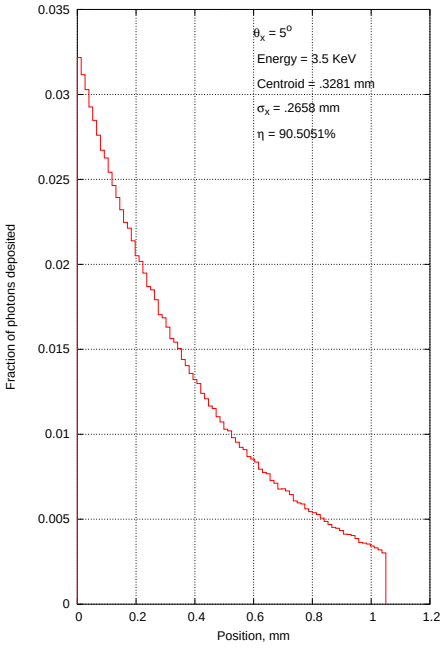

(c) 3.5 KeV X-ray photon incident at 5°

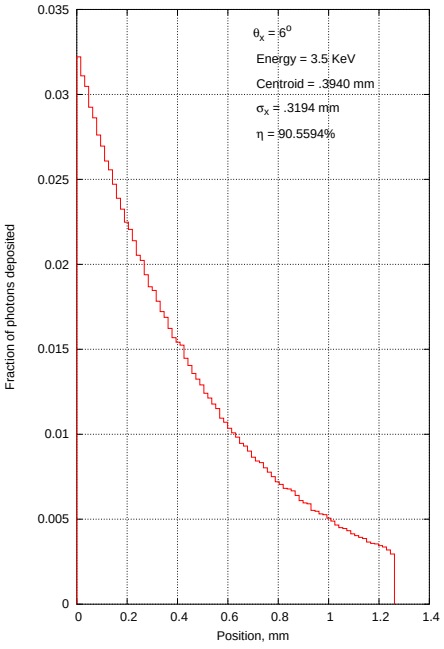

(d) 3.5 KeV X-ray photon incident at 6°

Figure 4.18: Probability of absorption of 3.5 KeV photon when incident at 3°, 4°, 5° and 6°

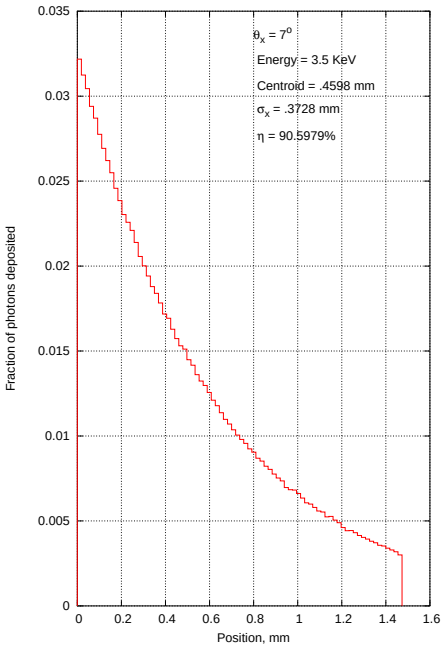

(a) 3.5 KeV X-ray photon incident at 7°

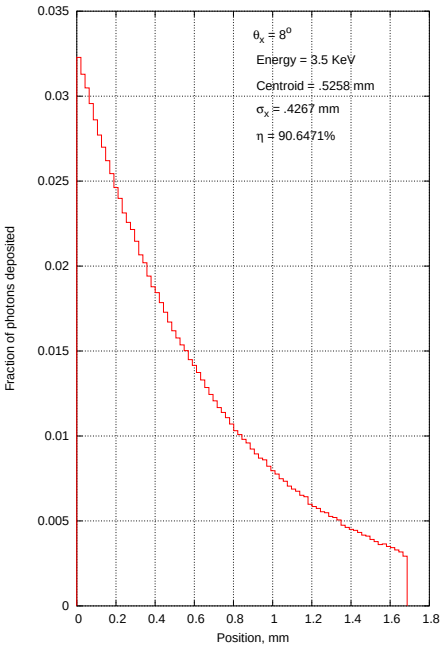

(b) 3.5 KeV X-ray photon incident at 8°

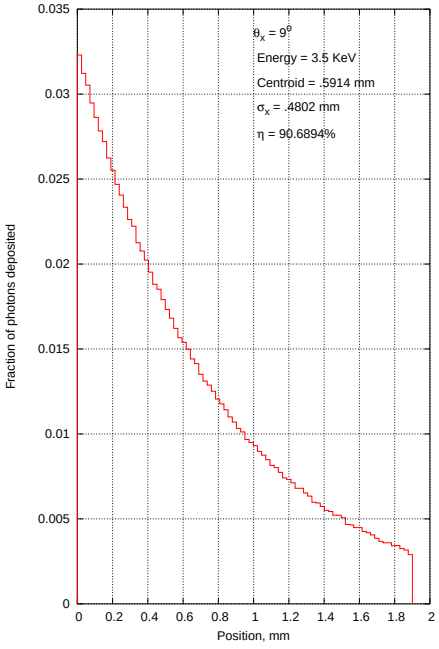

(c) 3.5 KeV X-ray photon incident at 9°

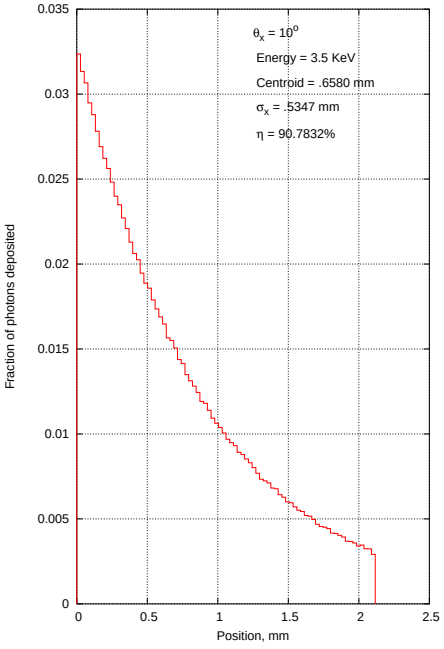

(d) 3.5 KeV X-ray photon incident at 10°

Figure 4.19: Probability of absorption of 3.5 KeV photon when incident at 7°, 8°, 9° and 10°

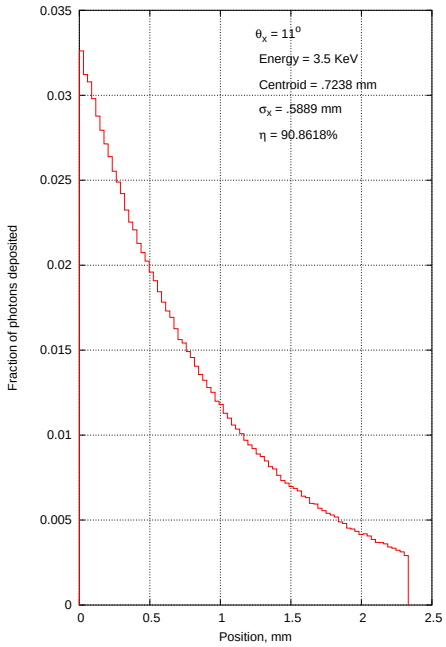

(a) 3.5 KeV X-ray photon incident at 11°

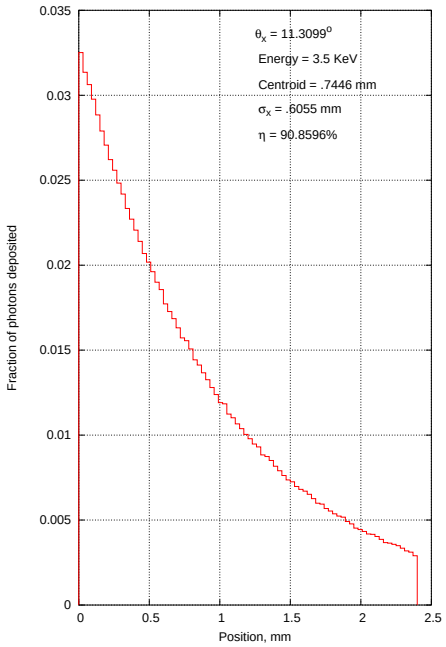

(b) 3.5 KeV X-ray photon incident at 11.3099°

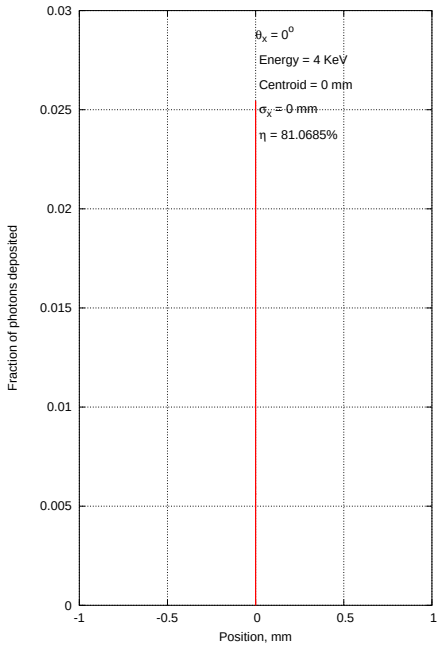

(c) 4 KeV X-ray photon incident at 0°

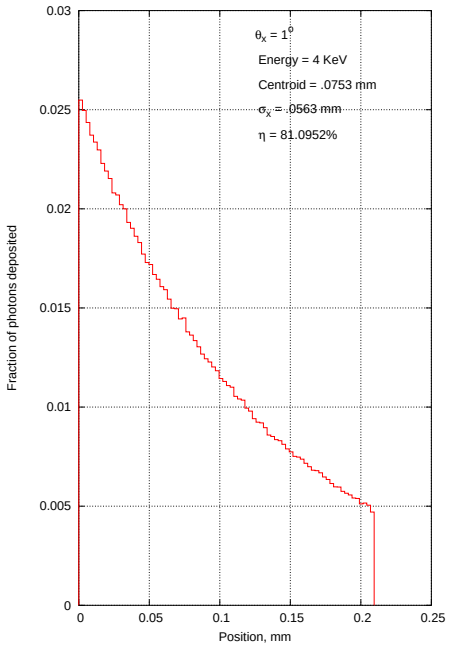

(d) 4 KeV X-ray photon incident at 1°

Figure 4.20: Probability of absorption of 3.5 KeV photon when incident at 11°, 11.3099° and 4 KeV at 0° and 1°

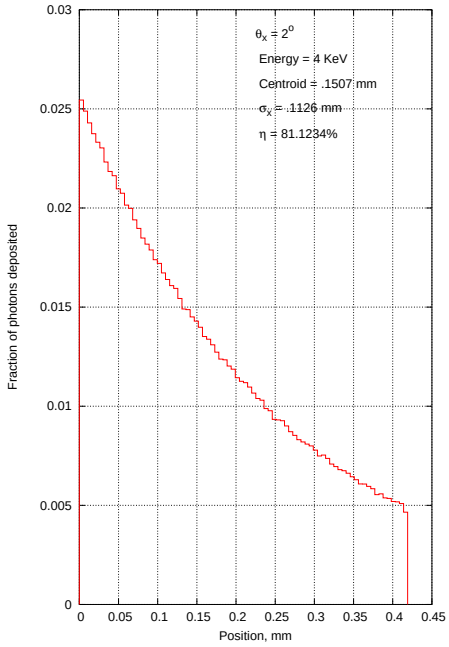

(a) 4 KeV X-ray photon incident at 2°

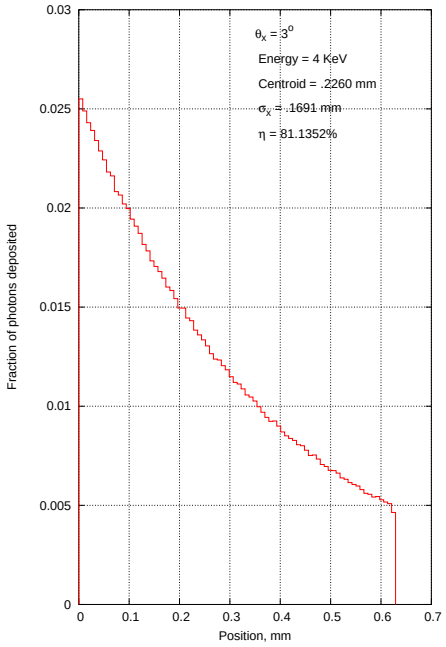

(b) 4 KeV X-ray photon incident at 3°

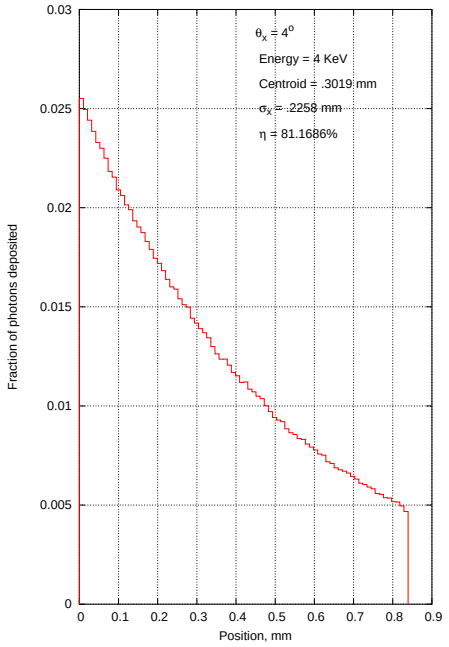

(c) 4 KeV X-ray photon incident at 4°

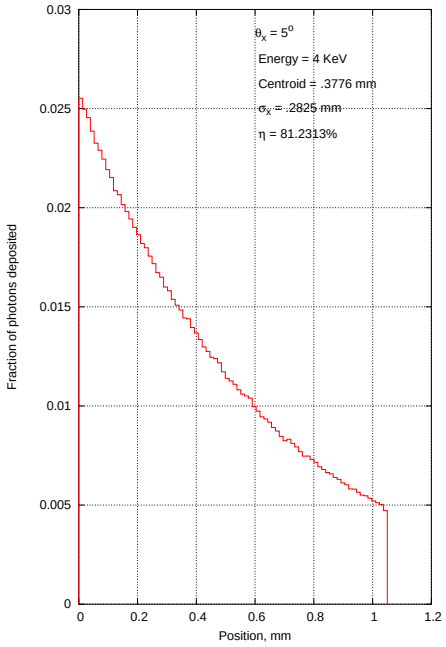

(d) 4 KeV X-ray photon incident at 5°

Figure 4.21: Probability of absorption of 4 KeV photon when incident at 2°, 3°, 4° and 5°

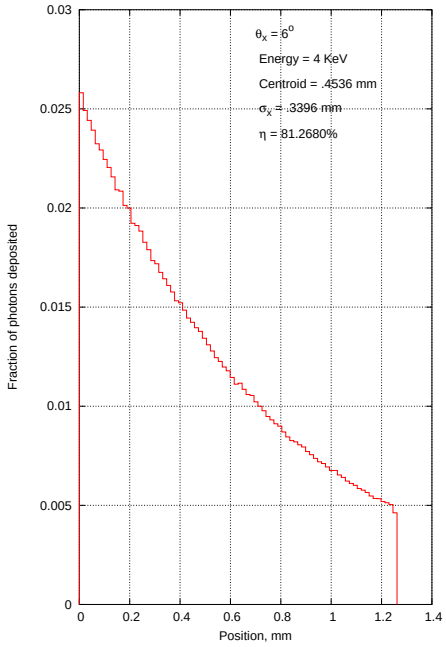

(a) 4 KeV X-ray photon incident at 6°

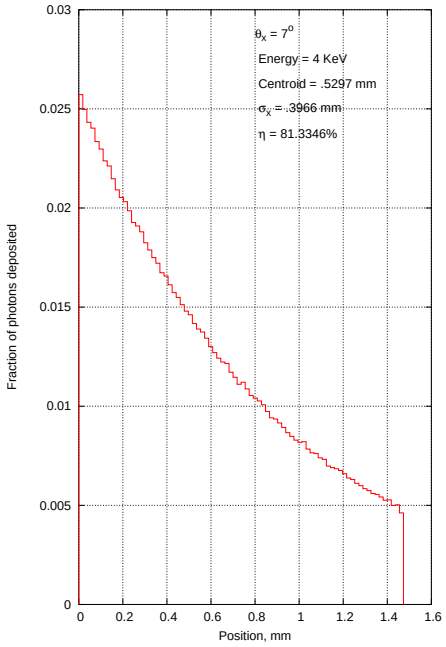

(b) 4 KeV X-ray photon incident at 7°

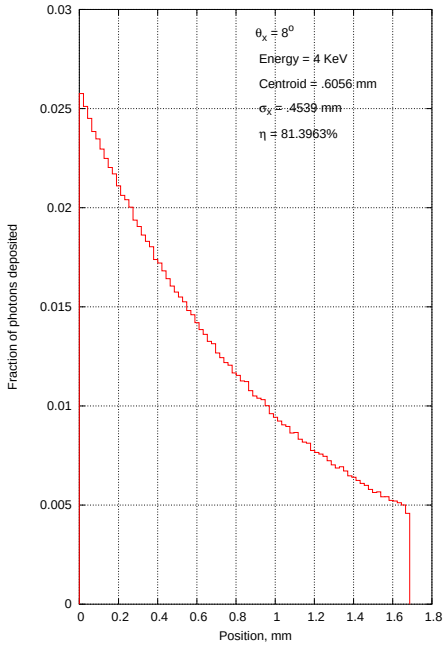

(c) 4 KeV X-ray photon incident at 8°

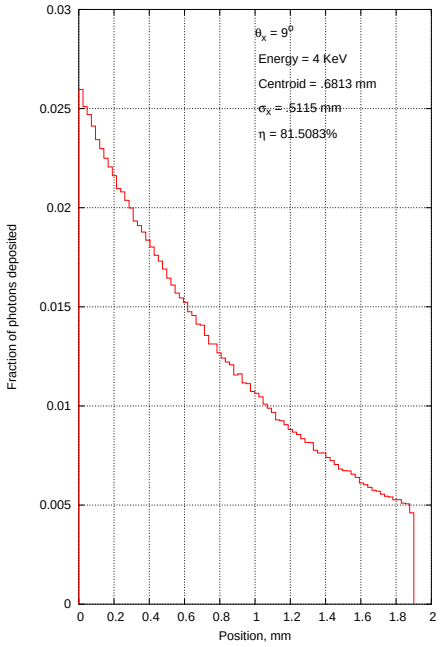

(d) 4 KeV X-ray photon incident at 9°

Figure 4.22: Probability of absorption of 4 KeV photon when incident at 6°, 7°, 8° and 9°

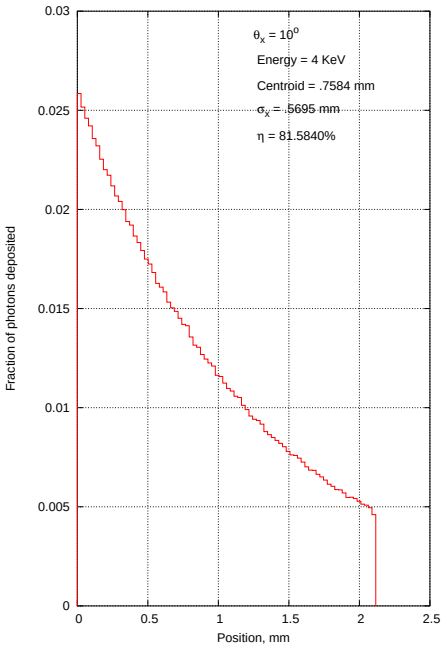

(a) 4 KeV X-ray photon incident at 10°

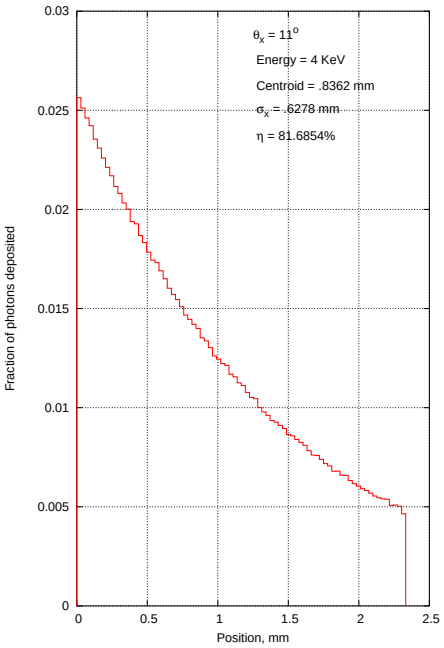

(b) 4 KeV X-ray photon incident at 11°

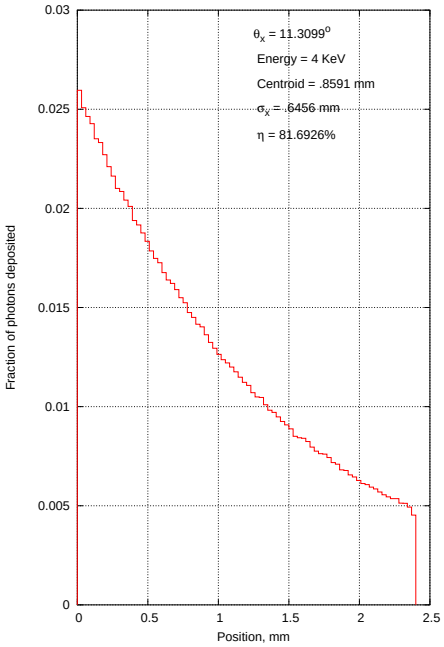

(c) 4 KeV X-ray photon incident at 11.3099°

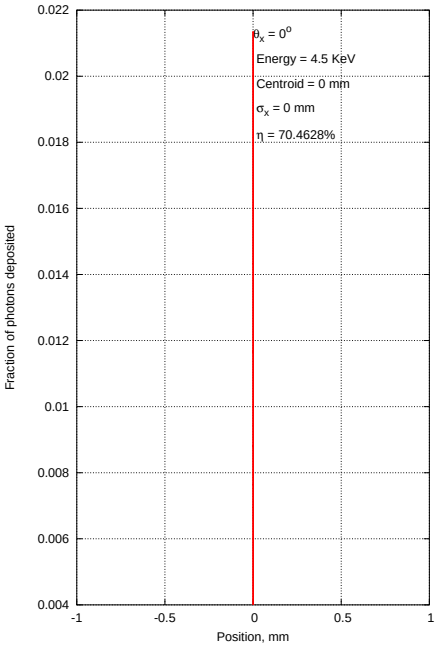

(d) 4.5 KeV X-ray photon incident at 0°

Figure 4.23: Probability of absorption of 4 KeV photon when incident at 10°, 11°, 11.3099° and 4.5 KeV at 0°

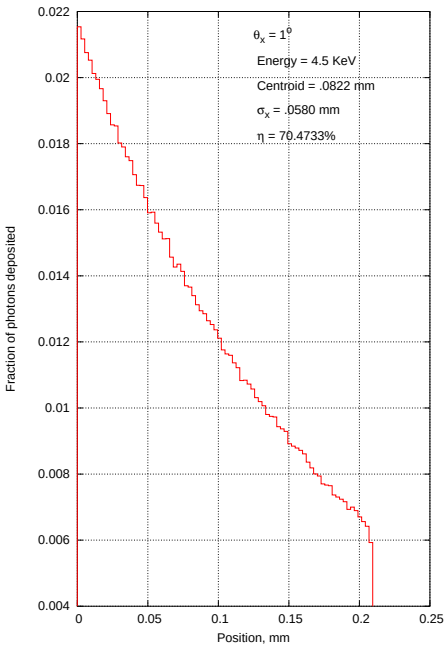

(a) 4.5 KeV X-ray photon incident at 1°

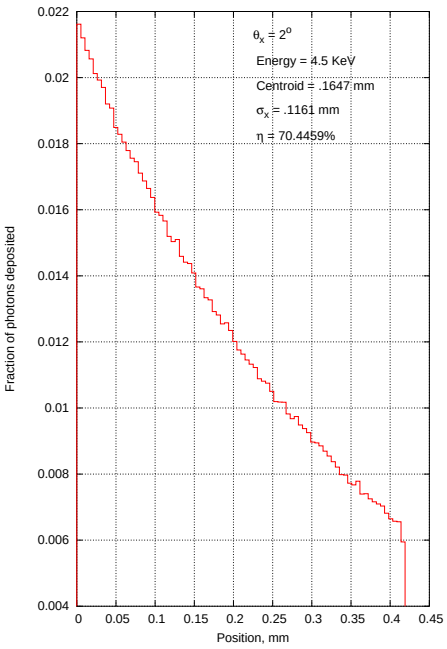

(b) 4.5 KeV X-ray photon incident at 2°

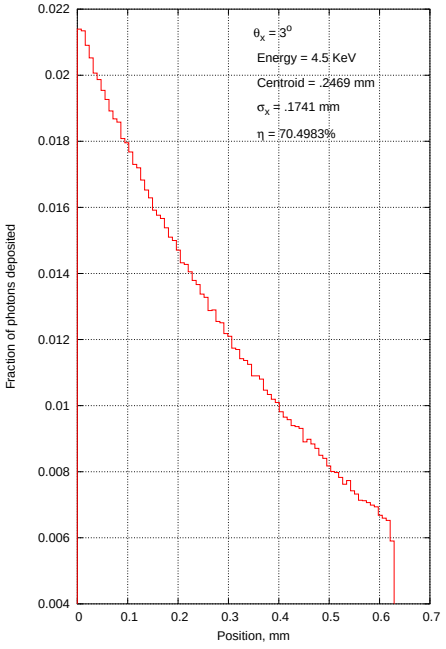

(c) 4.5 KeV X-ray photon incident at 3°

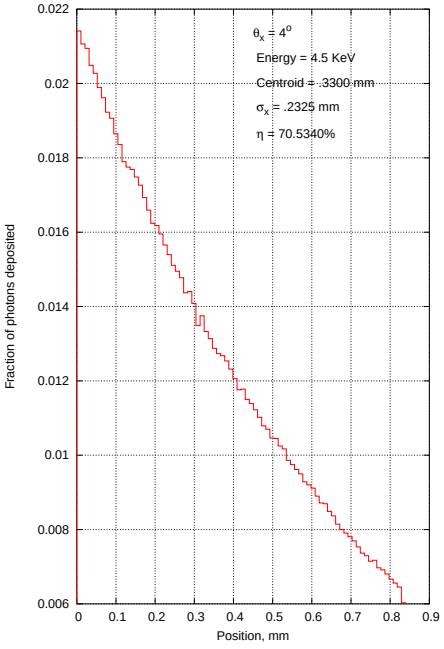

(d) 4.5 KeV X-ray photon incident at 4°

Figure 4.24: Probability of absorption of 4.5 KeV photon when incident at 1°, 2°, 3° and 4°

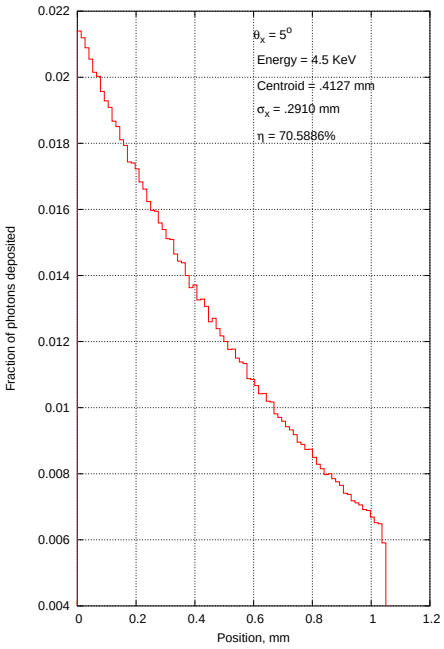

(a) 4.5 KeV X-ray photon incident at 5°

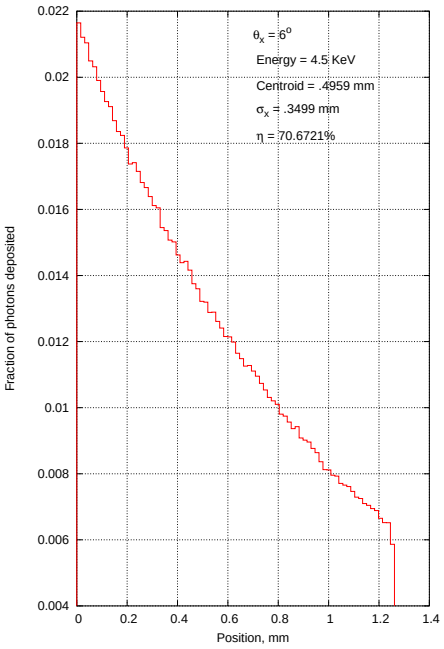

(b) 4.5 KeV X-ray photon incident at 6°

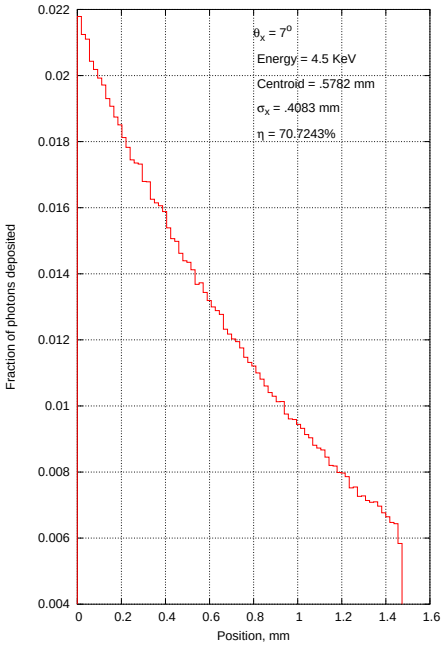

(c) 4.5 KeV X-ray photon incident at 7°

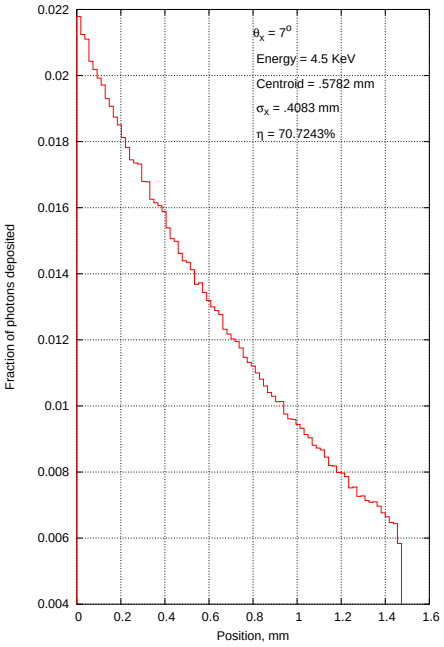

(d) 4.5 KeV X-ray photon incident at 8°

Figure 4.25: Probability of absorption of 4.5 KeV photon when incident at 5°, 6°, 7° and 8°

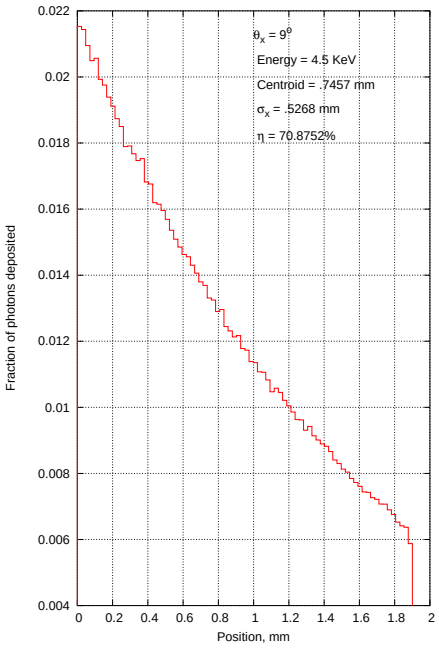

(a) 4.5 KeV X-ray photon incident at 9°

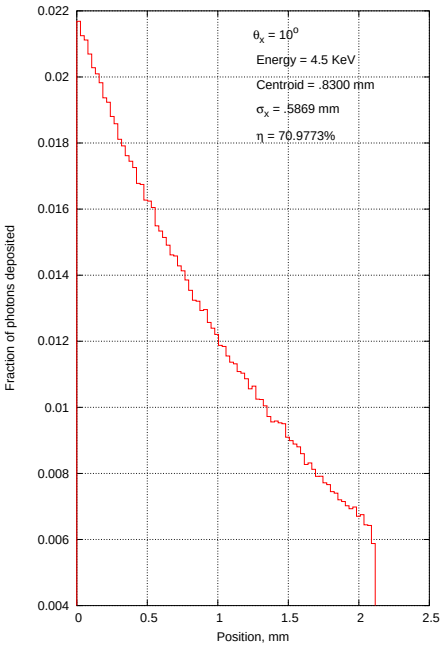

(b) 4.5 KeV X-ray photon incident at 10°

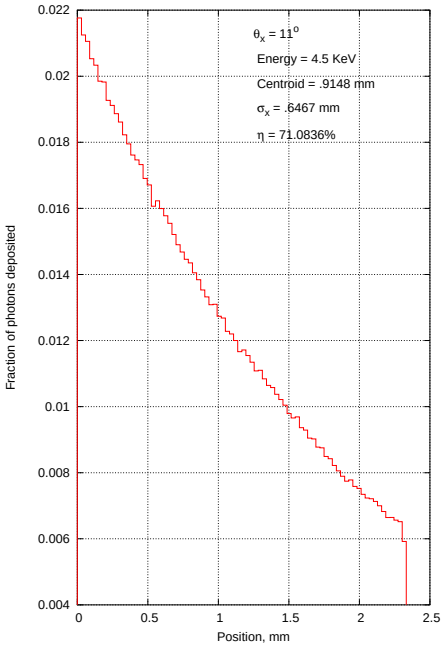

(c) 4.5 KeV X-ray photon incident at 11°

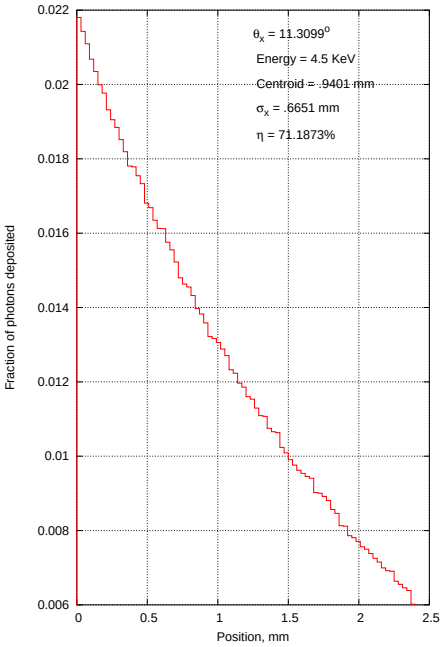

(d) 4.5 KeV X-ray photon incident at 11.3099°

Figure 4.26: Probability of absorption of 4.5 KeV photon when incident at 9°, 10°, 11° and 11.3099°

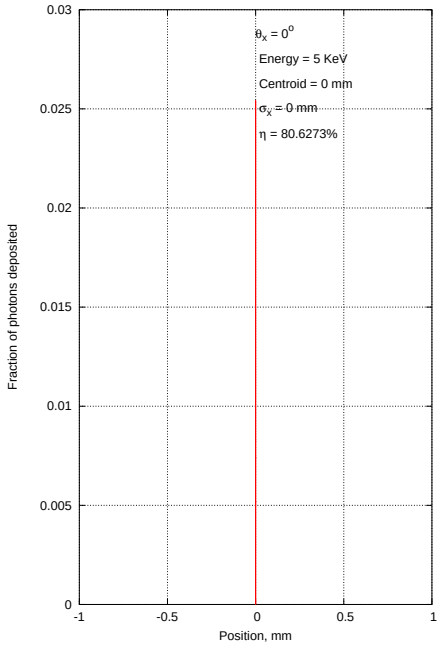

(a) 5 KeV X-ray photon incident at 0°

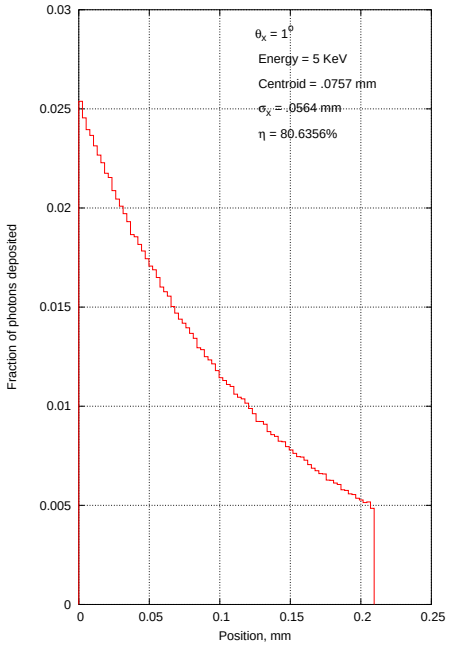

(b) 5 KeV X-ray photon incident at 1°

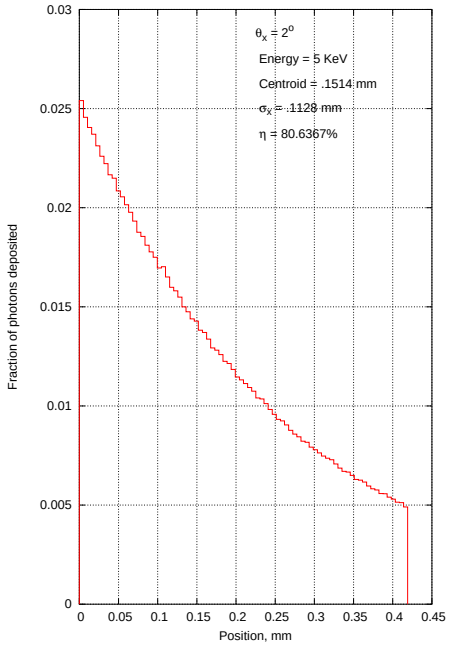

(c) 5 KeV X-ray photon incident at 2°

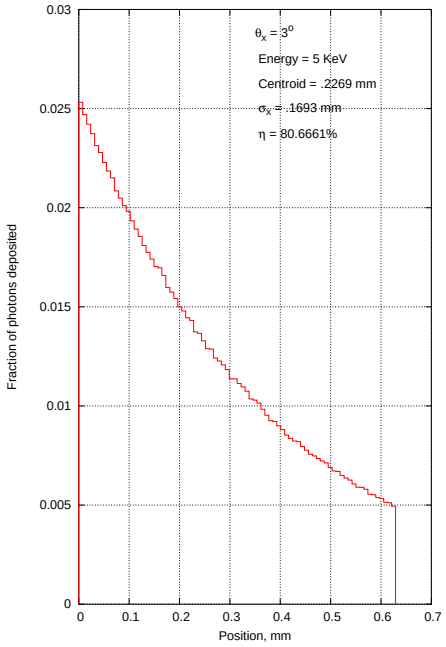

(d) 5 KeV X-ray photon incident at 3°

Figure 4.27: Probability of absorption of 5 KeV photon when incident at 0°, 1°, 2° and 3°

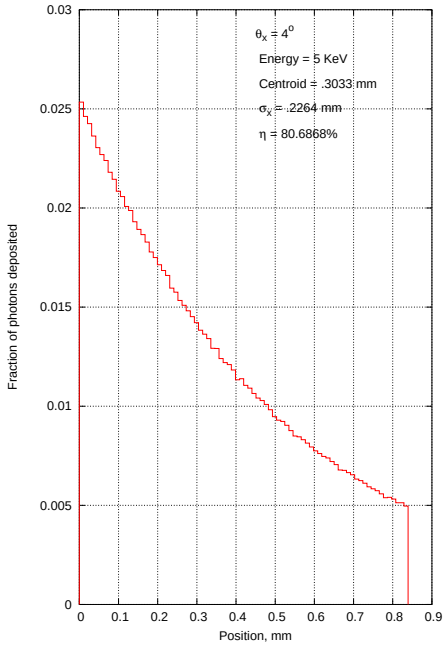

(a) 5 KeV X-ray photon incident at 4°

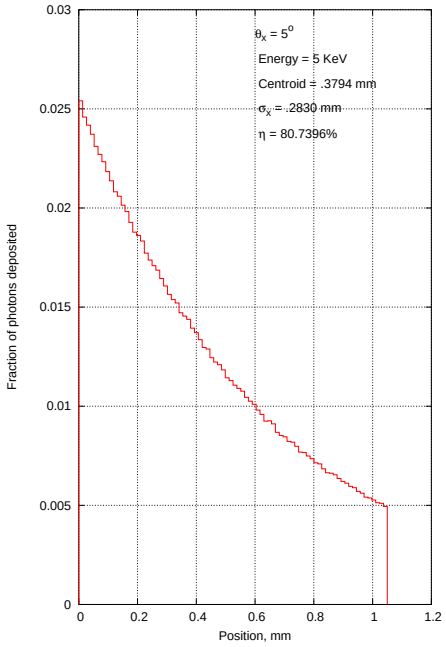

(b) 5 KeV X-ray photon incident at 5°

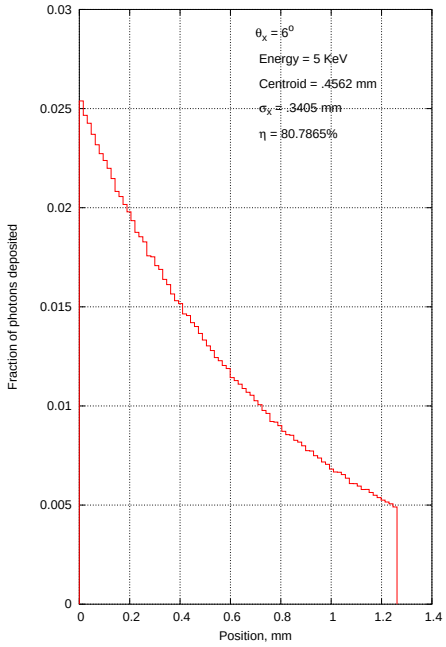

(c) 5 KeV X-ray photon incident at 6°

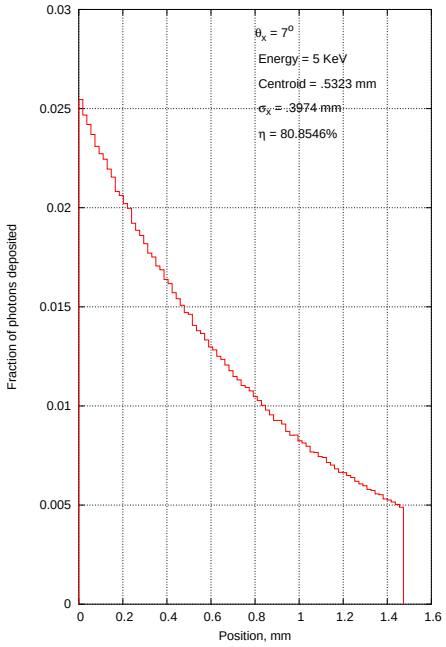

(d) 5 KeV X-ray photon incident at 7°

Figure 4.28: Probability of absorption of 5 KeV photon when incident at 4°, 5°, 6° and 7°

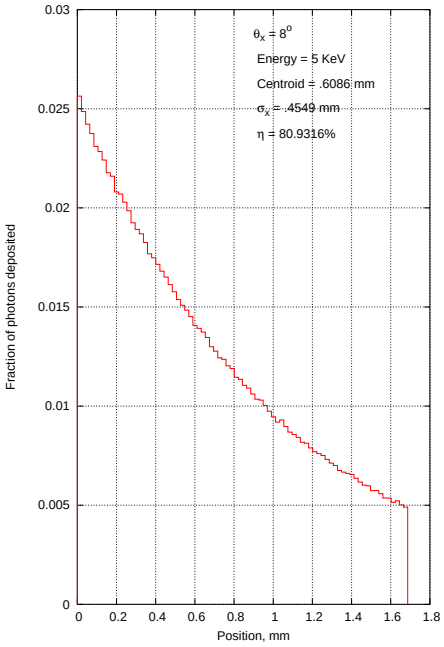

(a) 5 KeV X-ray photon incident at 8°

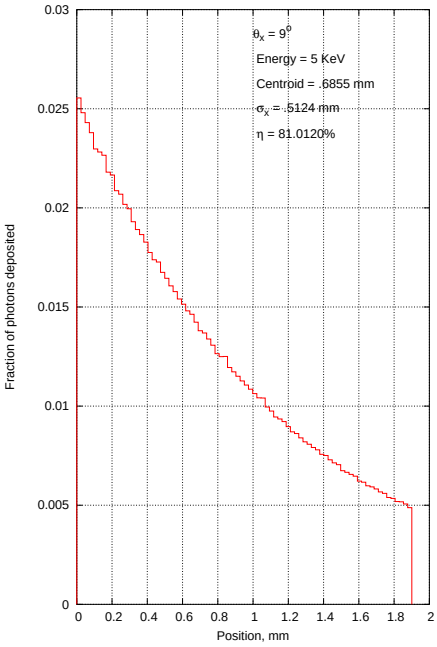

(b) 5 KeV X-ray photon incident at 9°

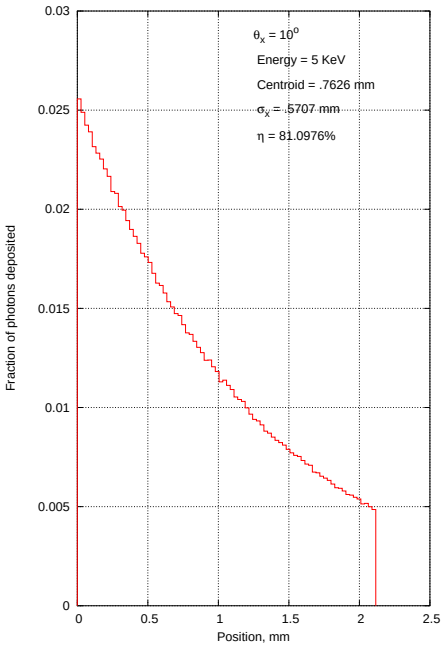

(c) 5 KeV X-ray photon incident at 10°

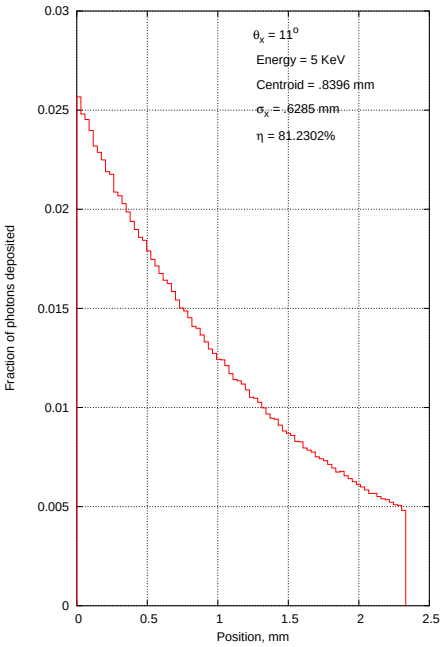

(d) 5 KeV X-ray photon incident at 11°

Figure 4.29: Probability of absorption of 5 KeV photon when incident at 8°, 9°, 10° and 11^o

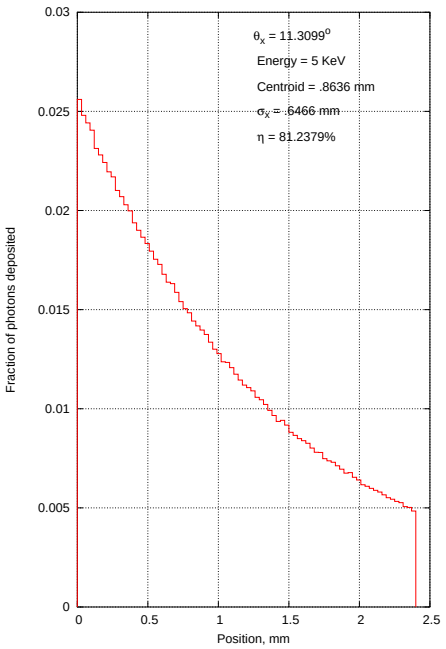

(a) 5 KeV X-ray photon incident at 11.3099°

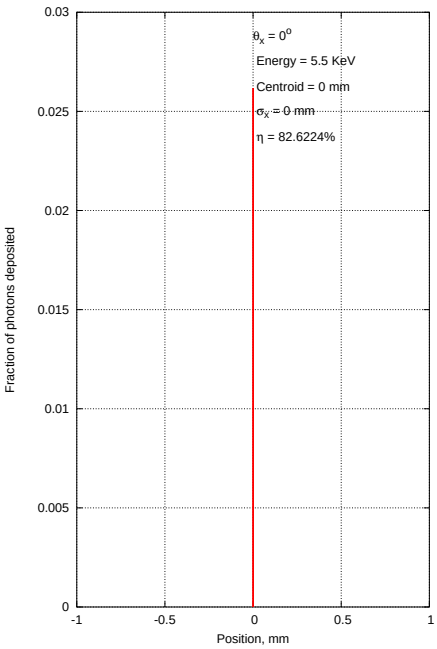

(b) 5.5 KeV X-ray photon incident at 0°

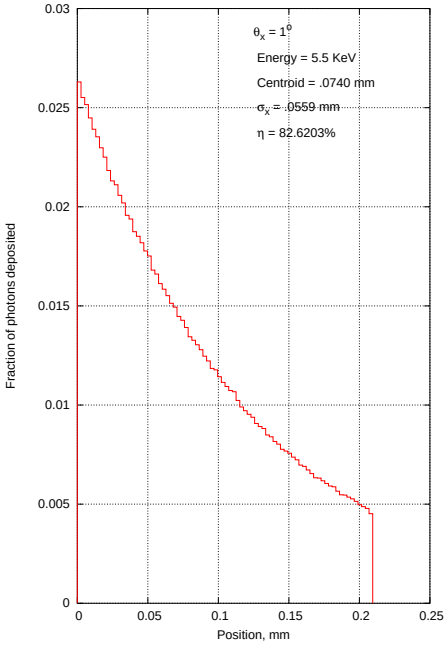

(c) 5.5 KeV X-ray photon incident at 1°

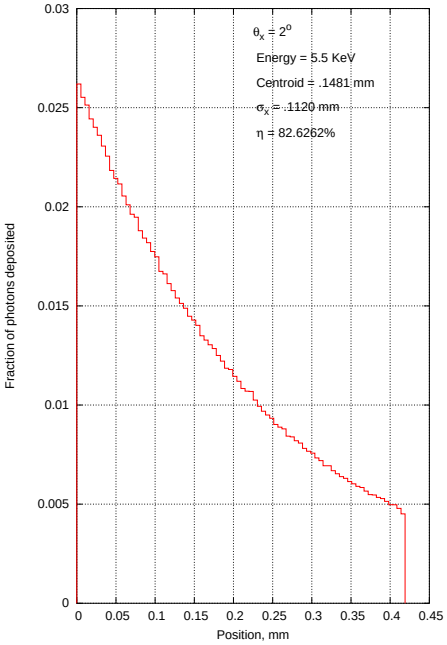

(d) 5.5 KeV X-ray photon incident at 2°

Figure 4.30: Probability of absorption of 5 KeV photon when incident at 11.3099° and 5.5 KeV at 0°, 1°, 2°

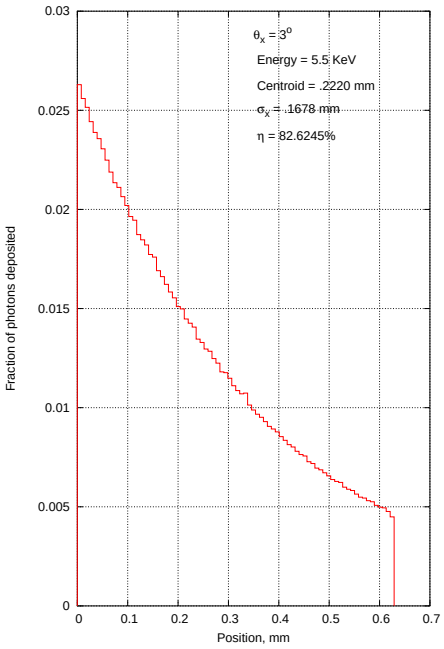

(a) 5.5 KeV X-ray photon incident at 3°

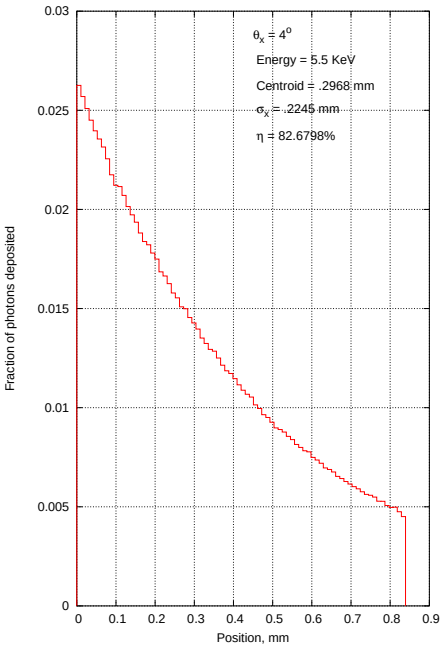

(b) 5.5 KeV X-ray photon incident at 4°

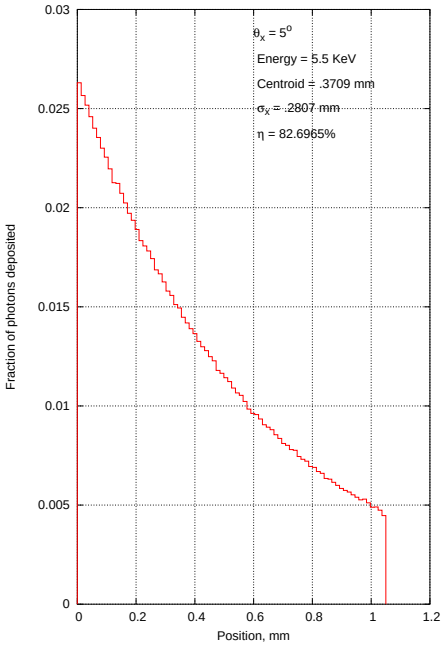

(c) 5.5 KeV X-ray photon incident at 5°

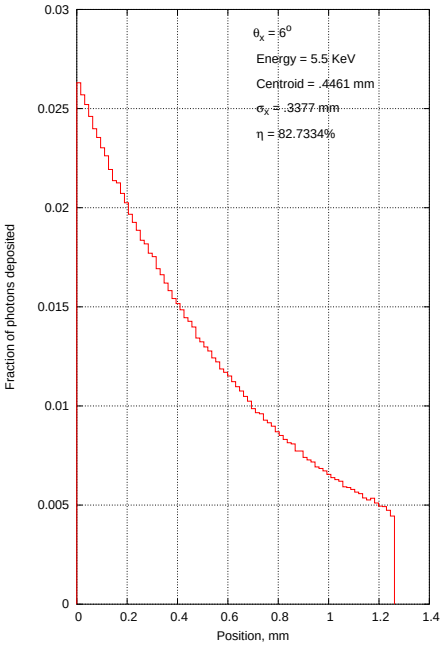

(d) 5.5 KeV X-ray photon incident at 6°

Figure 4.31: Probability of absorption of 5.5 KeV photon when incident at 3°, 4°, 5° and 6°

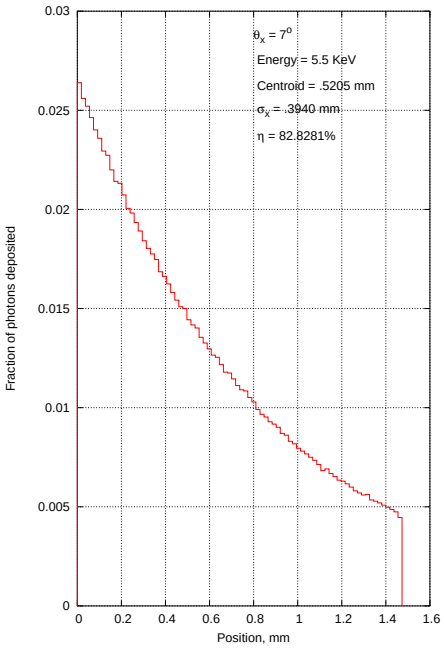

(a) 5.5 KeV X-ray photon incident at 7°

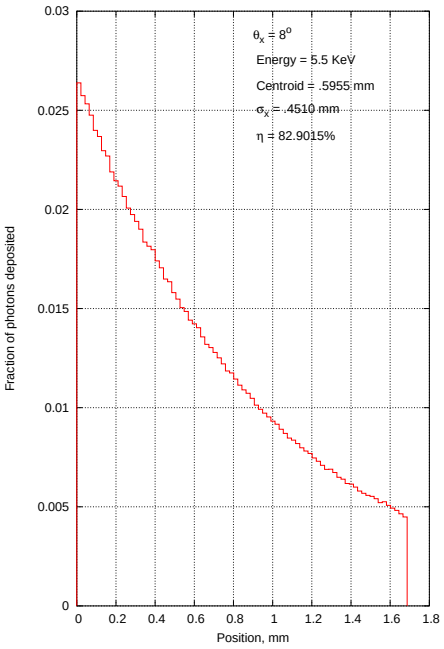

(b) 5.5 KeV X-ray photon incident at 8°

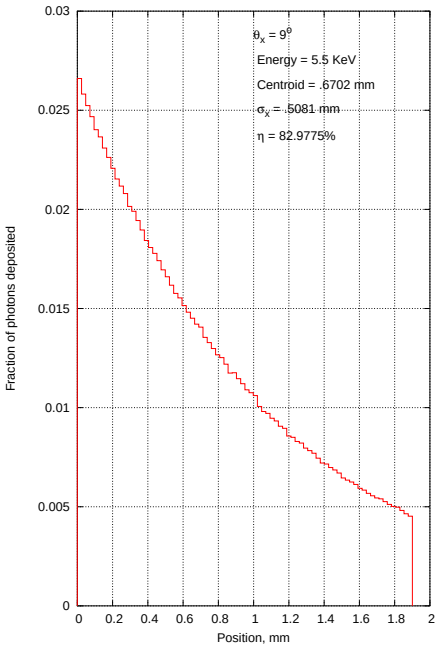

(c) 5.5 KeV X-ray photon incident at 9°

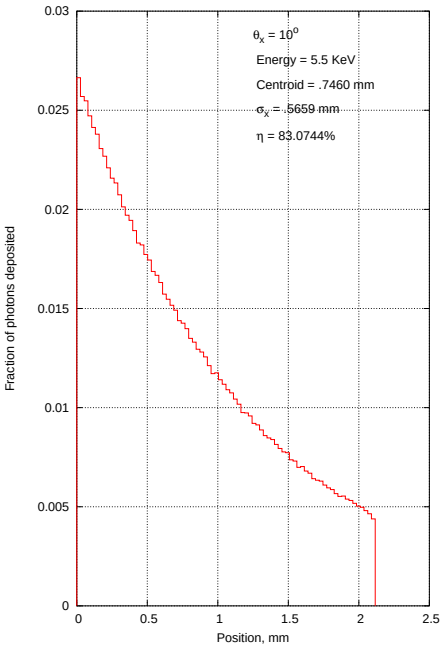

(d) 5.5 KeV X-ray photon incident at 10°

Figure 4.32: Probability of absorption of 5.5 KeV photon when incident at 7°, 8°, 9° and 10°

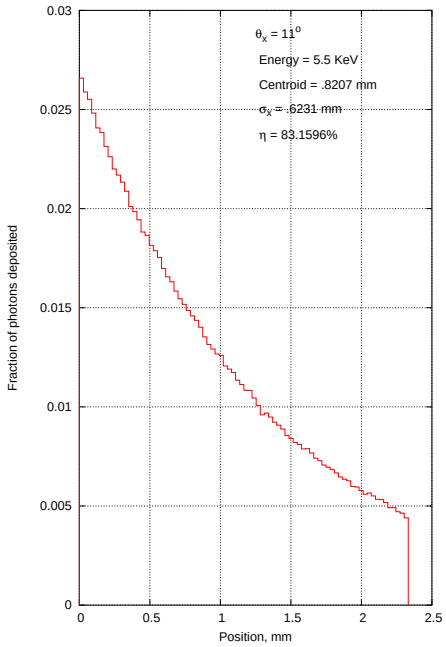

(a) 5.5 KeV X-ray photon incident at 11°

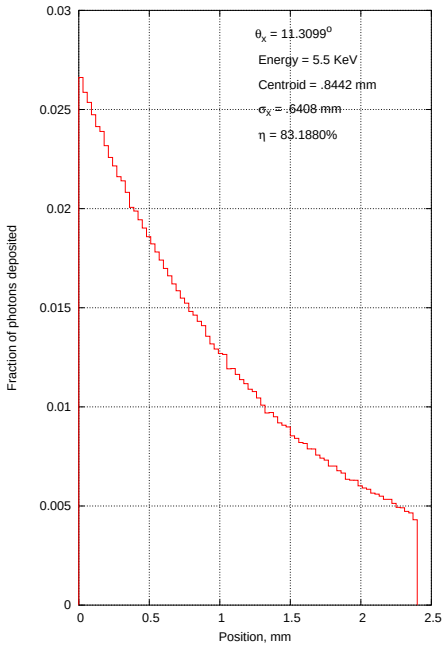

(b) 5.5 KeV X-ray photon incident at 11.3099°

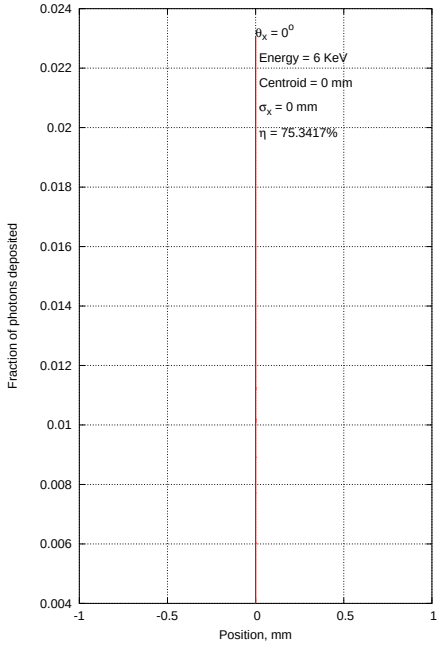

(c) 6 KeV X-ray photon incident at 0°

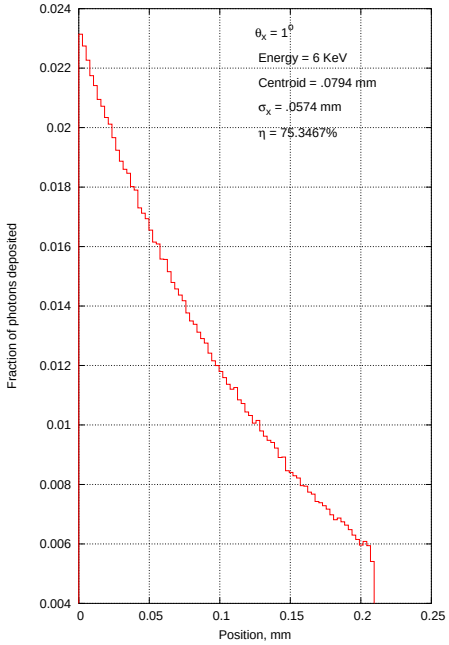

(d) 6 KeV X-ray photon incident at 1°

Figure 4.33: Probability of absorption of 5.5 KeV photon when incident at 11°, 11.3099° and 6 KeV at 0°, 1°

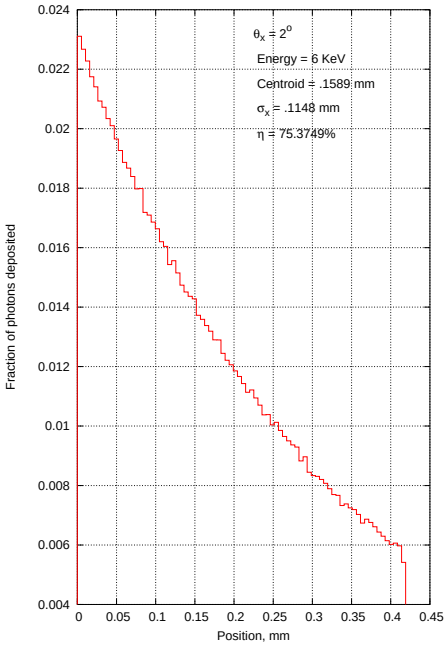

(a) 6 KeV X-ray photon incident at 2°

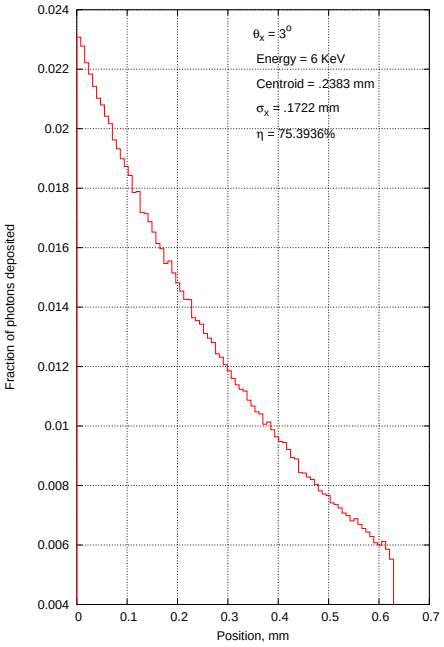

(b) 6 KeV X-ray photon incident at 3°

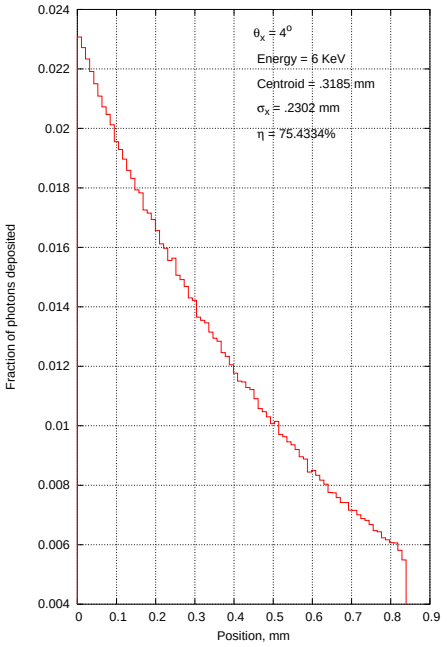

(c) 6 KeV X-ray photon incident at 4°

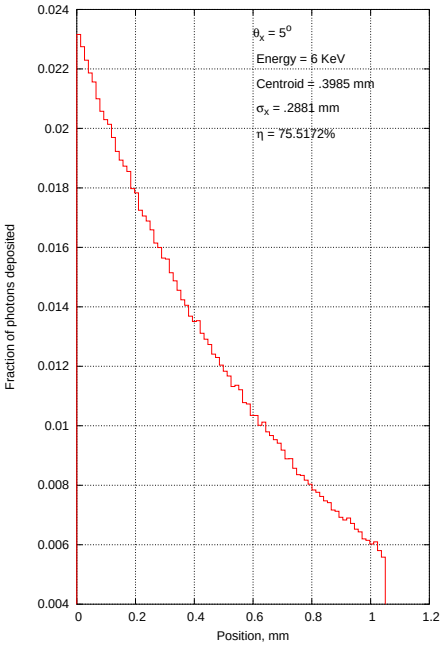

(d) 6 KeV X-ray photon incident at 5°

Figure 4.34: Probability of absorption of 6 KeV photon when incident at 2°, 3°, 4° and 5°

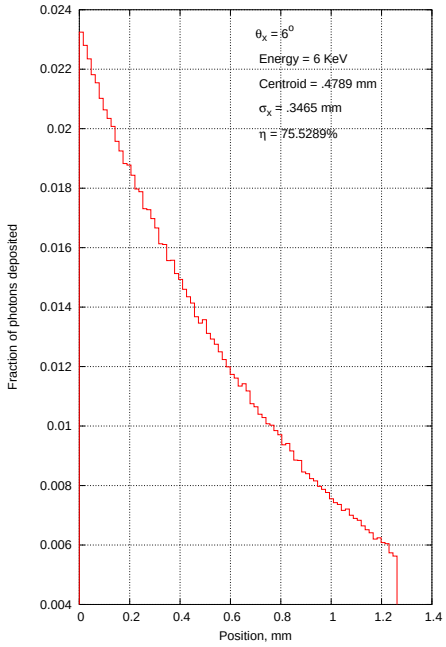

(a) 6 KeV X-ray photon incident at 6°

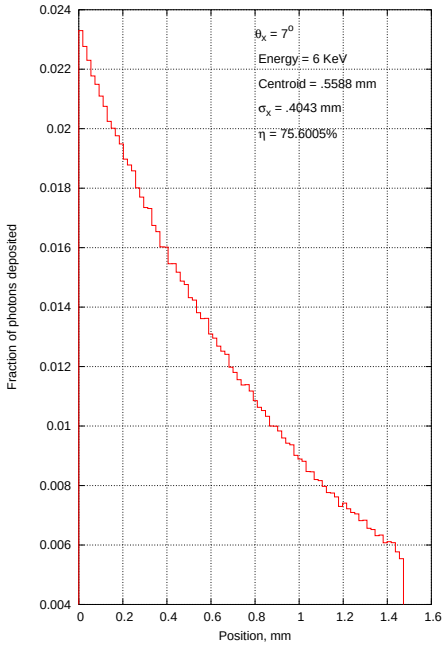

(b) 6 KeV X-ray photon incident at 7°

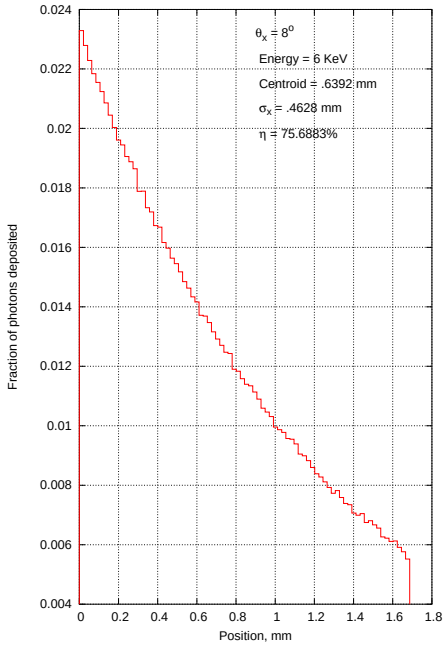

(c) 6 KeV X-ray photon incident at 8°

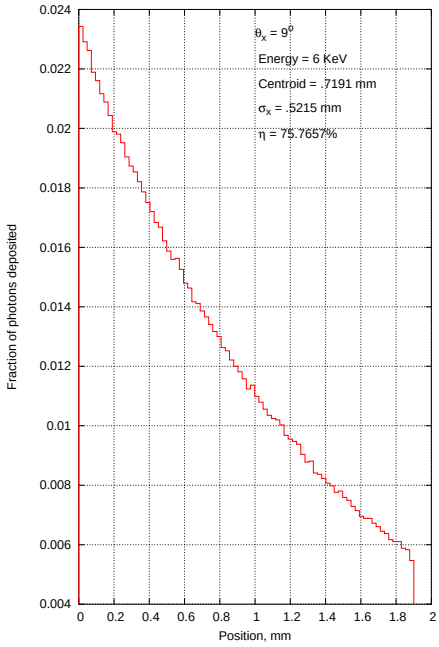

(d) 6 KeV X-ray photon incident at 9°

Figure 4.35: Probability of absorption of 6 KeV photon when incident at 6°, 7°, 8° and 9°

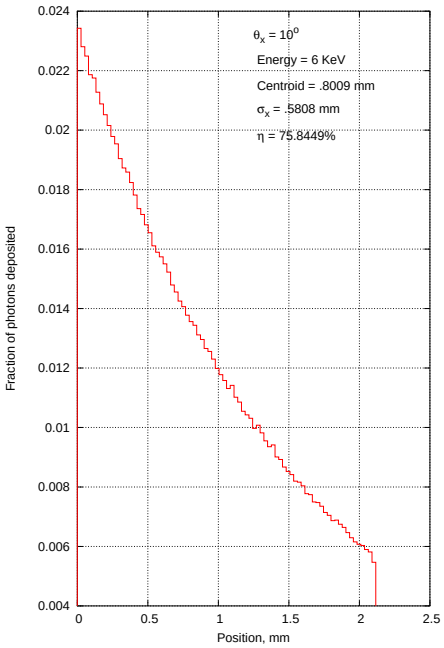

(a) 6 KeV X-ray photon incident at 10°

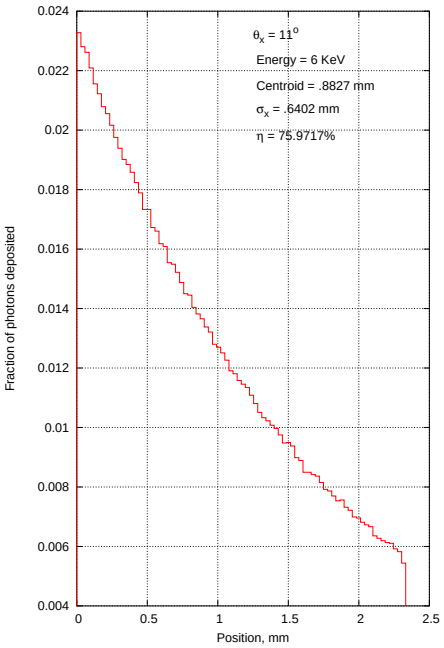

(b) 6 KeV X-ray photon incident at 11°

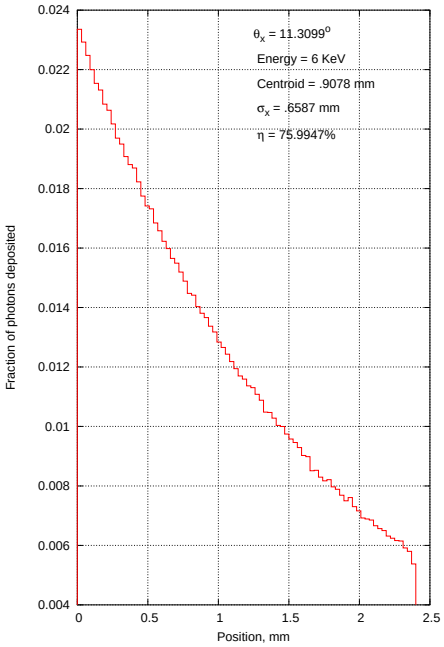

(c) 6 KeV X-ray photon incident at 11.3099°

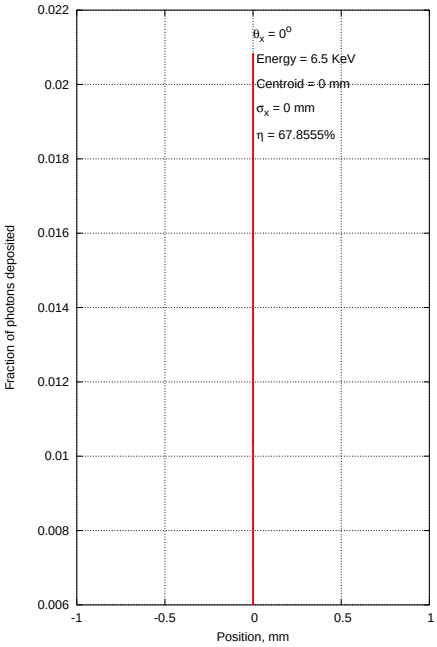

(d) 6.5 KeV X-ray photon incident at 0°

Figure 4.36: Probability of absorption of 6 KeV photon when incident at 10°, 11°, 11.3099° and 6.5 KeV at 0°

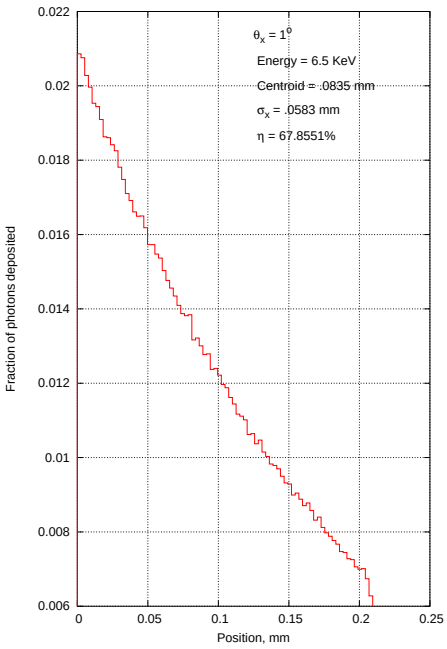

(a) 6.5 KeV X-ray photon incident at 1°

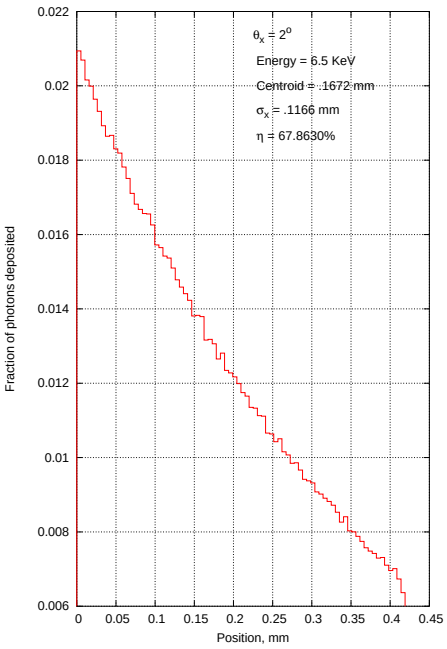

(b) 6.5 KeV X-ray photon incident at 2°

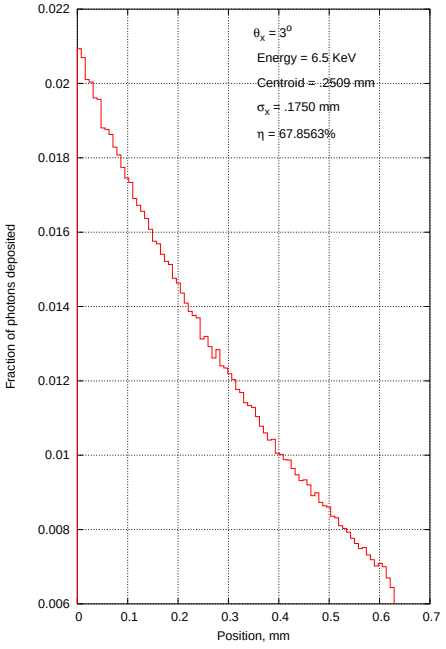

(c) 6.5 KeV X-ray photon incident at 3°

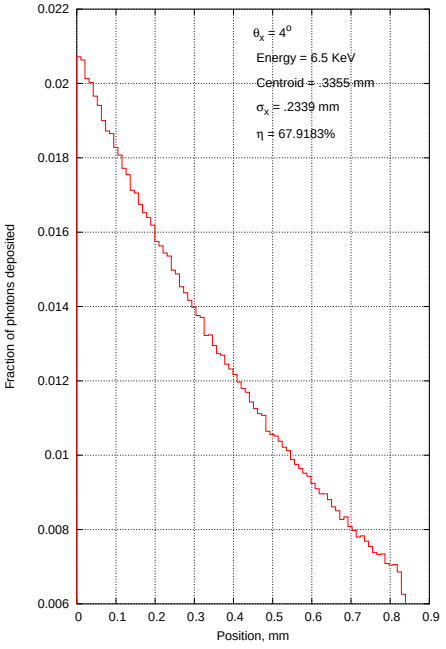

(d) 6.5 KeV X-ray photon incident at 4°

Figure 4.37: Probability of absorption of 6.5 KeV photon when incident at 1°, 2°, 3° and 4°

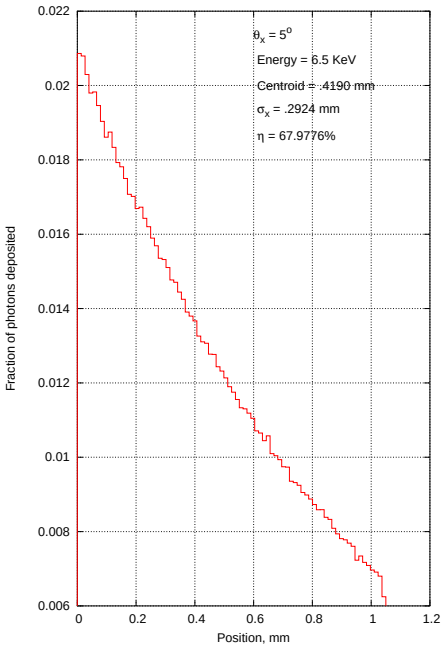

(a) 6.5 KeV X-ray photon incident at 5°

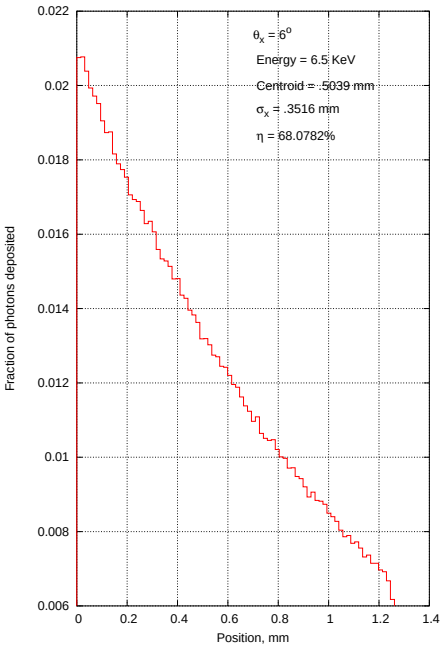

(b) 6.5 KeV X-ray photon incident at 6°

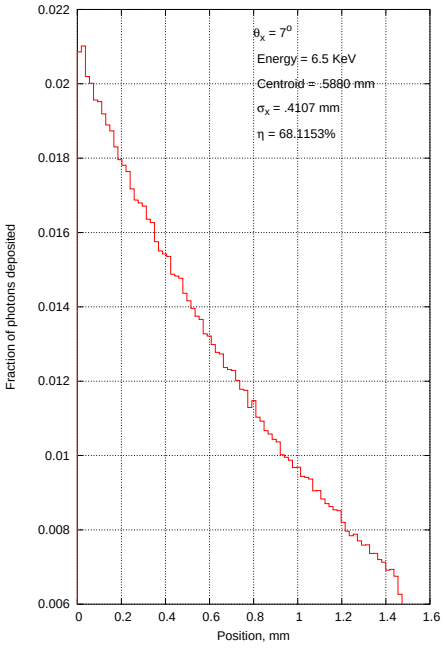

(c) 6.5 KeV X-ray photon incident at 7°

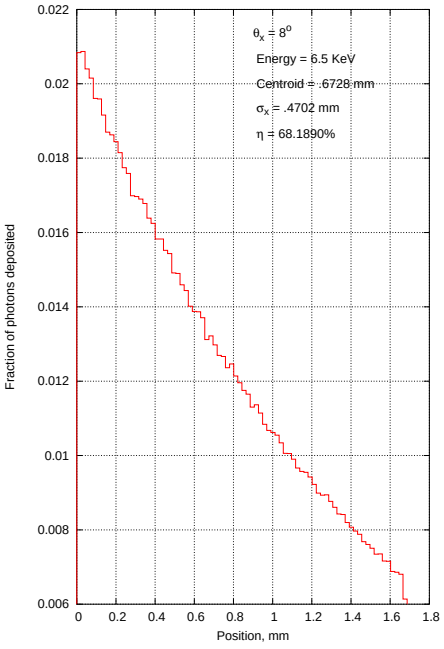

(d) 6.5 KeV X-ray photon incident at 8°

Figure 4.38: Probability of absorption of 6.5 KeV photon when incident at 5°, 6°, 7° and 8°

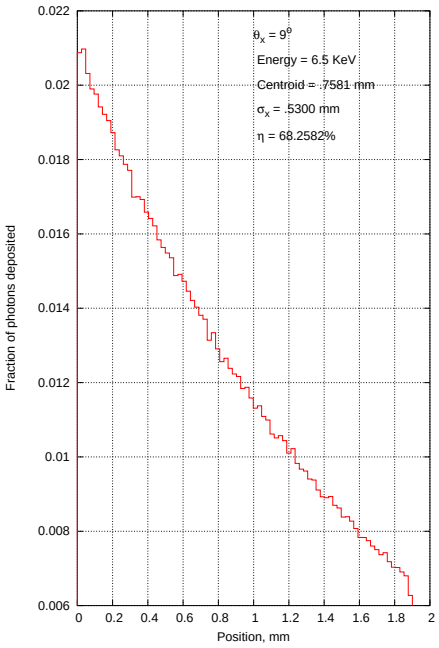

(a) 6.5 KeV X-ray photon incident at 9°

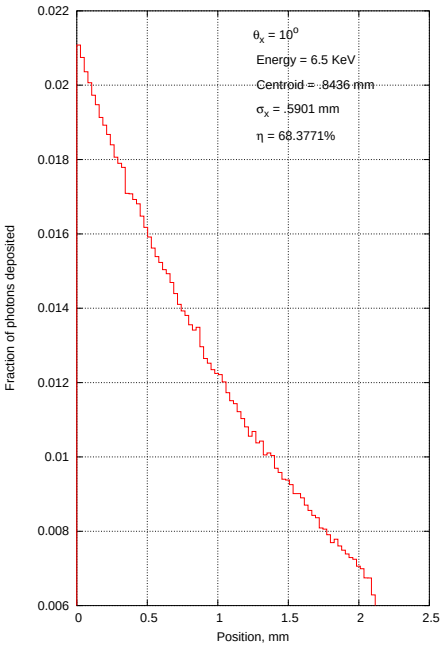

(b) 6.5 KeV X-ray photon incident at 10°

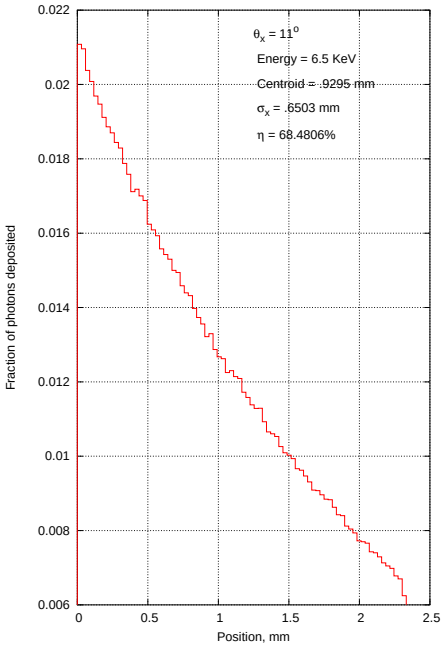

(c) 6.5 KeV X-ray photon incident at 11°

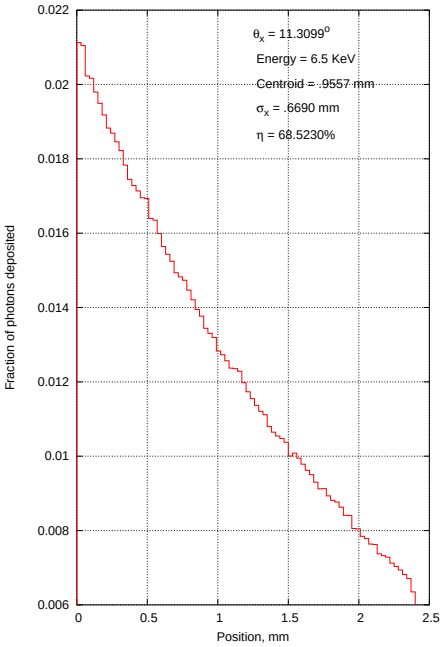

(d) 6.5 KeV X-ray photon incident at 11.3099°

Figure 4.39: Probability of absorption of 6.5 KeV photon when incident at 9°, 10°, 11° and 11.3099°

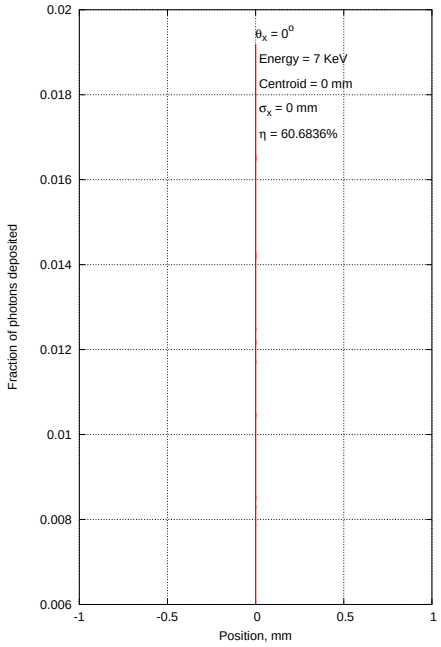

(a) 7 KeV X-ray photon incident at 0°

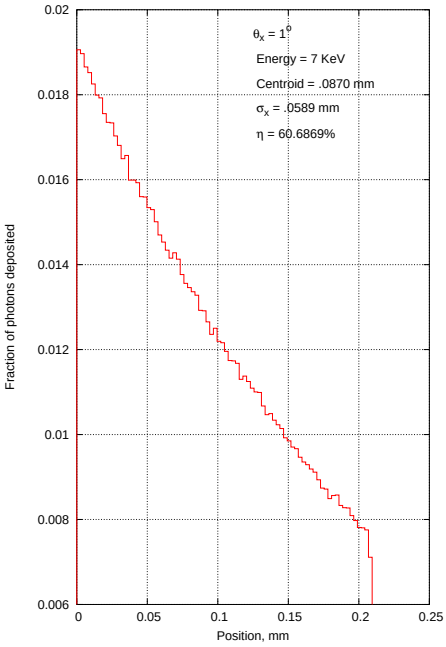

(b) 7 KeV X-ray photon incident at 1°

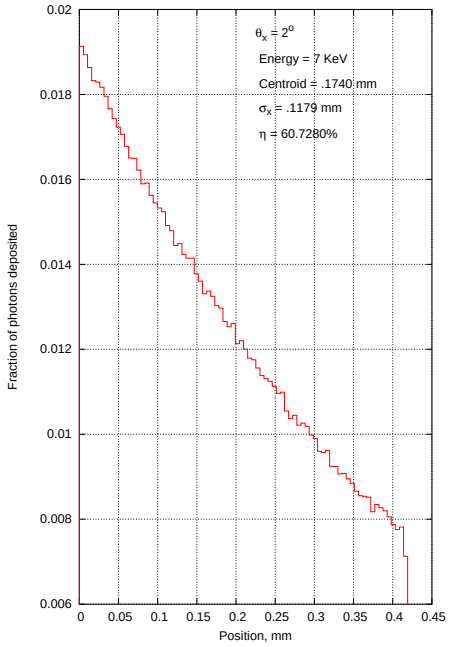

(c) 7 KeV X-ray photon incident at 2°

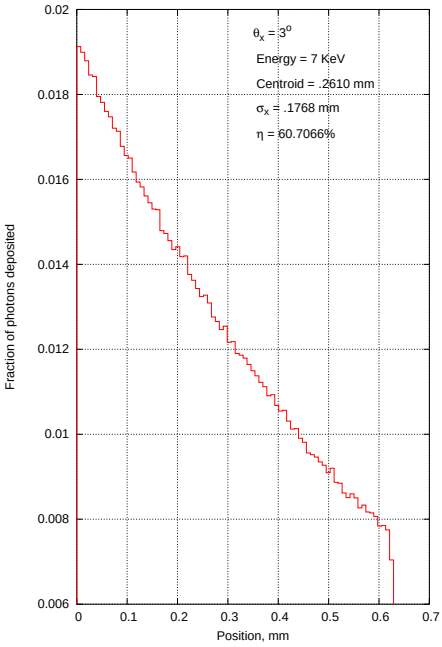

(d) 7 KeV X-ray photon incident at 3°

Figure 4.40: Probability of absorption of 7 KeV photon when incident at 0°, 1°, 2° and 3°

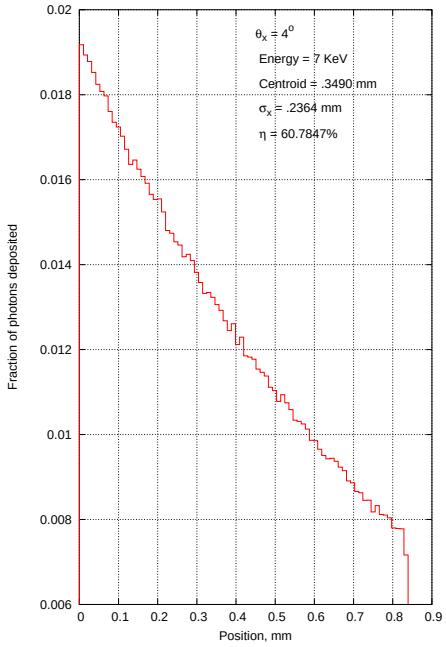

(a) 7 KeV X-ray photon incident at 4°

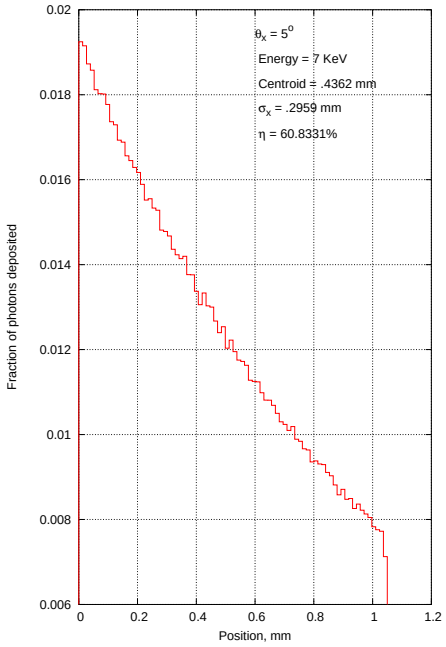

(b) 7 KeV X-ray photon incident at 5°

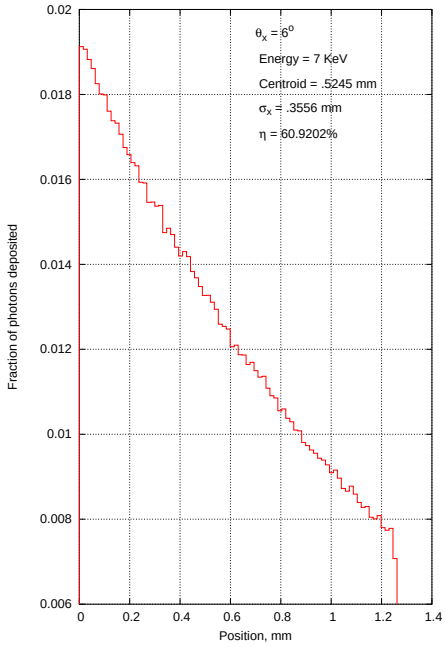

(c) 7 KeV X-ray photon incident at 6°

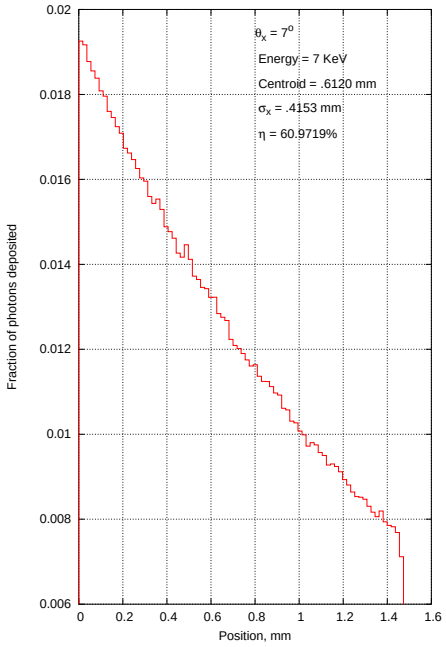

(d) 7 KeV X-ray photon incident at 7°

Figure 4.41: Probability of absorption of 7 KeV photon when incident at 4°, 5°, 6° and 7°

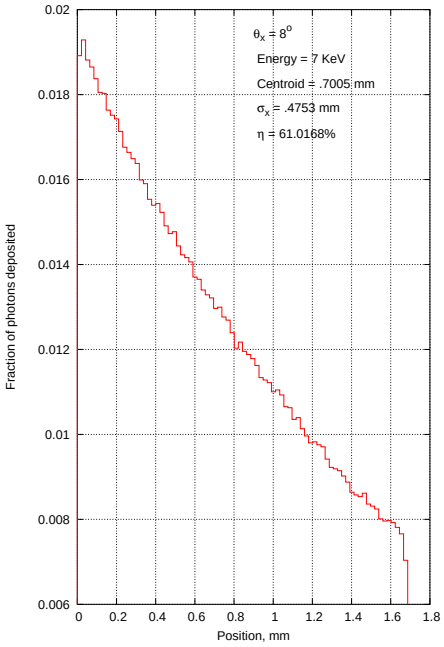

(a) 7 KeV X-ray photon incident at 8°

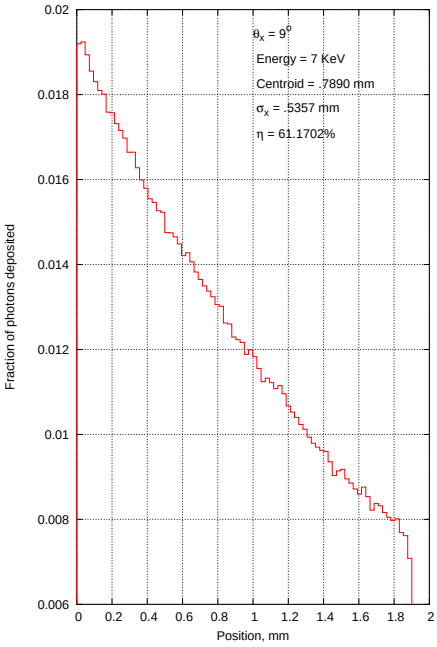

(b) 7 KeV X-ray photon incident at 9°

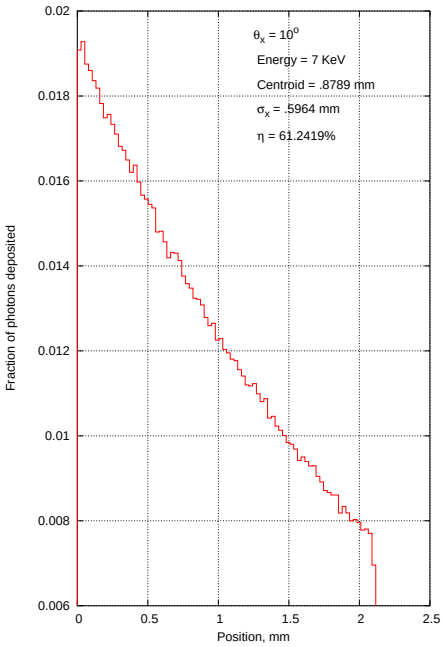

(c) 7 KeV X-ray photon incident at 10°

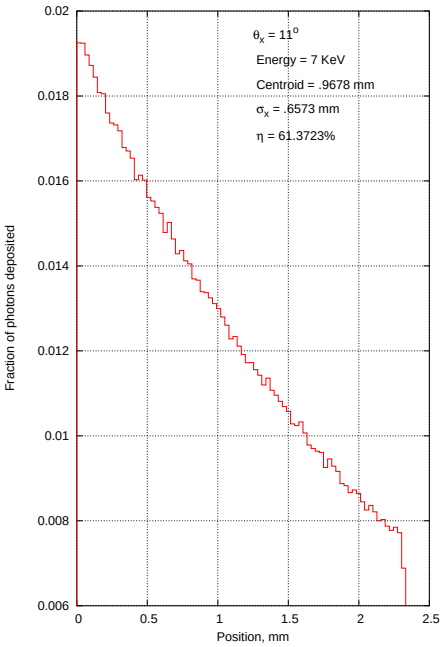

(d) 7 KeV X-ray photon incident at 11°

Figure 4.42: Probability of absorption of 7 KeV photon when incident at 8°, 9°, 10° and 11°

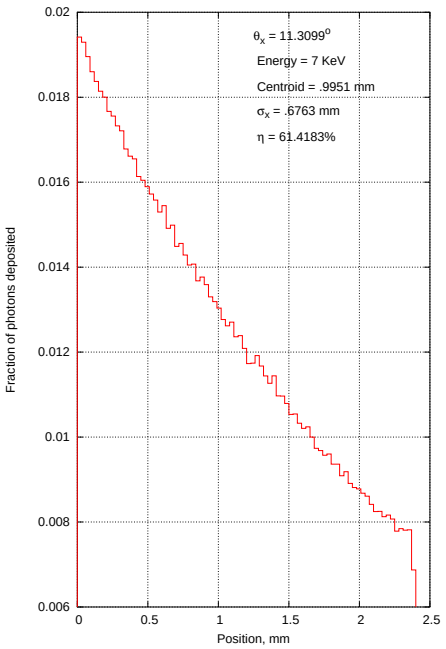

(a) 7 KeV X-ray photon incident at 11.3099°

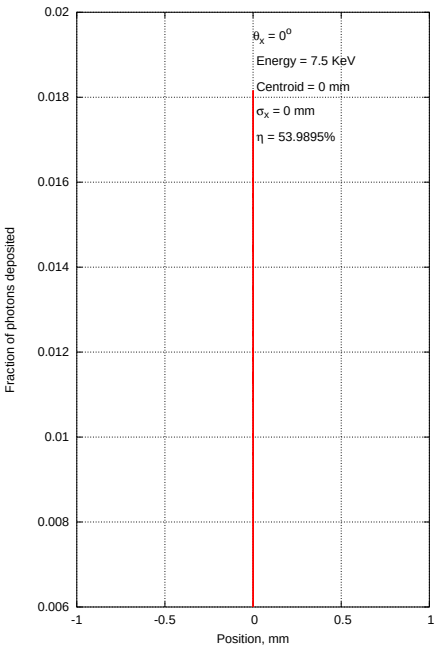

(b) 7.5 KeV X-ray photon incident at 0°

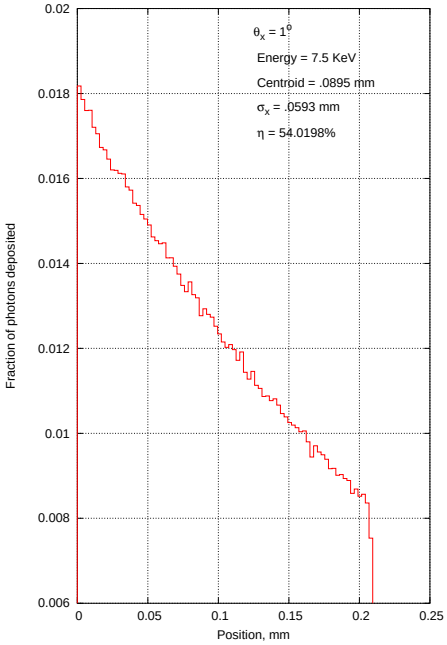

(c) 7.5 KeV X-ray photon incident at 1°

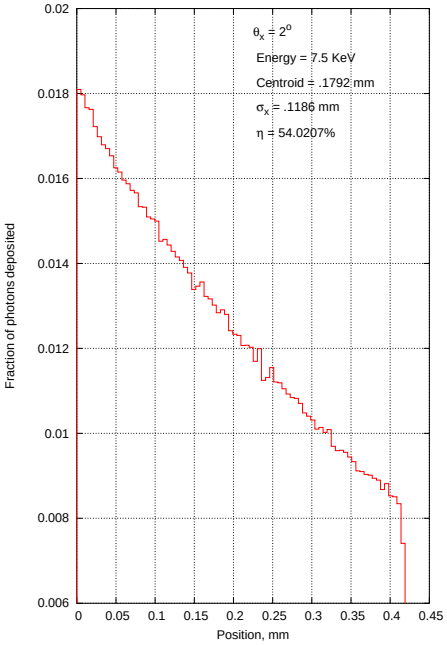

(d) 7.5 KeV X-ray photon incident at 2°

Figure 4.43: Probability of absorption of 7 KeV photon when incident at 11.3099° and 7.5 KeV at 0°, 1°, 2°

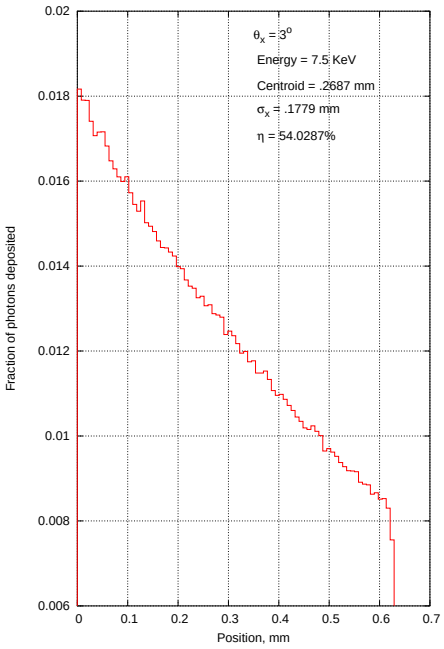

(a) 7.5 KeV X-ray photon incident at 3°

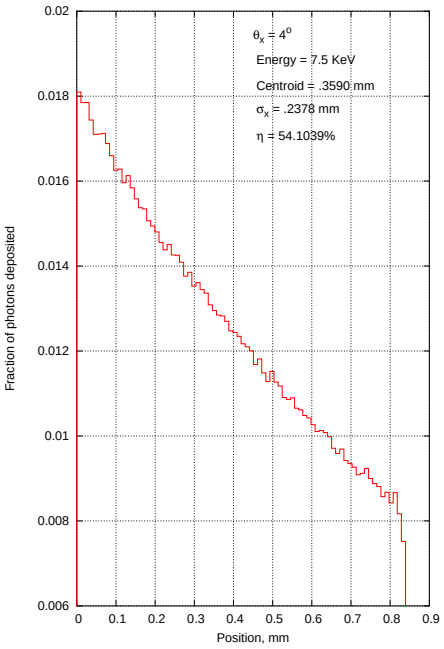

(b) 7.5 KeV X-ray photon incident at 4°

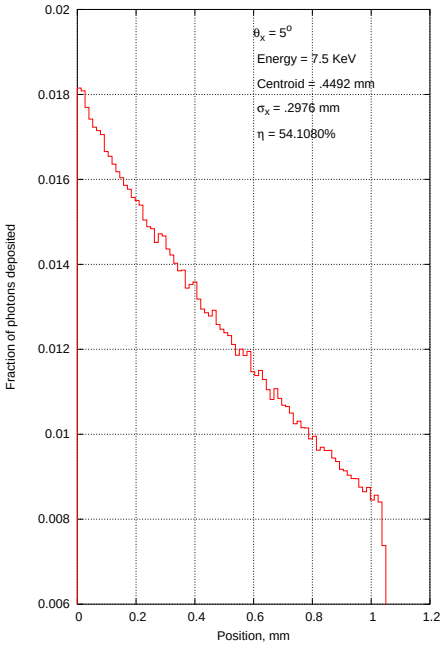

(c) 7.5 KeV X-ray photon incident at 5°

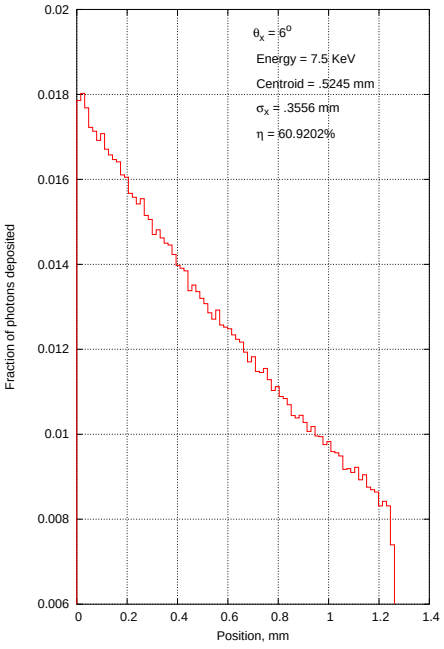

(d) 7.5 KeV X-ray photon incident at 6°

Figure 4.44: Probability of absorption of 7.5 KeV photon when incident at 3°, 4°, 5° and 6°

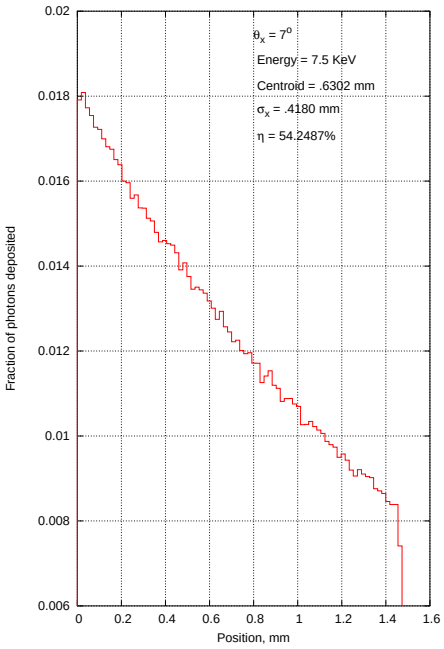

(a) 7.5 KeV X-ray photon incident at 7°

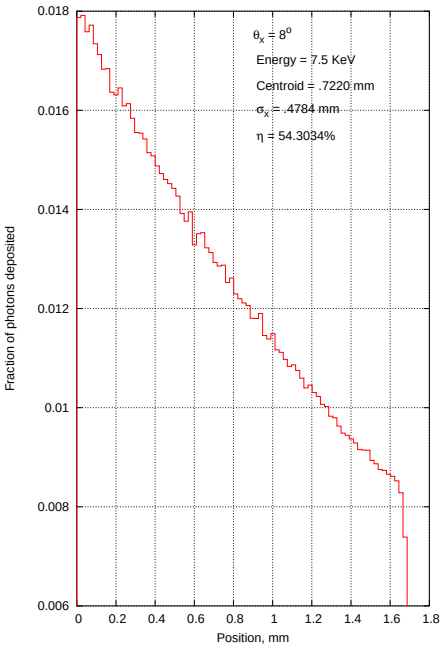

(b) 7.5 KeV X-ray photon incident at 8°

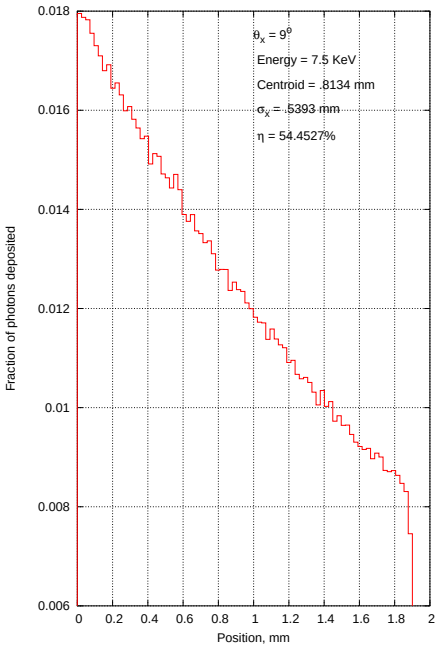

(c) 7.5 KeV X-ray photon incident at 9°

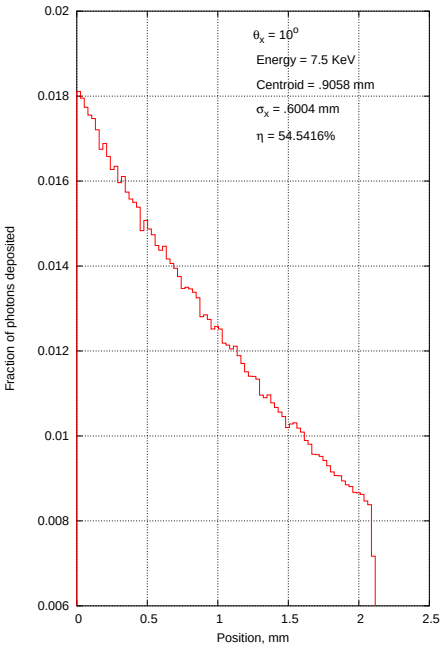

(d) 7.5 KeV X-ray photon incident at 10°

Figure 4.45: Probability of absorption of 7.5 KeV photon when incident at 7°, 8°, 9° and 10°

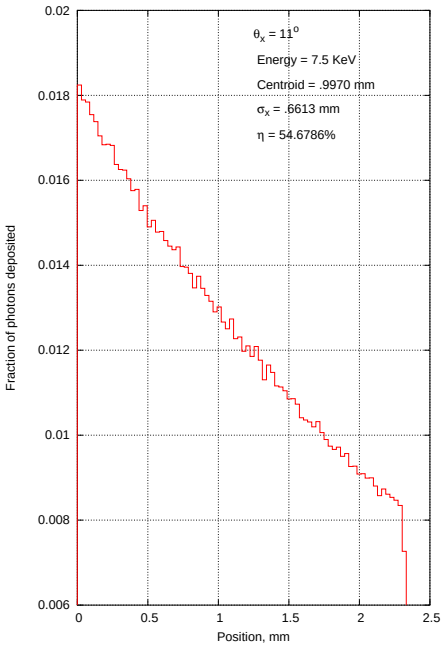

(a) 7.5 KeV X-ray photon incident at 11°

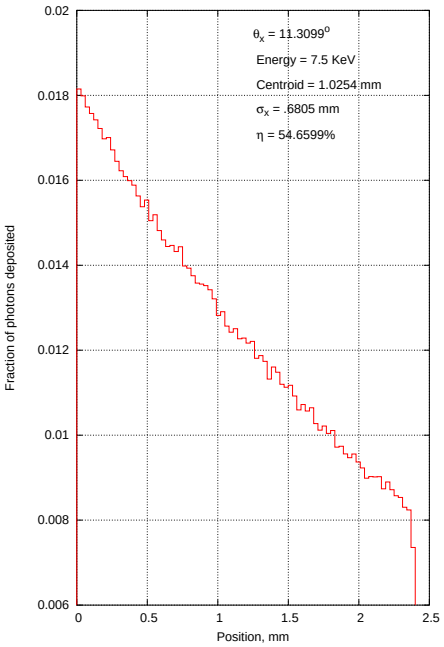

(b) 7.5 KeV X-ray photon incident at 11.3099°

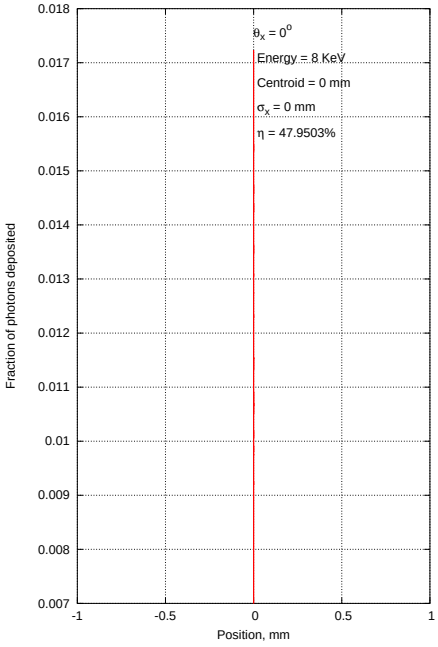

(c) 8 KeV X-ray photon incident at 0°

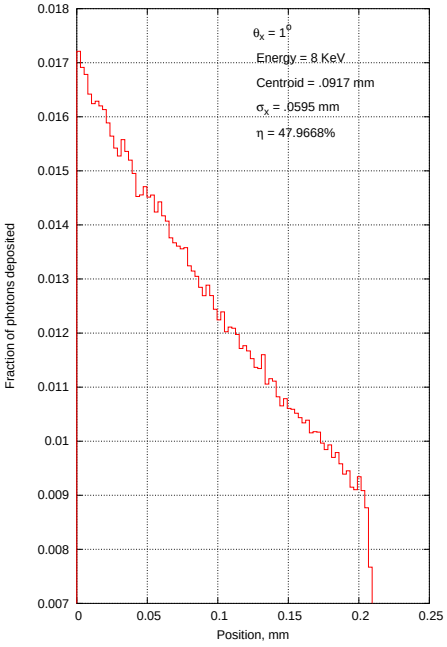

(d) 8 KeV X-ray photon incident at 1°

Figure 4.46: Probability of absorption of 7.5 KeV photon when incident at 11°, 11.3099° and 8 KeV at 0°, 1°

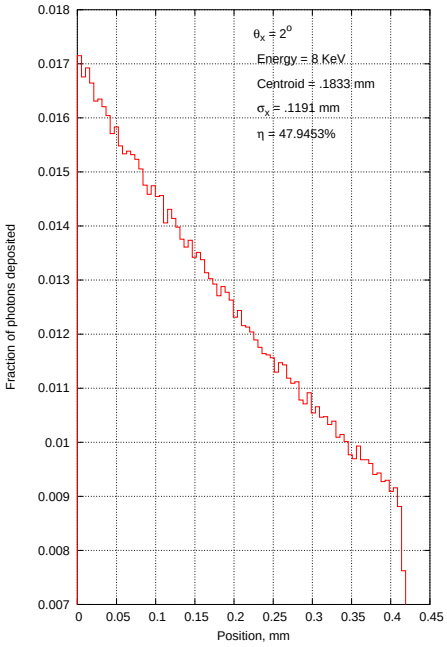

(a) 8 KeV X-ray photon incident at 2°

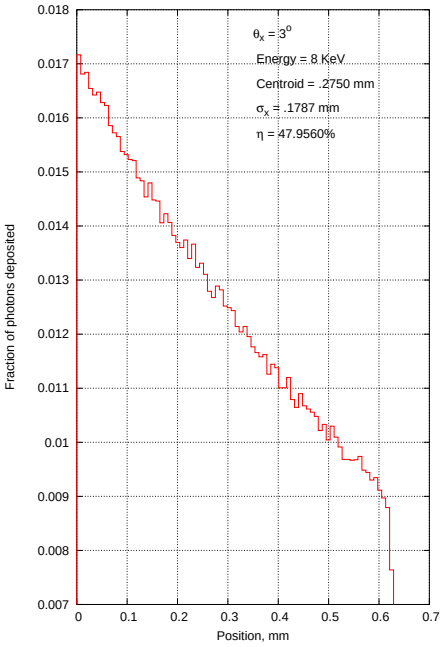

(b) 8 KeV X-ray photon incident at 3°

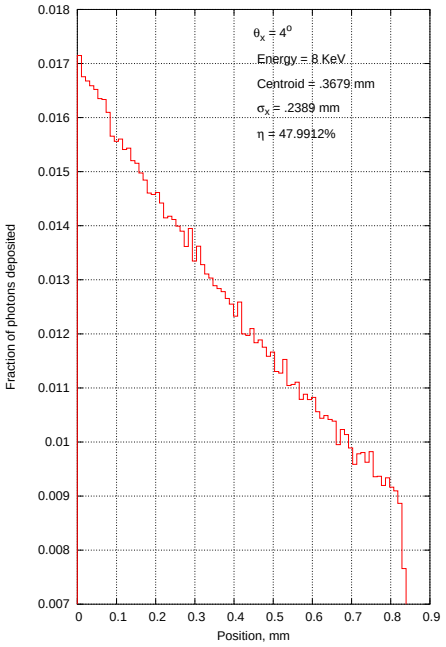

(c) 8 KeV X-ray photon incident at 4°

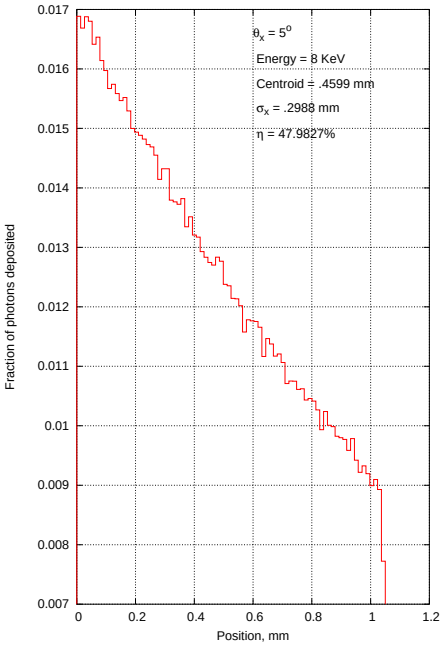

(d) 8 KeV X-ray photon incident at 5°

Figure 4.47: Probability of absorption of 8 KeV photon when incident at 2°, 3°, 4° and 5°

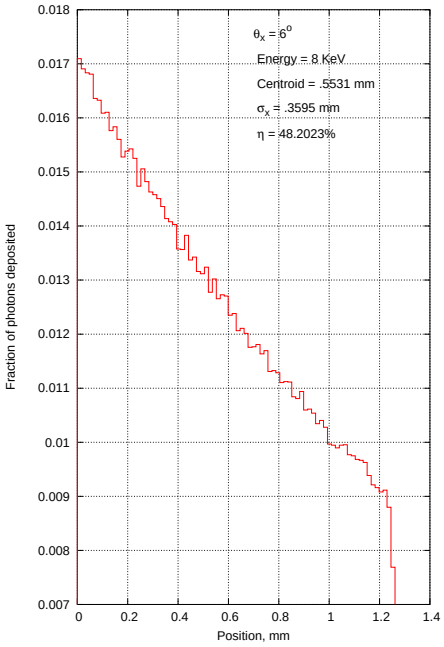

(a) 8 KeV X-ray photon incident at 6°

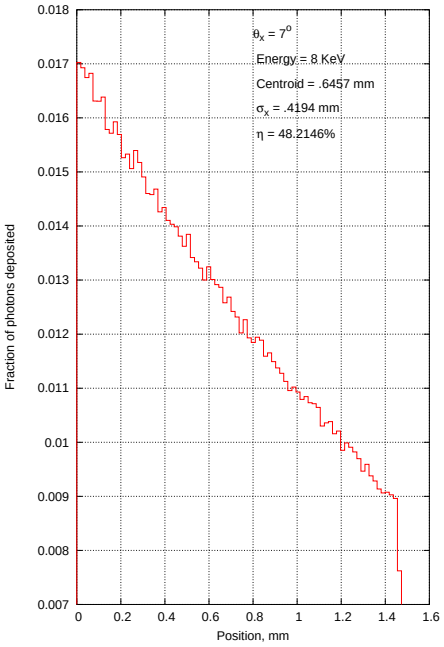

(b) 8 KeV X-ray photon incident at 7°

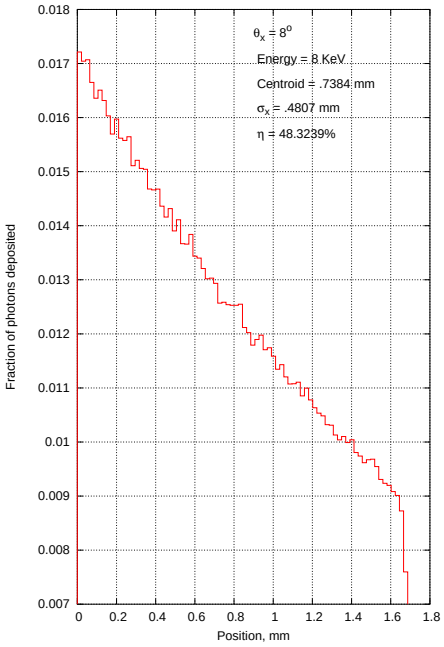

(c) 8 KeV X-ray photon incident at 8°

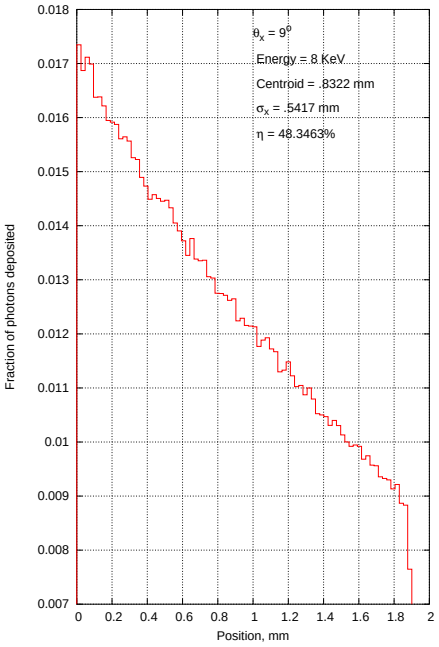

(d) 8 KeV X-ray photon incident at 9°

Figure 4.48: Probability of absorption of 8 KeV photon when incident at 6°, 7°, 8° and 9°

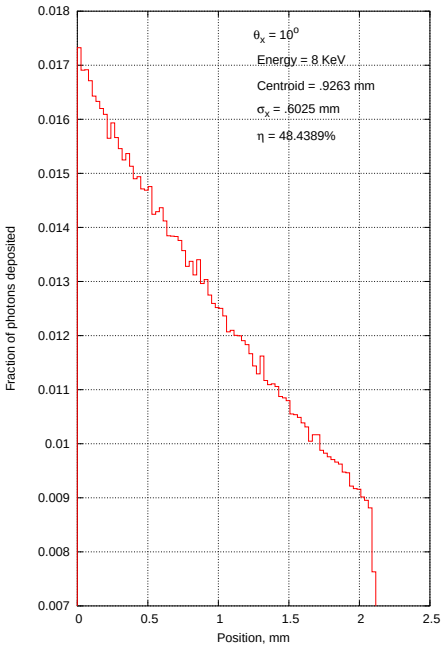

(a) 8 KeV X-ray photon incident at 10°

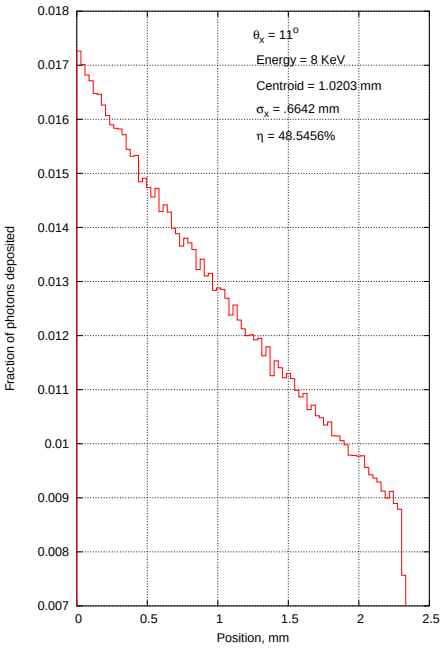

(b) 8 KeV X-ray photon incident at 11°

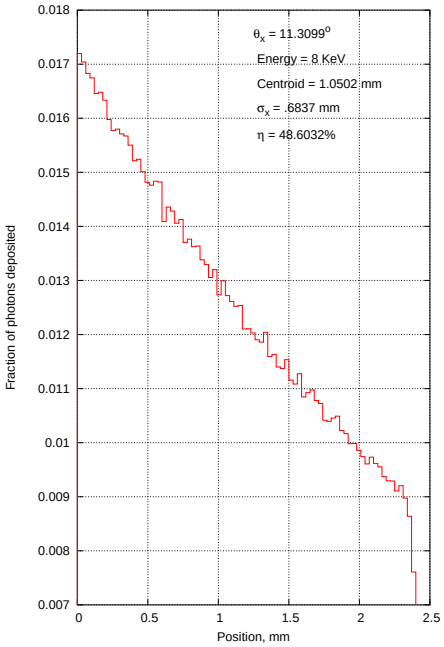

(c) 8 KeV X-ray photon incident at 11.3099°

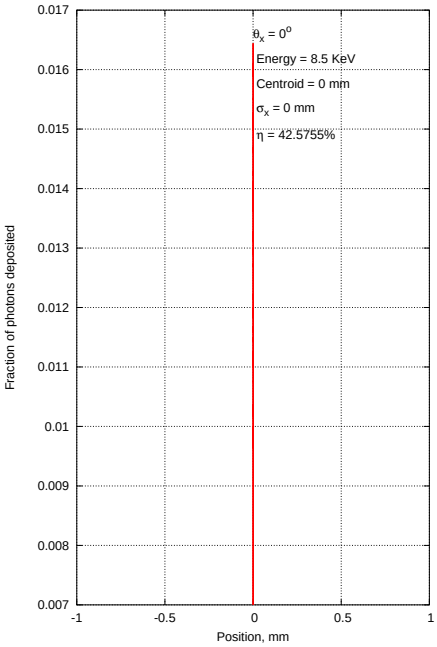

(d) 8.5 KeV X-ray photon incident at 0°

Figure 4.49: Probability of absorption of 8 KeV photon when incident at 10°, 11°, 11.3099° and 8.5 KeV at 0°

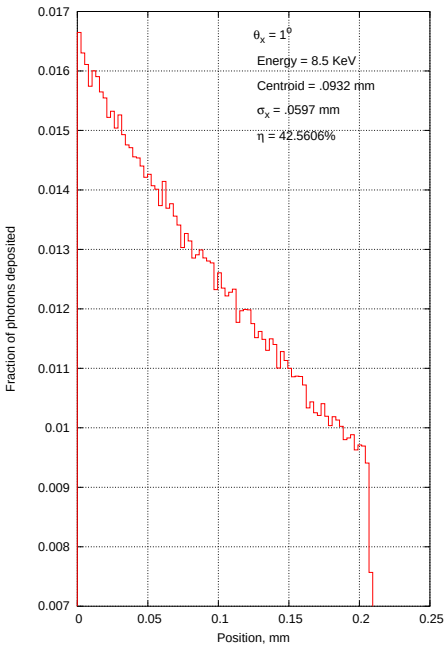

(a) 8.5 KeV X-ray photon incident at 1°

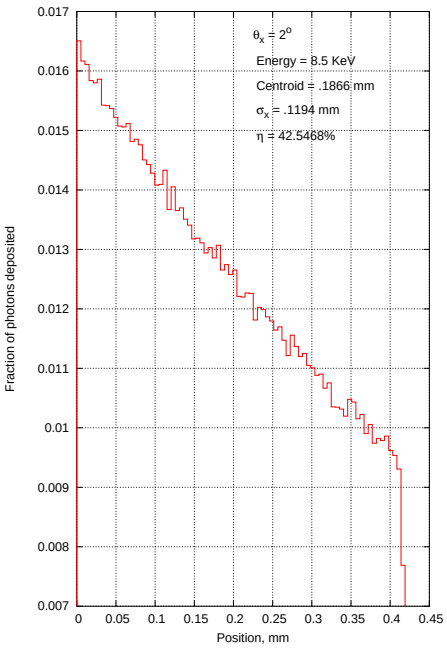

(b) 8.5 KeV X-ray photon incident at 2°

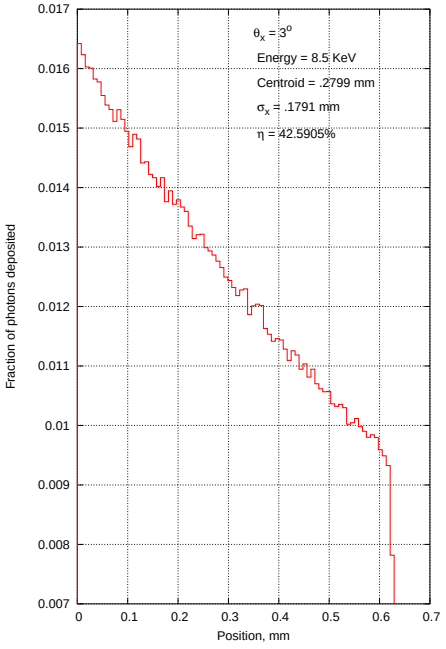

(c) 8.5 KeV X-ray photon incident at 3°

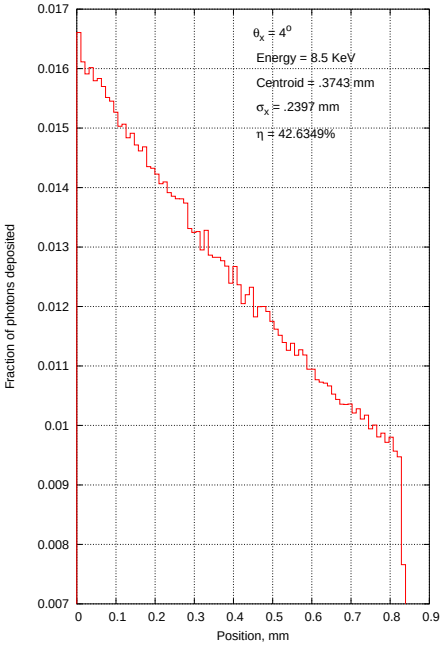

(d) 8.5 KeV X-ray photon incident at 4°

Figure 4.50: Probability of absorption of 8.5 KeV photon when incident at 1°, 2°, 3° and 4°

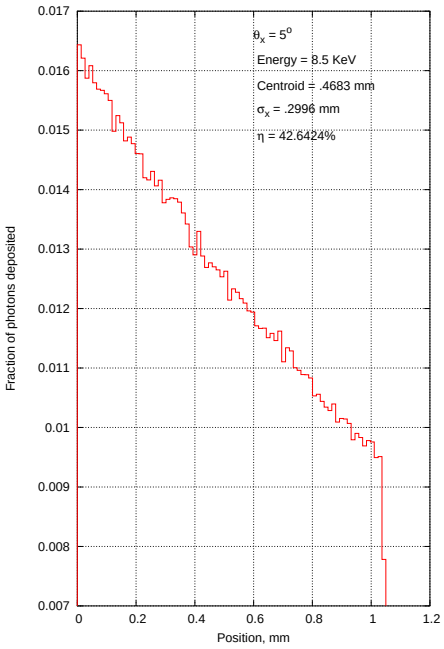

(a) 8.5 KeV X-ray photon incident at 5°

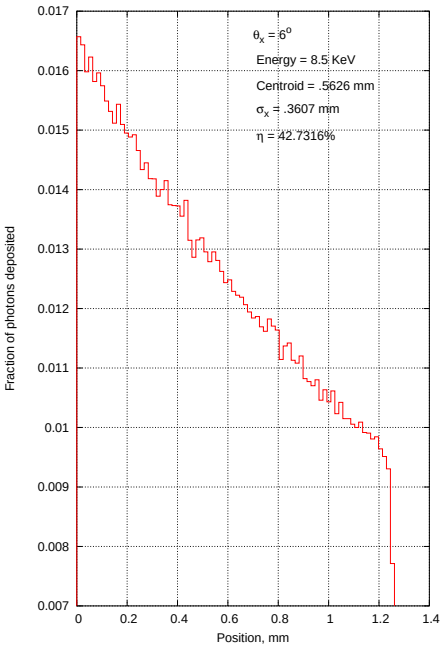

(b) 8.5 KeV X-ray photon incident at 6°

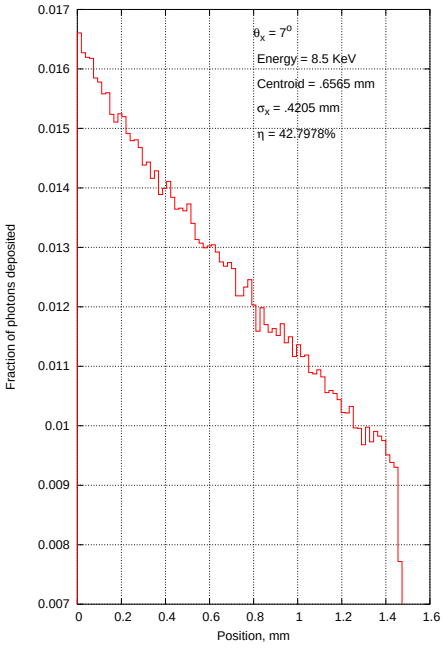

(c) 8.5 KeV X-ray photon incident at 7°

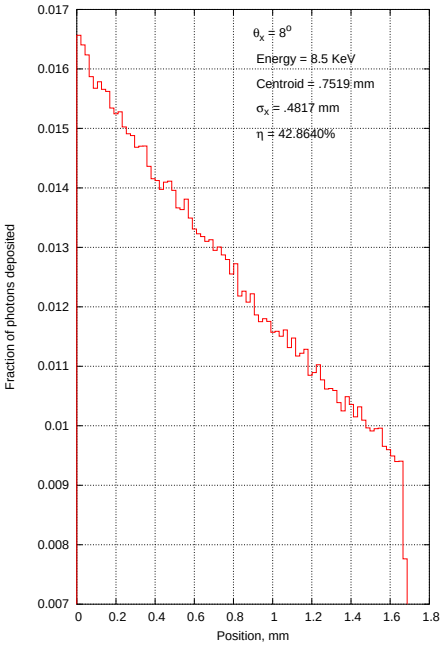

(d) 8.5 KeV X-ray photon incident at 8°

Figure 4.51: Probability of absorption of 8.5 KeV photon when incident at 5^o, 6^o, 7^o and 8^o

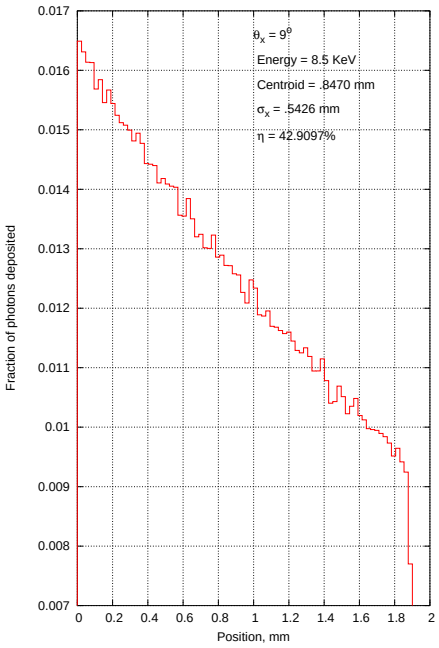

(a) 8.5 KeV X-ray photon incident at 9°

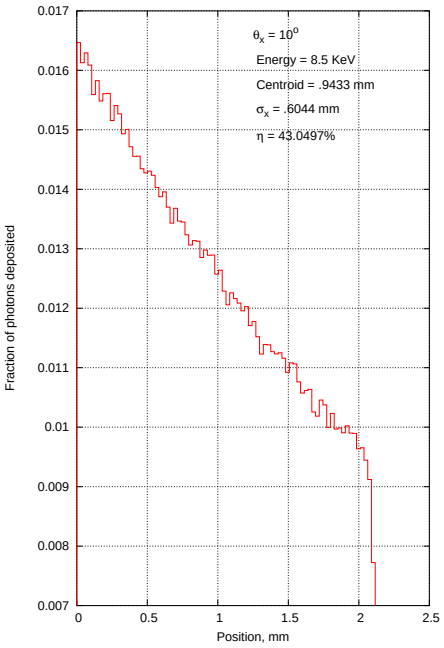

(b) 8.5 KeV X-ray photon incident at 10°

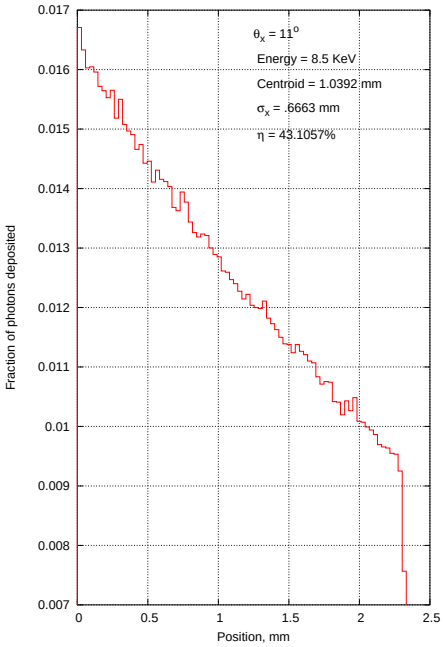

(c) 8.5 KeV X-ray photon incident at 11°

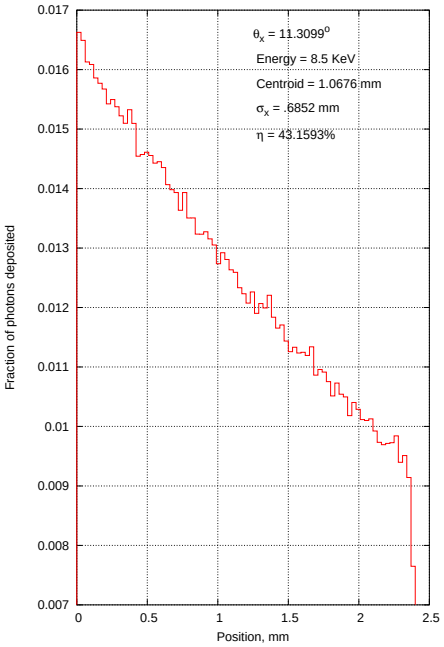

(d) 8.5 KeV X-ray photon incident at 11.3099°

Figure 4.52: Probability of absorption of 8.5 KeV photon when incident at 9°, 10°, 11° and 11.3099^o

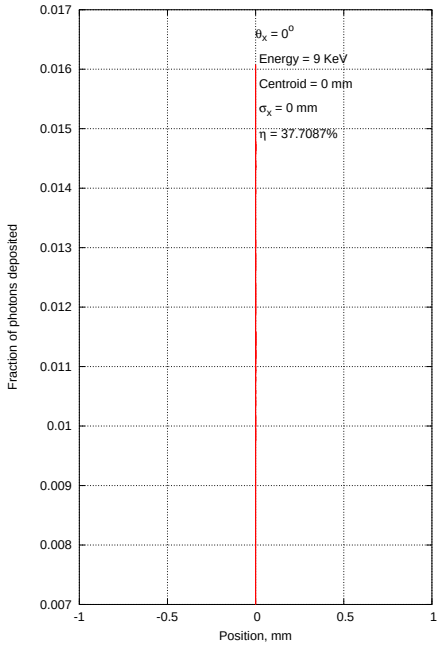

(a) 9 KeV X-ray photon incident at 0°

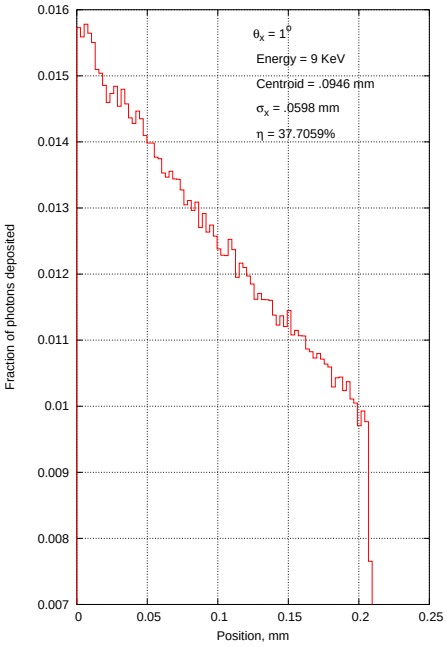

(b) 9 KeV X-ray photon incident at 1°

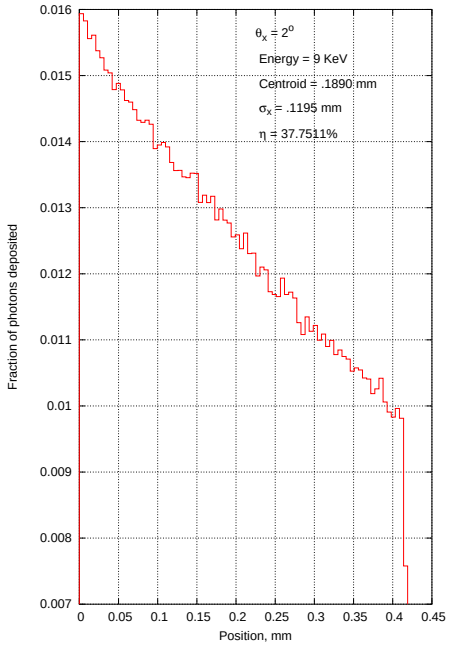

(c) 9 KeV X-ray photon incident at 2°

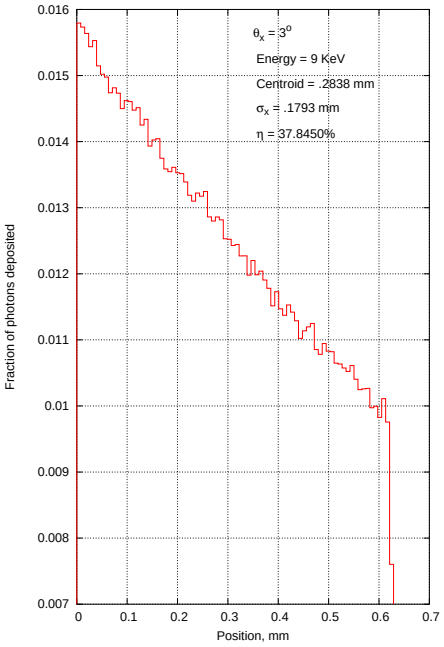

(d) 9 KeV X-ray photon incident at 3°

Figure 4.53: Probability of absorption of 9 KeV photon when incident at 0^o, 1^o, 2^o and 3^o

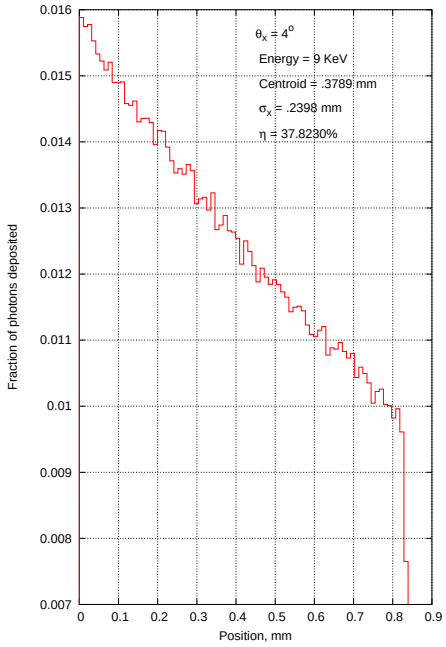

(a) 9 KeV X-ray photon incident at 4°

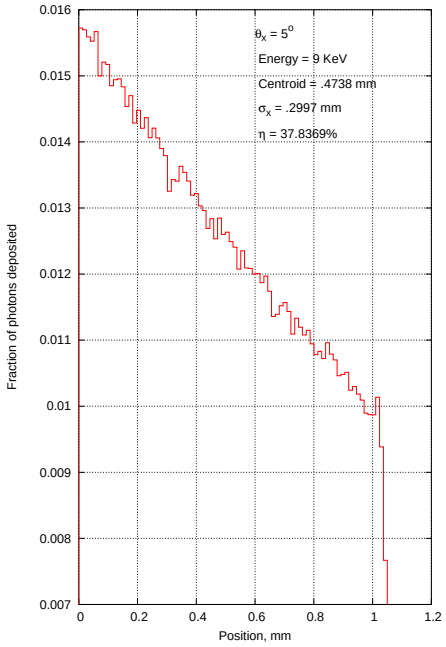

(b) 9 KeV X-ray photon incident at 5°

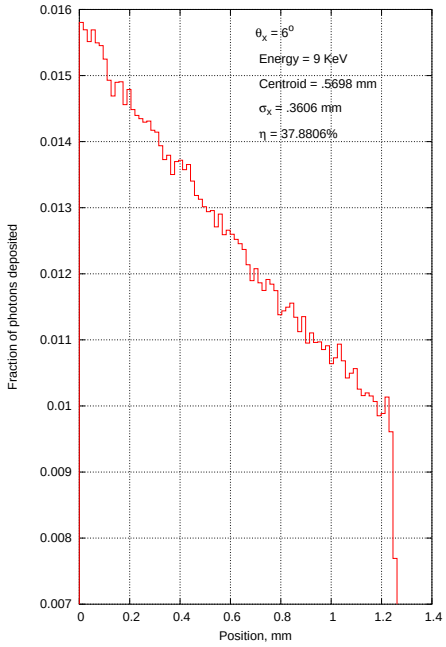

(c) 9 KeV X-ray photon incident at 6°

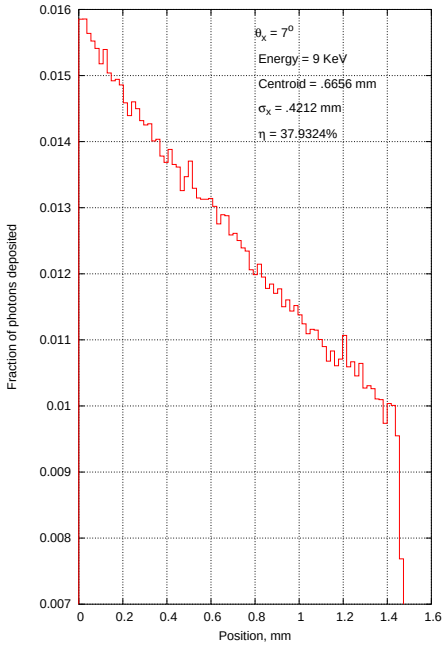

(d) 9 KeV X-ray photon incident at 7°

Figure 4.54: Probability of absorption of 9 KeV photon when incident at 4°, 5°, 6° and 7°

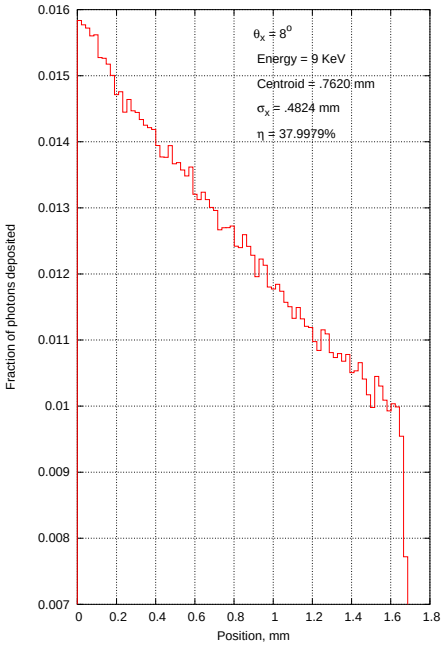

(a) 9 KeV X-ray photon incident at 8°

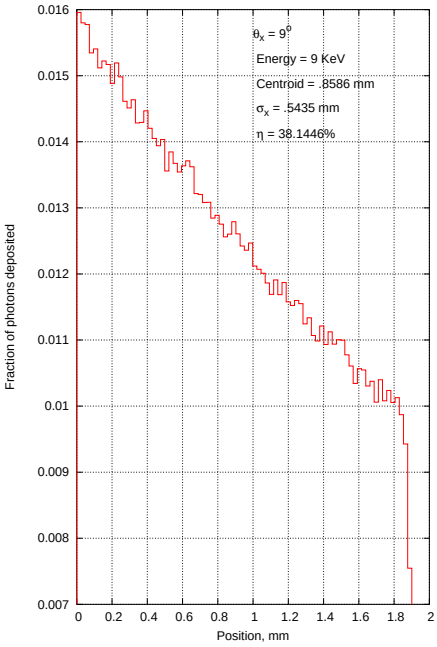

(b) 9 KeV X-ray photon incident at 9°

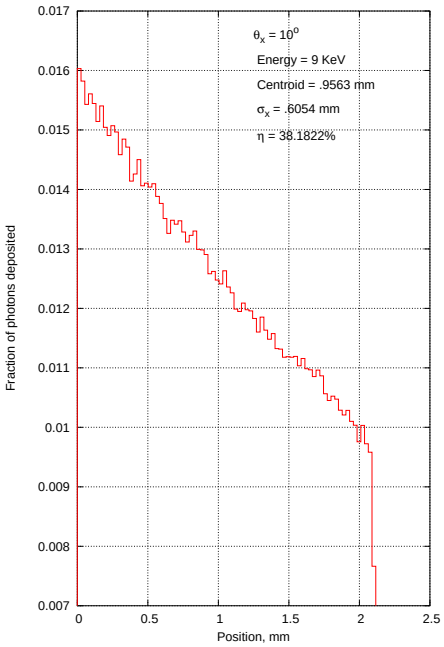

(c) 9 KeV X-ray photon incident at 10°

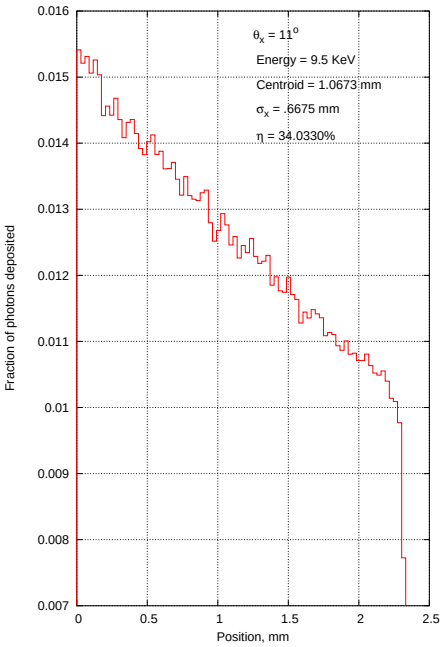

(d) 9.5 KeV X-ray photon incident at 11°

Figure 4.55: Probability of absorption of 9 KeV photon when incident at 8°, 9°, 10° and 11°

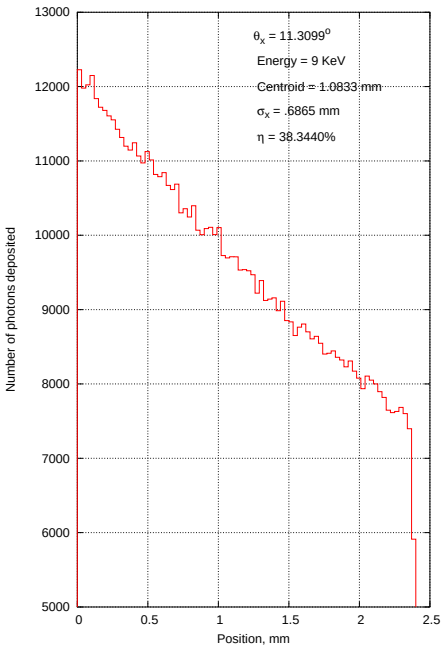

(a) 9 KeV X-ray photon incident at 11.3099°

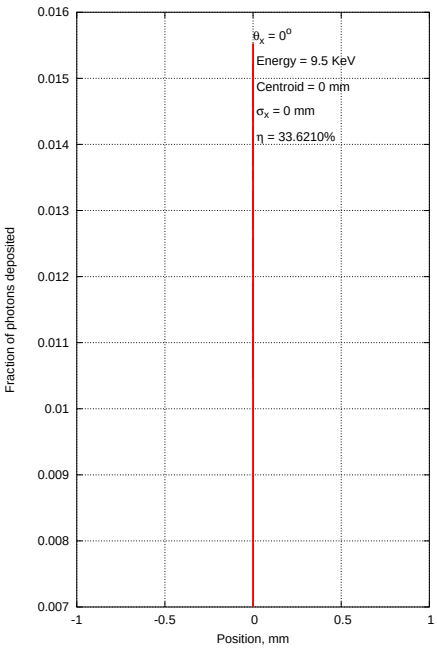

(b) 9.5 KeV X-ray photon incident at 0°

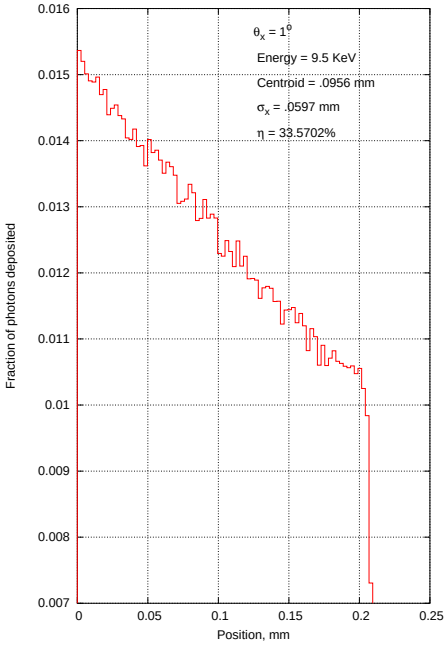

(c) 9.5 KeV X-ray photon incident at 1°

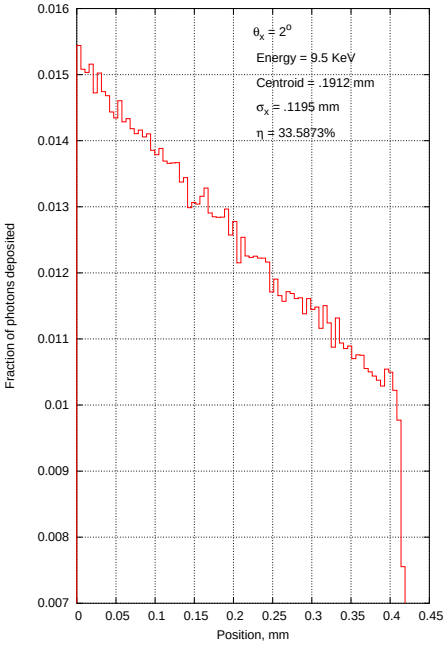

(d) 9.5 KeV X-ray photon incident at 2°

Figure 4.56: Probability of absorption of 9 KeV photon when incident at 11.3099° and 9.5 KeV at 0°, 1°, 2°

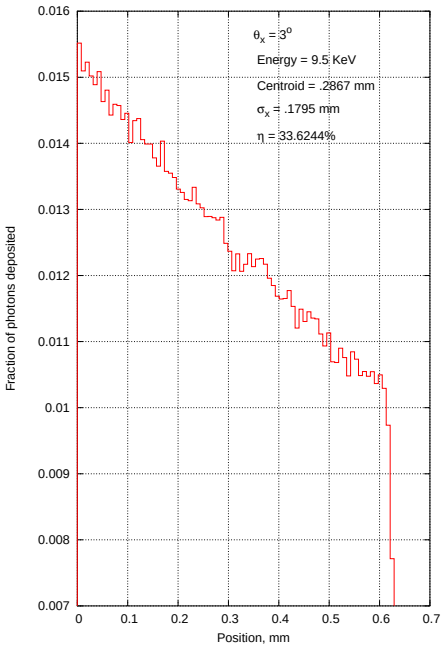

(a) 9.5 KeV X-ray photon incident at 3°

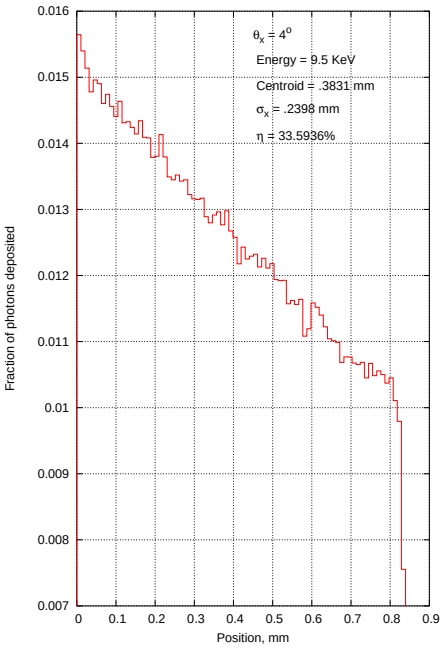

(b) 9.5 KeV X-ray photon incident at 4°

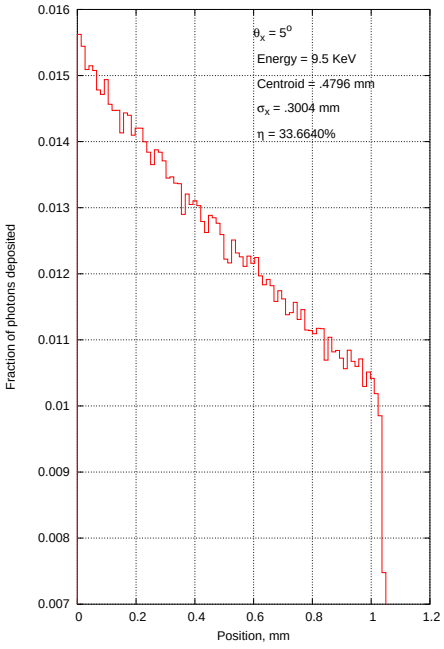

(c) 9.5 KeV X-ray photon incident at 5°

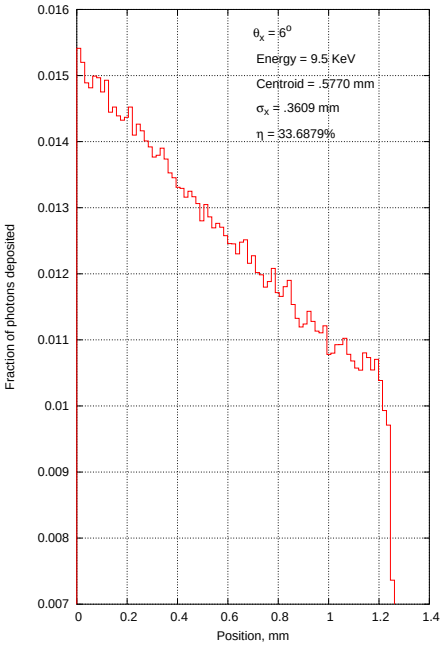

(d) 9.5 KeV X-ray photon incident at 6°

Figure 4.57: Probability of absorption of 9.5 KeV photon when incident at 3°, 4°, 5° and 6°

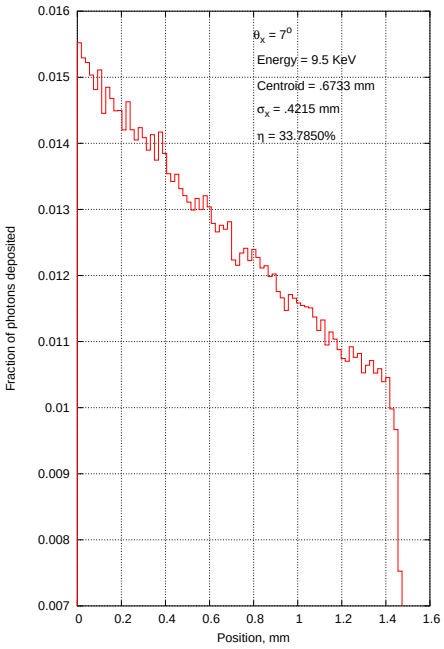

(a) 9.5 KeV X-ray photon incident at 7°

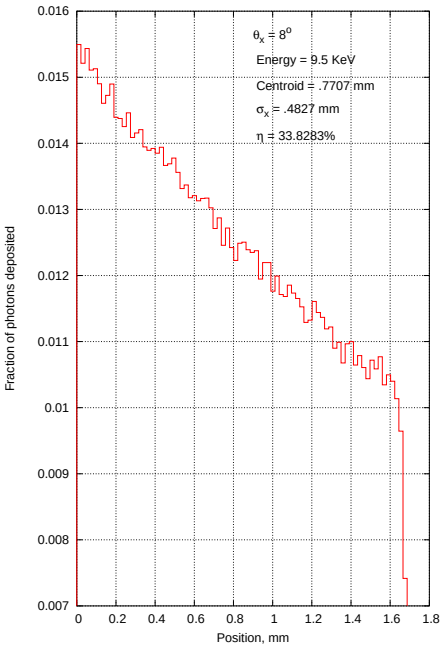

(b) 9.5 KeV X-ray photon incident at 8°

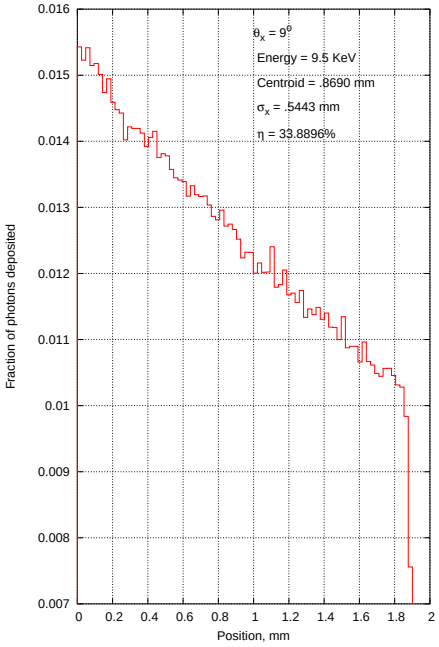

(c) 9.5 KeV X-ray photon incident at 9°

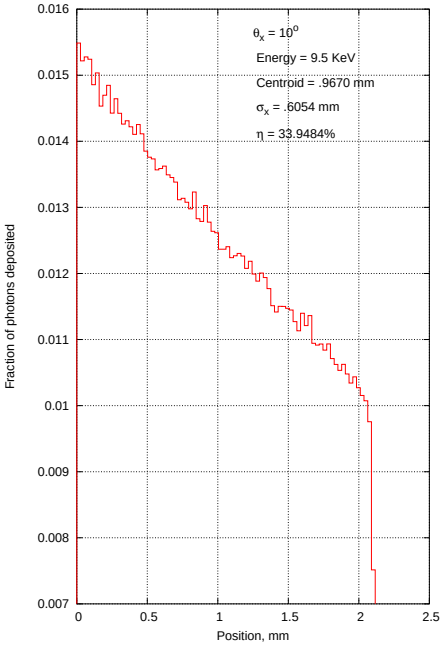

(d) 9.5 KeV X-ray photon incident at 10°

Figure 4.58: Probability of absorption of 9.5 KeV photon when incident at 7°, 8°, 9° and 10°

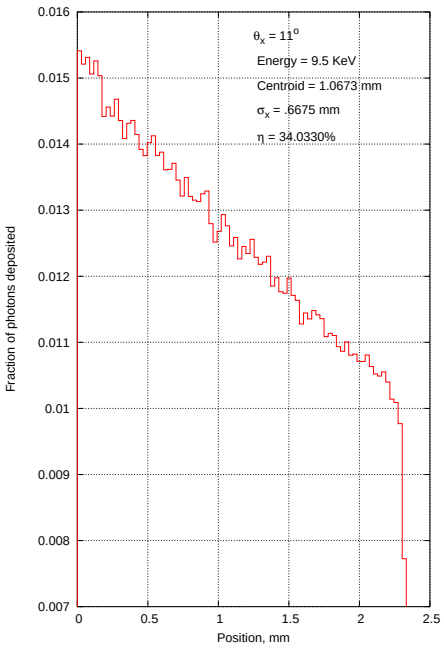

(a) 9.5 KeV X-ray photon incident at 11°

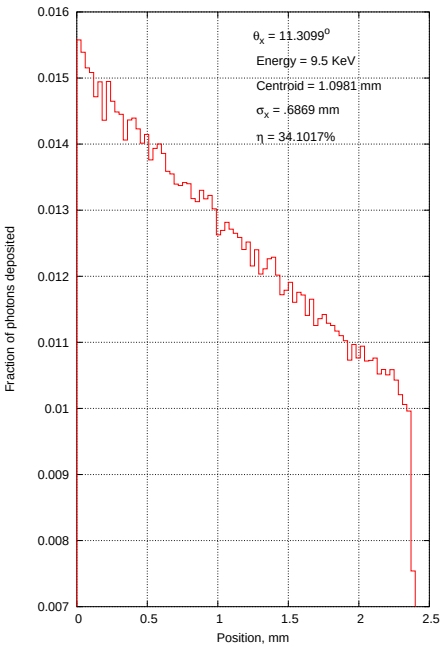

(b) 9.5 KeV X-ray photon incident at 11.3099°

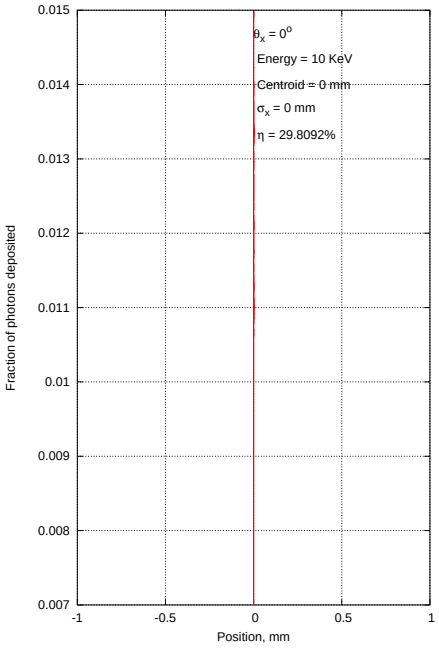

(c) 10 KeV X-ray photon incident at 0°

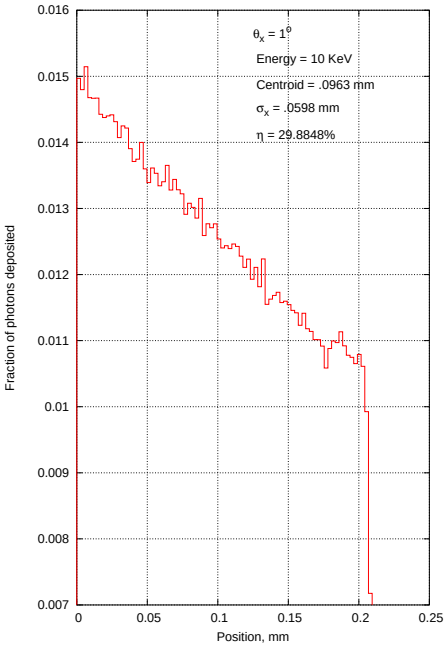

(d) 10 KeV X-ray photon incident at 1°

Figure 4.59: Probability of absorption of 9.5 KeV photon when incident at 11°, 11.3099° and 10 KeV at 0°, 1°

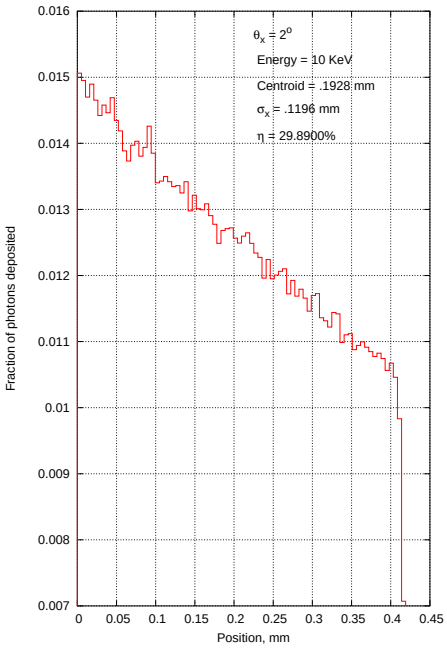

(a) 10 KeV X-ray photon incident at 2°

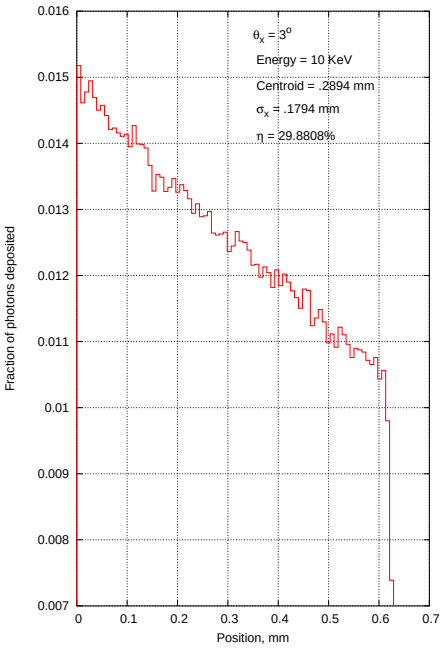

(b) 10 KeV X-ray photon incident at 3°

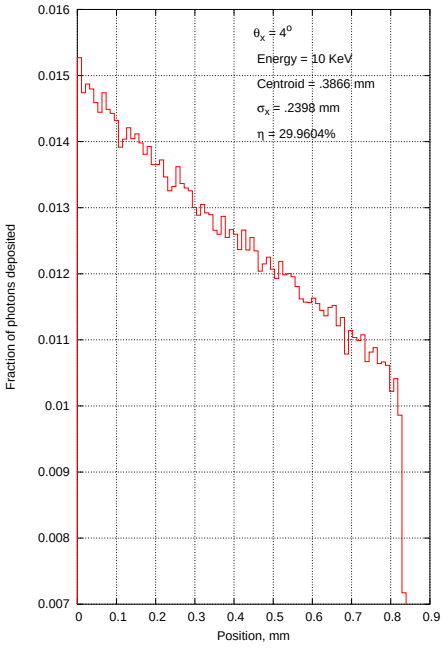

(c) 10 KeV X-ray photon incident at 4°

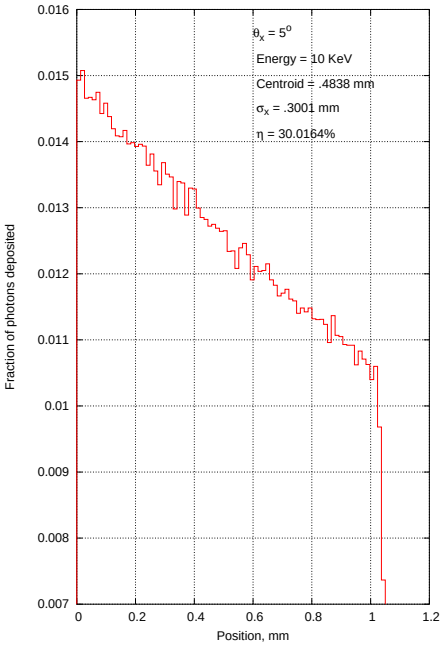

(d) 10 KeV X-ray photon incident at 5°

Figure 4.60: Probability of absorption of 10 KeV photon when incident at 2°, 3°, 4° and 5°

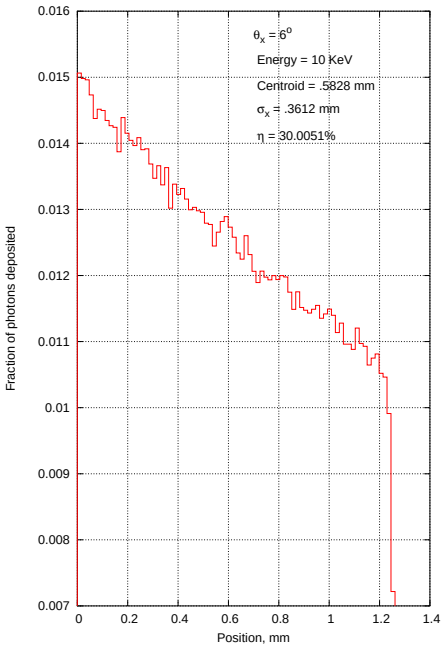

(a) 10 KeV X-ray photon incident at 6°

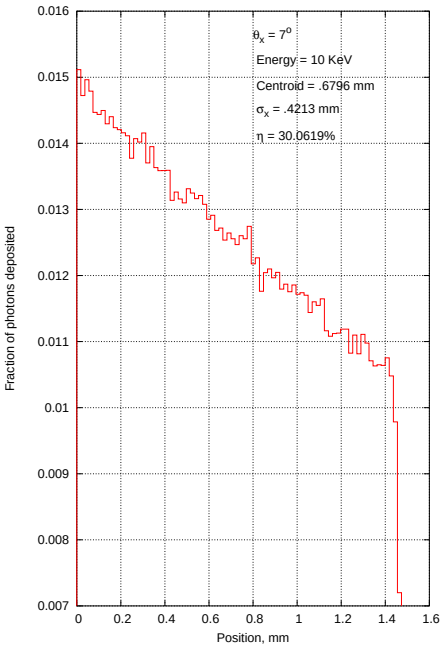

(b) 10 KeV X-ray photon incident at 7°

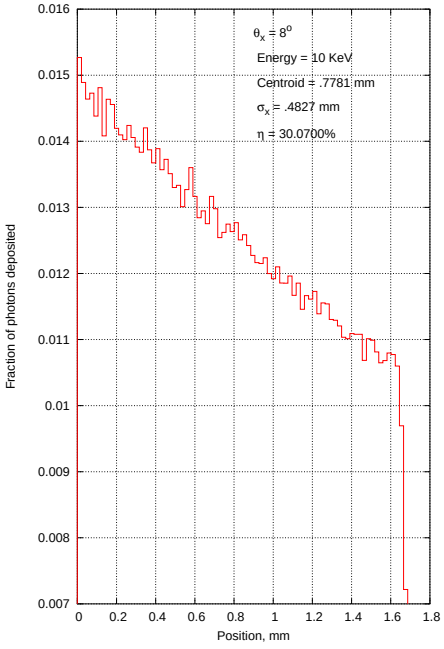

(c) 10 KeV X-ray photon incident at 8°

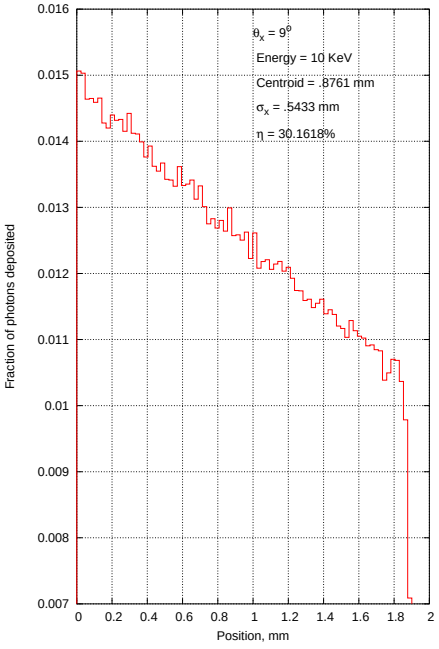

(d) 10 KeV X-ray photon incident at 9°

Figure 4.61: Probability of absorption of 10 KeV photon when incident at 6°, 7°, 8° and 9°

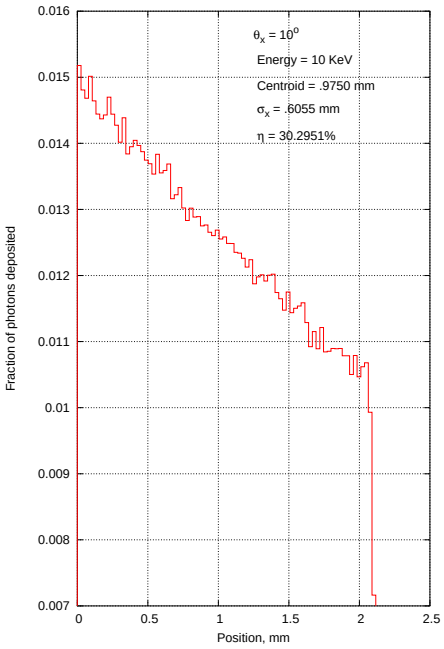

(a) 10 KeV X-ray photon incident at 10°

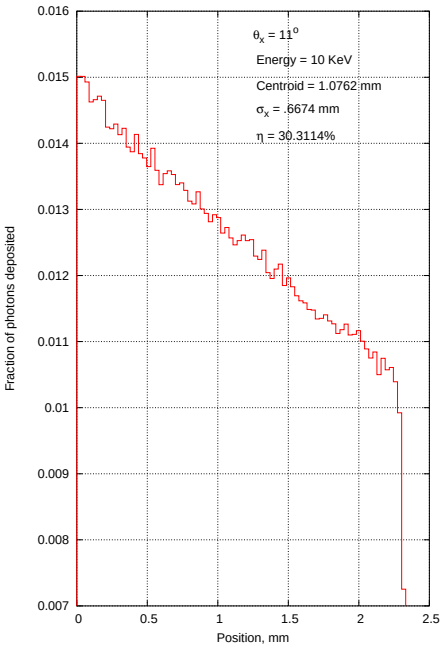

(b) 10 KeV X-ray photon incident at 11°

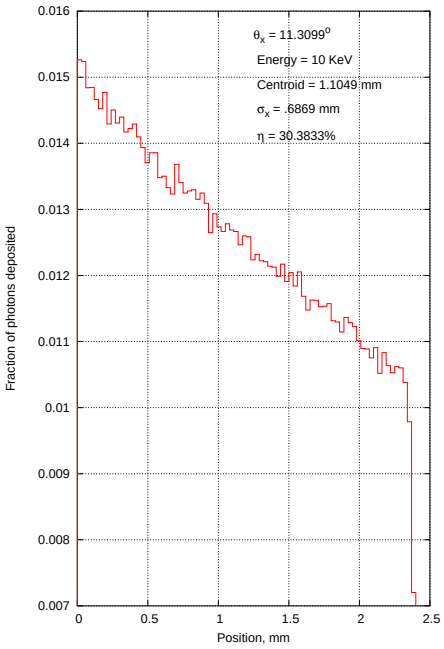

(c) 10 KeV X-ray photon incident at 11.3099°

Figure 4.62: Probability of absorption of 10 KeV photon when incident at 10°, 11°, 11.3099°.

The data obtained from the particle-matter simulation software Geant is named as **raw.dat**. The file raw.dat contains stream of energy values that are absorbed by each sub-cell for each incident photon process and data for 2×10^6 such processes is stored. This data file is then further processed, all the details of data analysis and processing is available in the chapter 5.

Aim of the exercise was to obtain the slant-ray blur caused due to the angular distribution of incident photons on the detector and the corrections made for suppressing its effect on imaging. The file **slantrayblurcorrection.dat** contains four columns, the first column contains **Energy**, second column contains **Angle**, third column contains **centroid** and fourth column contains **standard deviation**. The centroid and standard deviation for any energy and any angle is the correction factor.

4.1 Important Features to be looked upon:

While having a closer look at curve fitting for some energy ranges, dips in the slope were clearly observed. The energies where dips were present are 5.1 KeV and 5.467 KeV. These can be clearly observed in the Geant generated efficiency curve as shown in the figure 4.63.

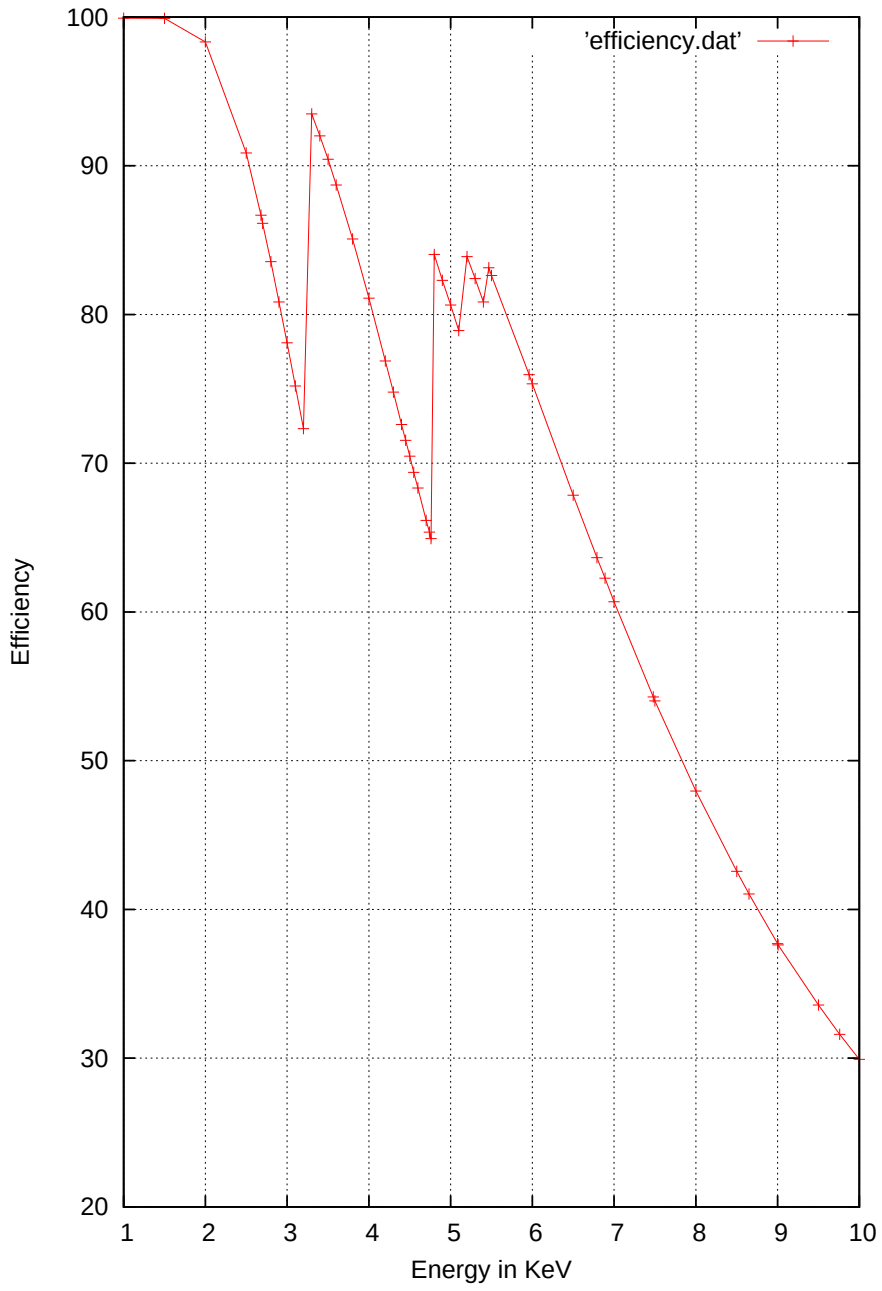

Figure 4.63: Efficiency curve for SSM detector generated by Geant 4.7

GEANT generated efficiency curve for SSM

Chapter 5

DATA ANALYSIS

The raw data is processed normalised and stored in different filenames each corresponding to a particular energy and angle for example: a file containing normalised data for a 5° angle and 4.7 keV energy is written as **nor_ThetaX5_Energy4.7_col.dat**. Each of these files contain commented explanation regarding the data present in the file, information about the mean,standard deviation and centroid of the position in the wire. These files for each angle and energy are stored in the folder **/sat12/amar/dataprogramjune17/Normalised_Data1/data** and the plots of these data are stored in **/sat12/amar/dataprogramjune17/Normalised_Data1/postscript**.

The processing of the raw data is done using a C-code **/sat12/amar/dataprogramjune17 /utilwithnor.c** and a shell script **/sat12/amar/dataprogramjune17/processrawdata_nor.sh**. This data gives us the values of centroid and standard deviation for a particular value of angle and energy but not for every angle and energy in the range of 0° to 11.309° and 1 keV to 10 keV. To obtain the values of centroid and standard deviation for any angle and energy for the required range we did curve fitting of some orders. In the first stage a shell script **/sat12/amar/dataprogramjune17/Normalised_Data1/data/curvefit.sh** is used to fit the equation $f(x) = b * exp(-x/(c * sin(ThetaX * dr)))$ to the data obtained and stores the values of the **b** and **c** coefficients in the following folders

- **/sat12/amar/dataprogramjune17/Normalised_Data1/data/bFitvarenergy/**
- **/sat12/amar/dataprogramjune17/Normalised_Data1/data/cFitvarenergy/**

In the second stage the shell script

- **/ sat12/ amar/ dataprogramjune17/ Normalised_ Data1/ data/ bFitvarenergy/ bfitgraphfinal.sh**
- **/ sat12/ amar/ dataprogramjune17/ Normalised_ Data1/ data/ cFitvarenergy/ cfitgraphfinal.sh**

are used to obtain further values of the coefficients and are stored in the files

- **/ sat12/ amar/ dataprogramjune17/ Normalised_ Data1/ data/ bFitvarenergy/ bFitfinal.dat**
- **/ sat12/ amar/ dataprogramjune17/ Normalised_ Data1/ data/ cFitvarenergy/ cFitfinal.dat**

The values of all the primary and secondary coefficients are copied into the folder **/ sat12/ amar/ dataprogramjune17/ Normalised_Data1/ data/ formula**. To generate the centroid and standard deviation from these coefficients for a given angle and energy in the range of 0° to 11.309° and 2 keV to 10 keV we have a script file and an awk file **/ sat12/ amar/ dataprogramjune17/ Normalised_Data1/ data/ formula/ slantray.sh**, **/ sat12/ amar /dataprogramjune17/ Normalised_Data1/ data/ formula/ eval2.awk**. The above mentioned shell script prints the centroid and standard deviation in the file **/ sat12/ amar/ dataprogramjune17/ Normalised_Data1/ data/ formula/file1.dat**. Presently the centroid and standard deviation for all the angles and energies in the range with a step size of 0.1° and 0.1 keV are stored in the file **/ sat12/ amar/ dataprogramjune17/ Normalised_Data1/ data/ formula/slantrayblurcorrection.dat**.

Chapter 6

CONCLUSION

Geant 4.7 a software for studying the particle-matter interaction was successfully used to obtain the data for the study of efficiency of the detector gas mixture and for the study of Slant Ray Blur in Scanning Sky Monitor. While studying the efficiency of the detector gas mixture and analyzing Slant Ray Blur we have come across two more dips in the efficiency curve for the detector at Energies 5.1 KeV and 5.467 KeV who's effect is present in the analysis of Slant Ray Blur which has been taken care. The Centroid and Standard Deviation for each Energy and Angle has been written in a file named **slantrayblurcorrection.dat**. This data is used for the corrections regarding blur in imaging, that takes place due to the photons that are incident in the off-normal angles.